Grand Accélérateur National d'Ions Lourds
Laboratoire commun CEA/DSM - CNRS/IN2P3

GANIL R 05 01

TECHNICAL REPORT ON OPERATING ACCELERATORS 2003 – 2004

Fig. 1

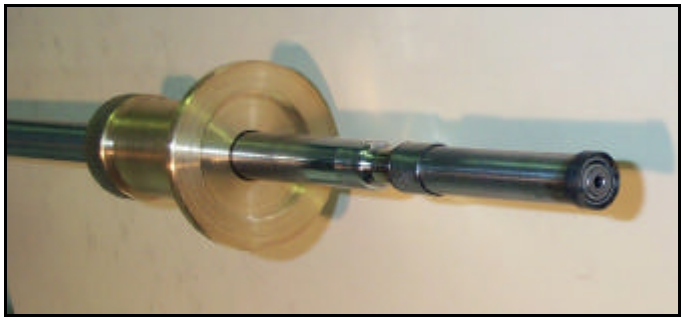

Fig. 2

GRAND ACCELERATEUR NATIONAL D'IONS LOURDS – LABORATOIRE COMMUN CEA / DSM – CNRS / IN2P3
BP 55027 – 14076 CAEN Cedex 5 – TEL: 02.31.45.46.47 – FAX: 02.31.45.46.65 – www.ganil.fr

CONTENTS

Cover page :
Fig.1 : LIRAT beam line view
Fig.2 : Large Capacity Oven for ECR Ion Source

FOREWORD

This issue of the Technical Report about the Accelerators describes the operation for physics experiments and beam tests, various technical improvements and projects for the years 2003-2004.

As usual the first chapter reports on the standard operation of GANIL with stable as well as radioactive beams, an analysis of the beam time distribution and statistics. Then there is a status report and an analysis of operation since 1996.

The second chapter, dedicated to beam tests, illustrates the importance of beam tests improving the performances concerning the delivery of radioactive beams. Great efforts have been made, firstly with stable beams, through THI beam tests and beam dynamic studies, and secondly with radioactive beams, through radioactive-ion production tests and the extension of the CIME working diagram.

Technical studies, essentially concerning ion-source developments on stable metallic beams and technical improvements to the accelerators , are described in chapter 3.

The last chapter deals with the installation of the new high-voltage platform of the injector C01 at the beginning of 2004 (PFI1 project).The aim of this project is to increase beam intensity at extraction from this new platform, especially for metallic ion beams, and to ensure a better stability with the high-intensity beams produced. The first results, obtained in beam operation during 2004 , are promising. In this last chapter a status report is given on the very low energy beam line for radioactive beams line, called LIRAT. This new facility has been commissioned in mid-2004 with stable beam. The last step is to obtain the permission from the Nuclear Safety authorities to expand the LIRAT operation to radioactive ions, which we hope to receive at the beginning of 2005. This will allow us to use radioactive beams produced with the SPIRAL target-and-source device directly, and thus to offer new possibilities for physics.

Eric PETIT
Head of the Accelerator Division

PREFACE

Ce numéro du rapport technique des accélérateurs décrit le fonctionnement pour la physique, les études machine, les améliorations techniques et les projets pour la période 2003-2004.

Le premier chapitre décrit comme il est de tradition le fonctionnement des accélérateurs avec des faisceaux d'ions stables mais également radioactifs, l'analyse de la distribution du temps de fonctionnement et les statistiques. Puis dans ce premier chapitre, un bilan et une analyse sont faits du fonctionnement des accélérateurs depuis 1996.

Le second chapitre, consacré aux études machine réalisées durant ces deux années, met en évidence la place importante faite aux études pour l'amélioration des performances dans le cadre de la fourniture des faisceaux radioactifs. Les efforts ont été portés tout d'abord côté faisceau primaire, avec des études machine THI et des tests d'optique faisceau, puis côté faisceaux radioactifs avec les mesures de taux de production en faisceaux radioactifs et l'étude de l'extension du diagramme de fonctionnement de CIME.

Au chapitre 3 sont évoqués les développements techniques avec les développements pour la production des ions métalliques sur les sources ECR en faisceau stable, mais également les développements et améliorations côté accélérateurs (trieur vertical dans CIME, projet CICS, la migration du commande-contrôle vers LINUX).

Le dernier chapitre décrit la mise en place, au début de l'année 2004, de la nouvelle configuration de la plateforme source de l'injecteur 1 (projet PFI1). L'objectif visé est d'augmenter l'intensité du faisceau à la sortie de cette plateforme, notamment pour les faisceaux métalliques, et de garantir une stabilité plus grande sur les faisceaux haute intensité produits. Les premiers résultats obtenus en exploitation sont prometteurs. Ce dernier chapitre est également l'occasion de faire le point sur la nouvelle ligne d'ions radioactifs très basse énergie, appelée LIRAT, qui a été testée avec succès en faisceau stable au cours de l'année 2004. La dernière étape à franchir est l'obtention de l'autorisation d'exploitation en faisceaux radioactifs de cette nouvelle ligne. Cette autorisation est espérée pour le printemps 2005, ce qui permettra d'utiliser directement les faisceaux issus de l'ensemble Cible/Source de SPIRAL et offrira ainsi de nouvelles possibilités pour la physique.

Eric PETIT
Chef du Secteur des Accélérateurs

1

ACCELERATOR OPERATION

ACCELERATOR OPERATION
In 2003 and 2004

A. Savalle

1) Highlights

2003

The accelerator operation was 35 weeks long, in 4 periods. This represents 5604 hours of operation. Among these 5604 hours, 3766 (67% of operating time) were used by physics experiments. This is a record since the beginning of GANIL in 1983.
Since the beginning of SPIRAL operation, SISSI was unavailable due to technical modifications and waiting for the safety authority authorization. This authorization was received in September and an experiment has been realized in October.
In parallel of high energy physics, about 240 hours of low energy beams (Xe, Pb, Kr) were available for users of the IRRSUD facility.
Several problems occurred during the SPIRAL beams :

- The production rate was too low for an experiment planned with ^{24}Ne beam
- Important failures during ^{8}He beam (CIME deflector, EINZEL lens at the source extraction, diagnostic failures...).

2004

The accelerator operation was 34.5 weeks long, in 5 periods. This represents 5532 hours of operation. Among these 5532 hours, 3352 (60.7% of operating time) were used by physics experiments.
In parallel of high energy physics, about 650 hours of low energy beams (Xe, Pb, Kr) were available for users of the IRRSUD facility. The Intermediate energy exit delivers about 1400 beam hours per year for atomic physics.

The high voltage platform, where is located the ECR source for C01 injector, was unavailable from march to may due to a major modification : a solenoid and a dipole have been included to separate ions and charge state before acceleration. The result is a better stability, better transmission in the cyclotron, and lower charge states needed for the same energy (the total acceleration voltage, source extraction + acceleration tube, is now equal to 100 kV).
Let us notice, since this modification, the following results :

- acceleration of 3 kW ^{13}C beam for SPIRAL
- acceleration of 1.2 kW ^{78}Kr beam for SPIRAL
- acceleration of 0.7 kW ^{48}Ca beam for SPIRAL and SISSI

A new SPIRAL target, designed for 3 kW primary beam, was tested with the production of 6 10^5 pps $^{8}He^{1+}$

2) Accelerated beams

2003

Stable beams

Period	Ion	Energy (MEV.A)	Accelerator	THI
1	^{32}S	95	SSC2	0.75 kW (D3)
1	^{36}S	77.5	SSC2	0.6 kW (D3) 1.4 kW (SPIRAL)
1	^{78}Kr	73	SSC2	
1	^{36}Ar	95	SSC2	1 kW (SPIRAL tests)
1	^{112}Sn	63.5	SSC2	
1	^{13}C	60	SSC2	
2	^{13}C	75	SSC2	1.4 kW (SPIRAL)
2	^{208}Pb	4.5 and 29	SSC1 and SSC2	
2	^{238}U	6.6	SSC1	
2	^{86}Kr	6.6 and 43.1	SSC1 and SSC2	
2	^{20}Ne	12	CIME	
2	^{238}U	5.9	SSC1	
2	^{13}C	75	SSC2	1.4 kW (SPIRAL)
2	^{129}Xe	7.5 and 50	SSC1 and SSC2	
2	^{36}S	11 and 77.5	SSC1 and SSC2	0.5 kW (D3)
3	^{129}Xe	50	SSC2	
3	^{208}Pb	4.5	SSC1	
3	^{36}S	77.5	SSC2	1.4 kW (SPIRAL)
3	^{40}Ar	4.8	CIME	
3	^{58}Fe	5	SSC1	
3	^{36}S	77.5	SSC2	1 kW (SISSI)
4	^{208}Pb	0.33	C02	
4	^{76}Ge	5	SSC1	
4	^{13}C	75	SSC2	1.4 kW (SPIRAL)
4	^{48}Ca	4.5	SSC1	

SPIRAL BEAMS		
Ion	**Energy (MeV.A)**	**INTENSITY (PPS)**
^{24}Ne	**4.7**	**$2\ 10^5$**
^{74}Kr	**4.6**	**$1.5\ 10^4$**
^{8}He	**15 .4**	**$1.5\ 10^4$**
^{8}He	**15 .4**	**$9\ 10^3$**
^{24}Ne	**10**	**$2\ 10^5$**
^{8}He	**15 .4**	**$2.5\ 10^4$**

2004

Stable beams

Period	Ion	Energy (MEV.A)	Accelerator	THI
1	^{36}Ar	95	SSC2	1 kW (SPIRAL tests)
1	^{129}Xe	35	SSC2	
1	^{58}Ni	74.5	SSC2	0.8 kW (SISSI)
2	^{36}S	77.5	SSC2	1 kW (SPIRAL)
2	^{58}Ni	74.5	SSC2	0.7 kW (SISSI)
2	^{15}N	1	C02	
3	^{48}Ca	60	SSC2	
3	^{208}Pb	29	SSC2	
3	^{13}C	75	SSC2	2.6 kW (SPIRAL)
3	^{78}Kr	70.4	SSC2	0.55 kW (SISSI)
4	^{13}C	75	SSC2	1.4 kW (SPIRAL)
4	^{56}Fe	9.7	SSC1	
4	^{57}Fe	9.7	SSC1	
4	^{78}Kr	70.4	SSC2	1.2 kW (SPIRAL)
4	^{48}Ca	60	SSC2	0.6 kW (SPIRAL)
4	^{86}Kr	60	SSC2	
4	^{78}Kr	64	SSC2	
5	^{129}Xe	35	SSC2	
5	^{18}O	55	SSC2	
5	^{18}O	5.3	CIME	
5	^{36}S	77.5	SSC2	0.6 kW (D3)
5	^{48}Ca	60	SSC2	0.7 kW (SISSI)
5	^{15}N	1.2	CIME	
5	^{48}Ca	6.6	SSC1	
5	^{208}Pb	29	SSC2	
5	^{48}Ca	60	SSC2	0.7 kW (SISSI)

SPIRAL BEAMS		
Ion	**Energy (MeV.A)**	**INTENSITY (PPS)**
^{26}Ne	**10**	**$3\ 10^3$**
^{44}Ar	**10.8**	**$2\ 10^5$**
^{8}He	**3.5**	**$6\ 10^5$**
^{8}He	**15.4**	**$2.5\ 10^4$**
^{76}Kr	**4.34**	**$7\ 10^5$**
^{46}Ar	**10.3**	**$2.5\ 10^4$**

3) Operating statistics :

2003

The time available for users was a record since the beginning of GANIL in 1983. This good result is due to a relatively low failure rate, as well as the organization of beam tunings and beam machine studies with one accelerator (ex. SSC1/SSC2) in parallel with experiments realized with another one (ex. CIME).

Scheduled beam time distribution from March 10th to December 19th 2003		
	Hours	%
Preparation of beams	757	13.8
Nuclear Physics (HE)	3413	62.2
Non Nuclear Physics (HE)	488	8.9
Non Nuclear Physics (ME)	97,00	1.8
Physics Tests	348	6.3
Machine beam tests	288,00	5.2
Not defined	97	1.8
total	**5488**	100.0

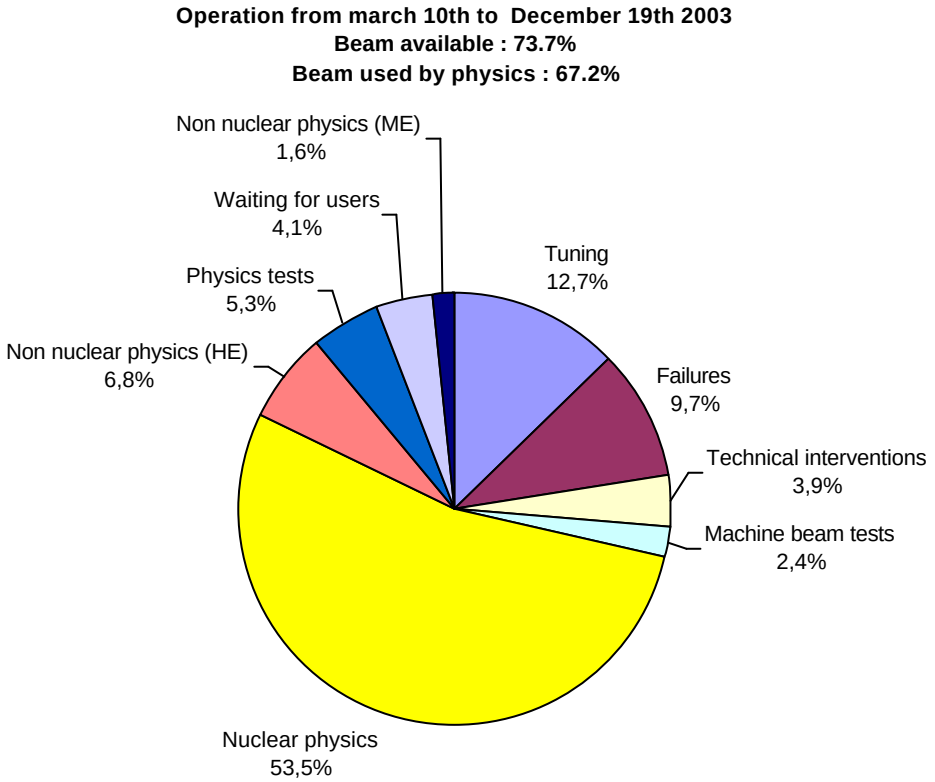

2004

The availability for users has decreased, due to an increase of the failure rate, and more time allocated to machine beam tests (in particular production tests with SPIRAL facility).

Scheduled beam time distribution from February 28th to December 17th 2004		
	Hours	**%**
Preparation of beams	1015,00	*18,34*
Nuclear Physics (HE)	3153,00	*56,96*
Non Nuclear Physics (HE)	498,00	*9,00*
Physics Tests	226,00	*4,08*
Machine beam tests	391,00	*7,06*
Not defined	252,00	*4,55*
total	**5535,00**	*100,00*

Operation from February 28th to December 17th 2004
Beam available : 72.3%
Beam used by physics : 60,6%

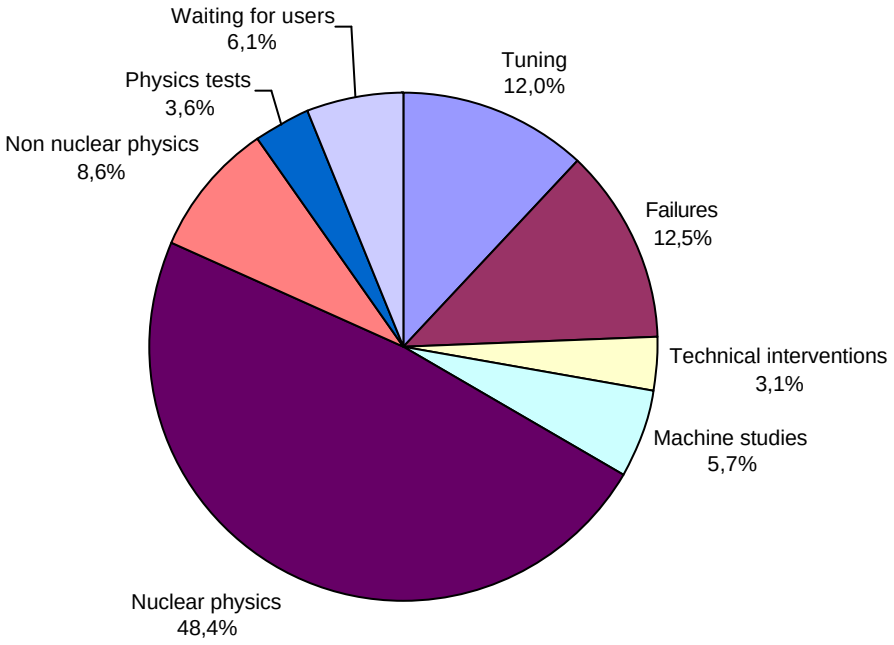

It can been seen, also, that waiting time is important. It is due to reduced tuning times, as well as to technical difficulties in experimental areas which make the use of the beam by physics impossible.

4) Failures Statistics

The distribution of the failures is the following :

2003	Hours	%
Power supplies	**82**	*15,06*
Electronics	**7,00**	*1,29*
Control-command	**14,25**	*2,62*
Logic controllers	**12,25**	*2,25*
R.F.	**57.25**	10,52
ECR Sources	**15,25**	*2,80*
SISSI	**18,50**	*3,40*
Cooling circuit	**29,50**	*5,42*
Vacuum	**54**	*9,92*
Surety systems	**51,50**	*9,46*
Beam stops	**14,50**	*2,66*
Electricity	**34,50**	*6,34*
Target and Source System	**53,50**	*9,83*
Instability	**13,50**	*2,48*
Diagnostics	**19**	*3,49*
Other equipments	**67,75**	*12,45*
total	**435,00**	*100,00*

While the failure rate is relatively low, important failures occurred during ^{8}He beams (CIME deflector, EINZEL lens at the source extraction, diagnostic failures...).

2004	Hours	%
Power supplies	**61,50**	*8,90%*
Control-command	**9,75**	*1,41%*
Logic controllers	**44,25**	*6,41%*
R.F.	**60**	*8,69%*
Electronics	**0,00**	*0,00%*
High voltage equipments	**10,75**	*1,56%*
Diagnostics	**13,75**	*1,99%*
Beam stops	**24,25**	*3,51%*
Cooling circuit	**36,50**	*5,29%*
Vacuum	**40,50**	*5,87%*
Surety systems	**20,75**	*3,01%*
ECR Sources	**4,00**	*0,58%*
Target and Source System (SPIRAL)	**75,25**	*10,90%*
SISSI	**193,75**	*28,06%*
Electricity	**74,00**	*10,72%*
Instability	**21,50**	*3,11%*
	690,50	*100,00%*

The main cause of failure concerns SISSI, with problems encountered with the rotation of the target, and the broke of a cooling circuit inside.

EVOLUTION OF OPERATION SINCE 1996

A. Savalle

1) Beam availability and availability for physics

Beam availability was slightly increased in 2003-2004, with a maximum of 73.7% in 2003. Simultaneously, the machine studies rate was low in 2003, resulting to a high availability for physics. In fact, 2003 is a record for beam availability for physics in percentage and in hours since twenty years of GANIL existence. In 2004, the machine studies part was increased. Furthermore, waiting time (beam ready in advance or unavailable experimental areas/devices) was important. Thus the percentage rate of beam used by physics is decreasing compared to 2003.

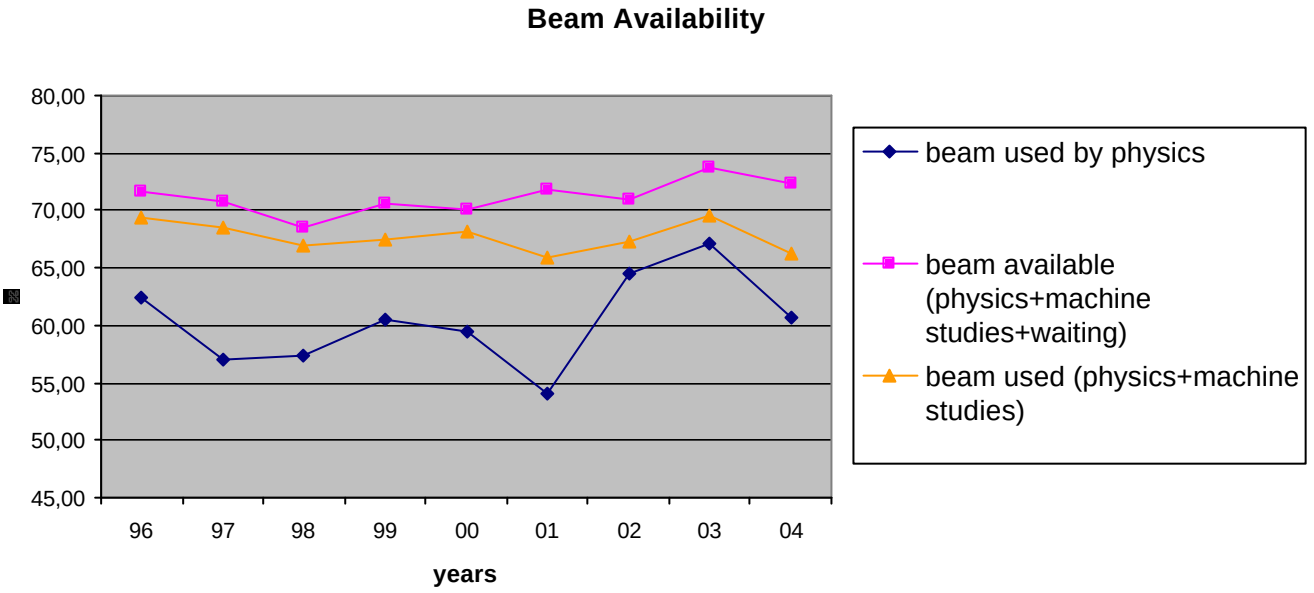

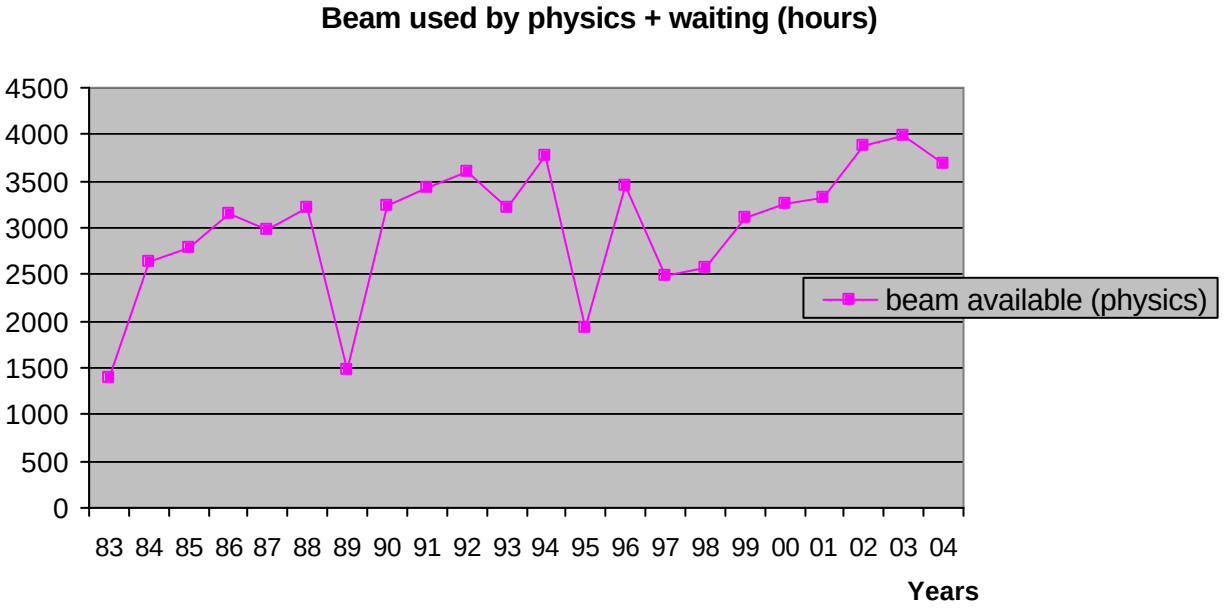

2) Machine studies

Since the start of operation with SPIRAL, the machine studies are, if possible, planned in parallel with physics : machine studies with CIME cyclotron in parallel with physics using SSC1/SSC2 beam, machine studies with SSC1/SSC2 in parallel with physics using CIME beam. This is the reason why the machine studies rate appears, in 2002-2003, inferior to 3%. In 2004, about 130 hours were devoted to production tests with SPIRAL Target and Source System. The tests use a SSC2 primary beam bombarding a SPIRAL target-source, so that no SSC2 nor CIME stable beam can be delivered.

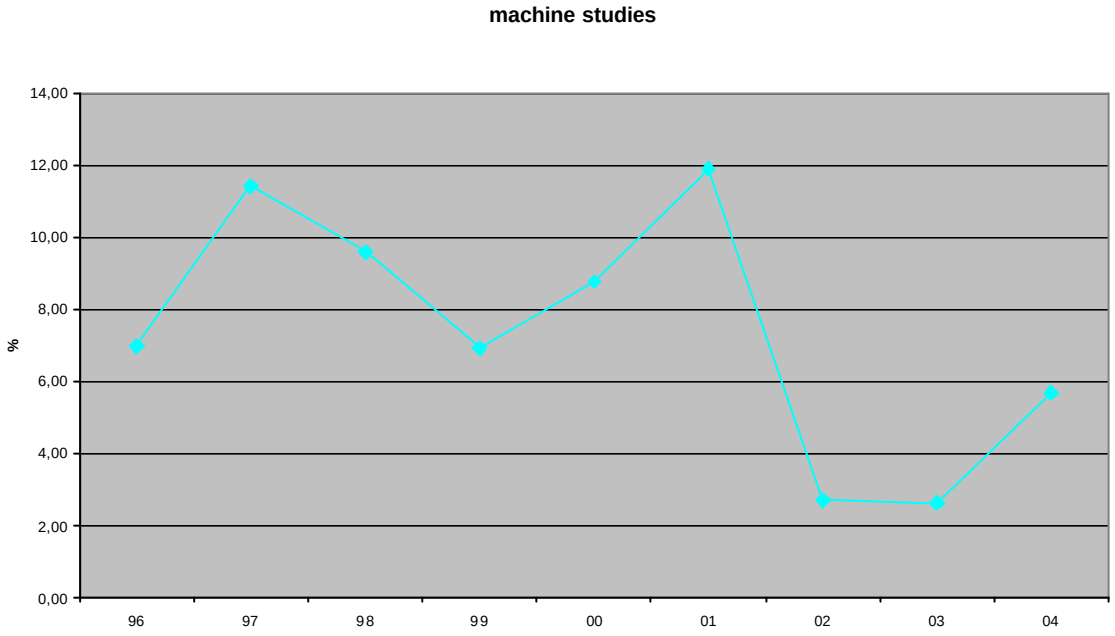

3) Evolution of tuning time

The tuning time is still decreasing in 2003-2004, despite an increasing ratio (number of accelerated beams / number of operation weeks).
It can be explained by two ways :

- improvement of the tuning methods
- organization of beam tuning in parallel with physics : the CIME (respectively SSC1 /SSC2) beams are planned so that the main part of the tuning is realized while a SSC1 or SSC2 (respectively CIME) beam is delivered to physics.

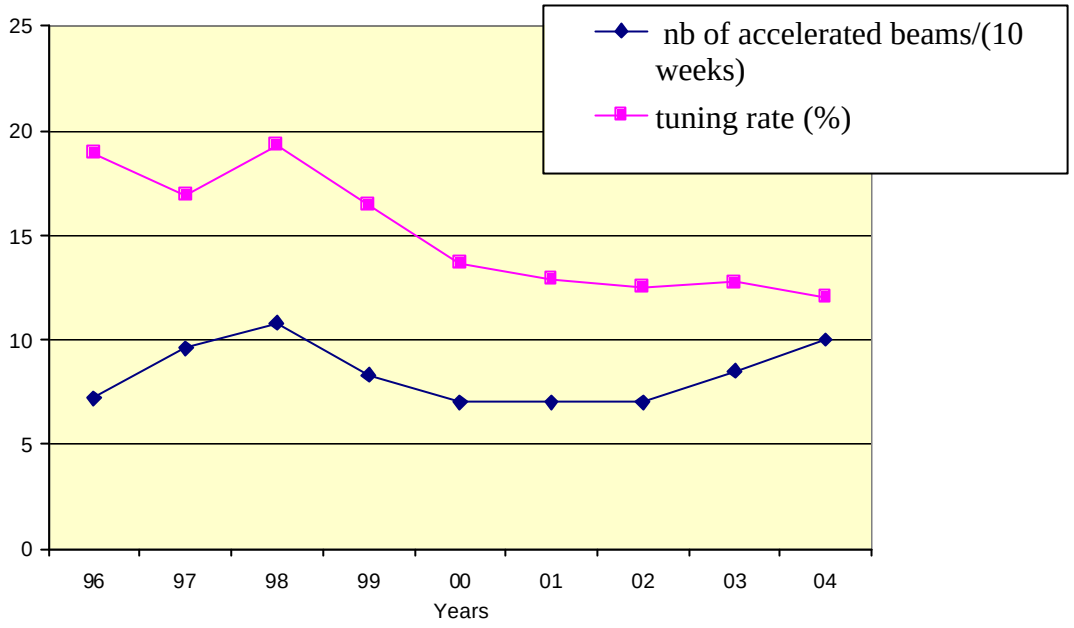

4) Evolution of failure rate

No clear tendency is shown by the graph bellow. Since 2001, are counted as technical interventions, not only the maintenance operation, but also changes of SISSI targets or of Targets and Source Systems.

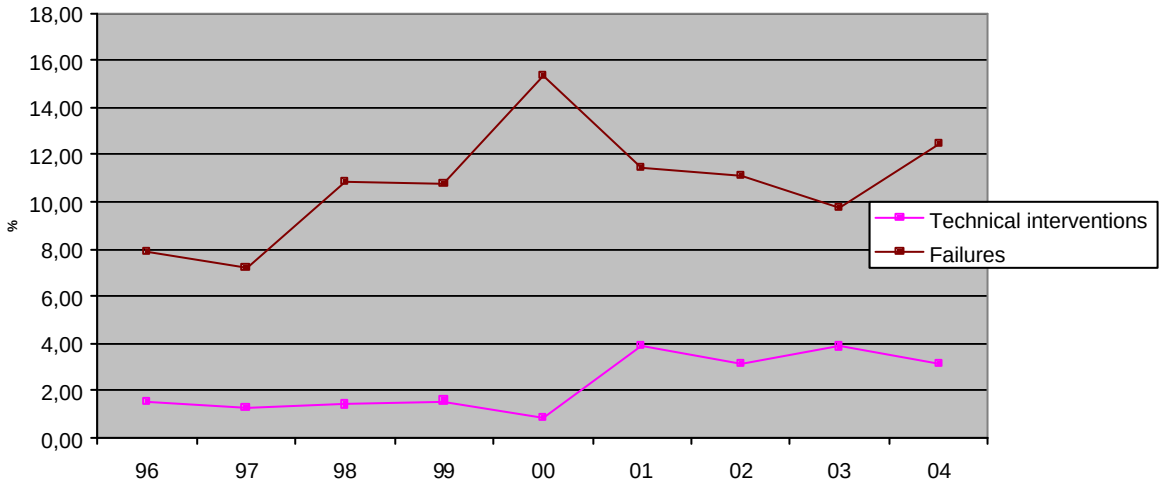

2
MACHINE STUDIES

SUMMARY OF MACHINE STUDIES IN 2003-2004

A. Savalle

2003:

2.4 % of operation time were devoted to machine studies. The different subjects were :

- Measurement of electrical power consumption depending to the characteristics of the accelerated beams
- Production tests with SPIRAL
- Automatic beam tuning

THI :

- The deflector of SSC2 was replaced by another, with a narrower septum. The aim was to decrease the losses at SSC2 extraction. This new deflector and its instrumentation (measurement of losses) was tested.
- Concluding the OPTHI project, the new system that guaranties the security of equipments in case of high power beams was tested
- Tests were made to obtain and maintain over 24 hours RF voltages of 240 kV in SSC2 (necessary for 6kW beams)

In addition, other tests were made in parallel with physics. The different subjects were :

- Beam instrumentation
- Beam tuning software
- Development of digital feedbacks to stabilize the beam
- Study of the beam dynamics in C01 injector: the reason of the large emittance observed (up to 40 π mm.mrad) was discovered and the emittance decreased to 10 π mm.mrad

2004

5.7 % (315 hours) of operation time were dedicated to machine studies :

- almost one half of this beam time concerns production tests of SPIRAL beams : ^{24,25,26,27}Ne, ^{31,32,33,35}Ar, ^{44,46}Ar

The other subjects were :

- developments of digital feedbacks
- beam instrumentation
- beam tuning software (longitudinal emittance measurement)
- tests of SSC2 RF voltage at high level
- tests of the optics of beam lines L3 and L4 (from SSC2 to the Target-Source of SPIRAL), with or without the use of the SISSI solenoids
- Test of the future system of control of the primary beam intensity, for SPIRAL (CICS project)
- Validation of the calculations of the radiological protections (LCG project)

In addition, other tests were made in parallel with physics. The different subjects were :

- Beam instrumentation
- mass measurements : stable beam tests to prepare an experiment with ^{31}Ar, ^{32}Ar, ^{33}Ar
- test of the LIRAT beam line (dedicated to very low energy exotic beams)
- test of a vertical deviator, which enables to improve the CIME resolution, for SPIRAL I beams but also in view of SPIRAL II
- Extension of CIME working diagram: some experiments demand a CIME energy lower than the low limit of the diagram (i.e. 1.7 MeV.A with harmonics 5). For that reason, tests of CIME working in harmonics 6 have been realized, and it has been proved that it was possible to get an energy as low as 1.2 MeV.A

CIME Harmonic 6 studies

F. Chautard

1. Introduction

The CIME working diagram allows to accelerate ion beam from 1.74 to 25 MeV/A as a function of their charge over mass ratio.
In order to respond to a new demand from the physicists, one has tried to extend the working diagram towards the low energies.
The lowest energy achievable is 1,74 MeV/A and is fixed by the lowest frequency (F_{rf} =9.6 MHz) reached by the RF cavities. Then, the change of harmonic is the only choice. The harmonic 6 would theoretically delivers beams from 1.2 MeV/A up to 2.7 MeV/A.

We will show in the following that we were able to accelerate ion beams at this harmonic. However, limitations appear, showing that, if the physicist demand grows, an adaptation of CIME injection is probably required

2. Simulations

One can recall the relation between the RF frequency and the harmonic number. $F_{rev} = \frac{F_{RF}}{h} = \frac{v}{2\pi R}$, where F_{rev} is the beam revolution frequency, F_{RF} the RF cavity frequency, h the harmonic number, v is the ion beam speed and R the orbit radius. The energy required is $W \approx v^2 \approx F_{rev}^2 = \left(\frac{F_{RF}}{h}\right)^2$. To reduce the limit energy at the extraction radius, one can whether reduce the RF frequency (F_{RF} = 9.6 MHz minimum for 1.74 MeV/A and h=5) or increase the harmonic number h.

The low energy limit for F_{RF} = 9.6 MHz and h=6 becomes 1.21 MeV/A.

The first objective is to find, for two CIME field levels (corresponding to a physicist experimentation proposal) a central rays compatible with the actual injection point constituted by a spiral inflector and electrostatic quadrupole placed behind.

The computation is done with the code LIONS and the trajectory found is shown on Figure 1 with the isochronism curve Figure 2.

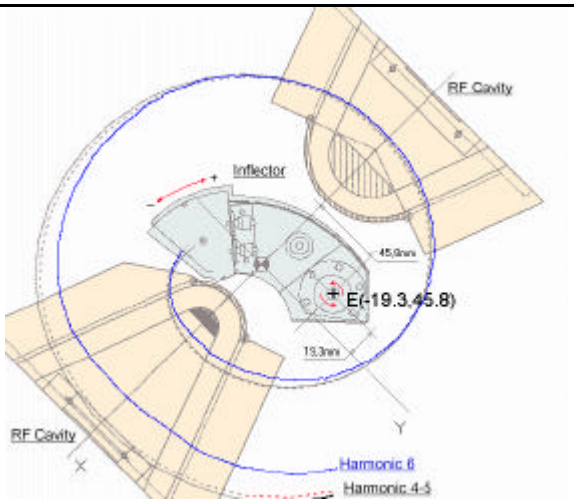

Figure 1 : Ion beam trajectories for various harmonics (h=4, 5 and 6).

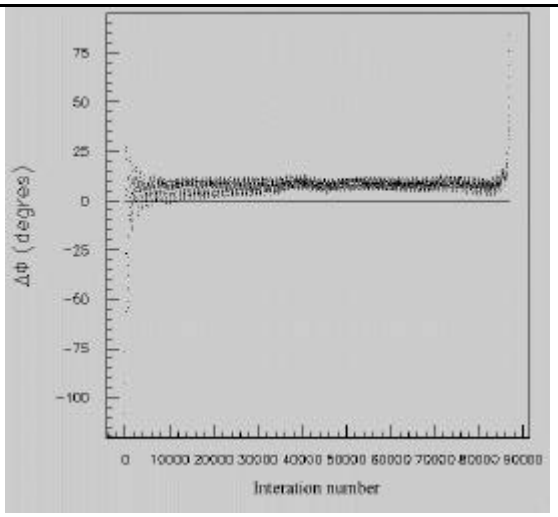

Figure 2 : Isochronism curve simulated from the injection to the ejection of CIME

The energy gain at each turn through the four cavity gaps is given by $\partial W = 4\frac{Q}{A} V_0 \sin(\frac{h\alpha}{2})$, where α is the azimuthal aperture of the cavity and h the harmonic (Figure 3 and Figure 4).

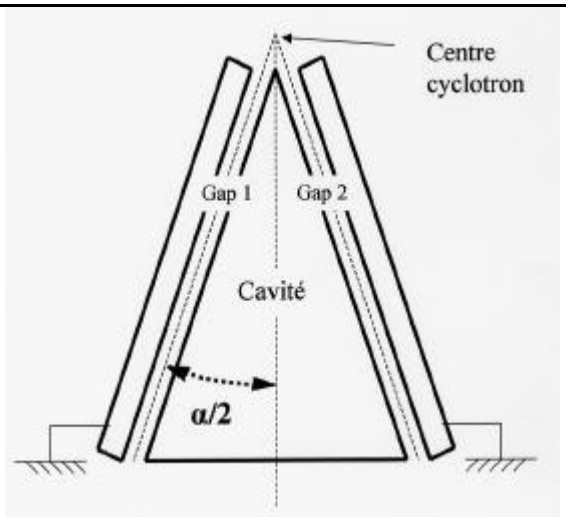

Figure 3 : CIME RF cavity Geometry

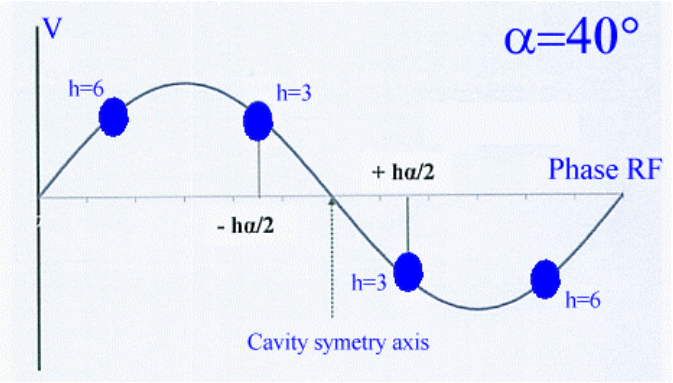

Figure 4 : Acceleration phase of the beam with respect to the RF phase as a function of the harmonic

The isochronism condition, $B(r)= \gamma(r)B_{inj}$, has to be fulfilled to accelerate the beam. We assume that the $\gamma(r)$ variation for energy in the 1 to 2 MeV/A range is not significant compared to higher energy. We use then the current value of the isochronism coils calculated for the harmonic 5. Additionally, the harmonic 5 and 6 have a common RF frequency region for 1,7 MeV/A. The $\gamma(r)$ is the same at this point. It will be our first study energy.

3. Machine study

The machine study was split into 3 from march 2004 to March 2005. It was decided to take advantage of the operators in order to benefit from their presence the evenings, weekend and public holidays. This continuity in the machine tuning largely contribute to converge to a tuning solution. Indeed, one could consider that the maximum in output for a given adjustment had been reached when the operators acknowledged themselves overcome.

The Figure 5 shows the various tuned beams (green dots) over the three harmonic 6 machine studies.

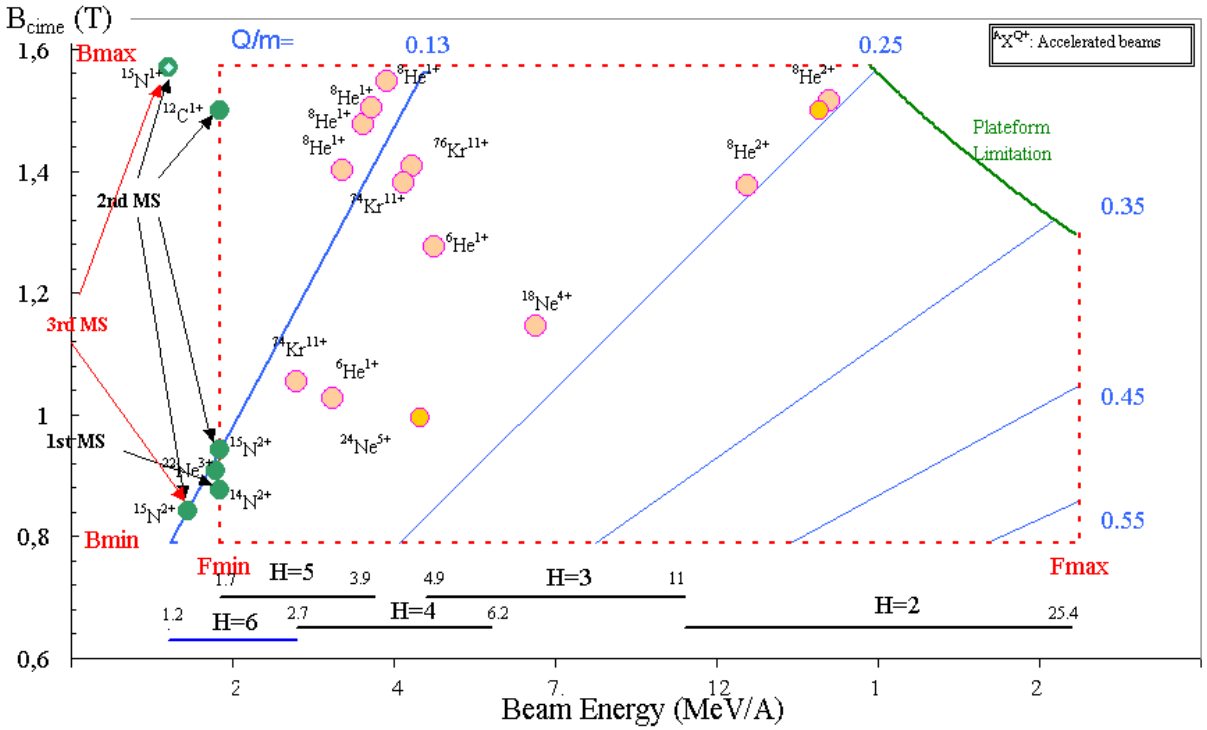

Figure 5 : CIME working diagram. In orange dots the SPIRAL accelerated beams. Green dots represent different beams done for the harmonic 6 study machine.

The table below, summarizes the machine parameters for the different tunings.

Beams	12C1+	12C1+	15N1+	15N2+	15N2+	15N2+	15N1+	15N2+	15N1+
Harmonic	H5	H6	H6	H5	H6	H6	H6	H6	H6
Energy [MeV/A]	1.74	1.74	1.21	1.74	1.74	1.4	1.2	1.4	1.2
Frequency [MHz]	9.6	11.52	9.6	9.6	11.52	10.34	9.6	10.34	9.6
Extraction magnetic rigidity [T.m]	2.28	2.28	2.376	1.425	1.425	1.278	2.376	1.272	2.376
Magnetic field [T]	19786	19783	20580	12331	12331	11052	20578	11053	20576
Efficiency Output / input CIME	25%	16%	15%	20%	18%	10%	17%	10%	15%

12C1+ at 1.74 MeV/A and H5 and H6

As told in §2, there is an energy, (1,74 MeV/A) common to the harmonic 5 and 6. The RF frequency is respectively 9.6 MHz and 11.52 MHz (Figure 5).
It is then possible to tune a beam in harmonic 5, with known parameters (25% transport efficiency, from the analyze point to the CIME ejection line) and flip to the harmonic 6 with the same beam and magnetic field configuration and by changing simply the phase between cavity, the frequency and applying the new RF cavity voltage (calculated with LIONS code) to pass correctly through the RF cavity gaps.
An efficiency of 16% was achieved.

15N1+ at 1.2 MeV/A and H6

The overall transport efficiency is around 15 to 17%. One can expect to gain few percent with more tuning time. Figure 6 shows the beam turns. There is 86 turns well defined. An excellent isochronism is reached, Figure 7.

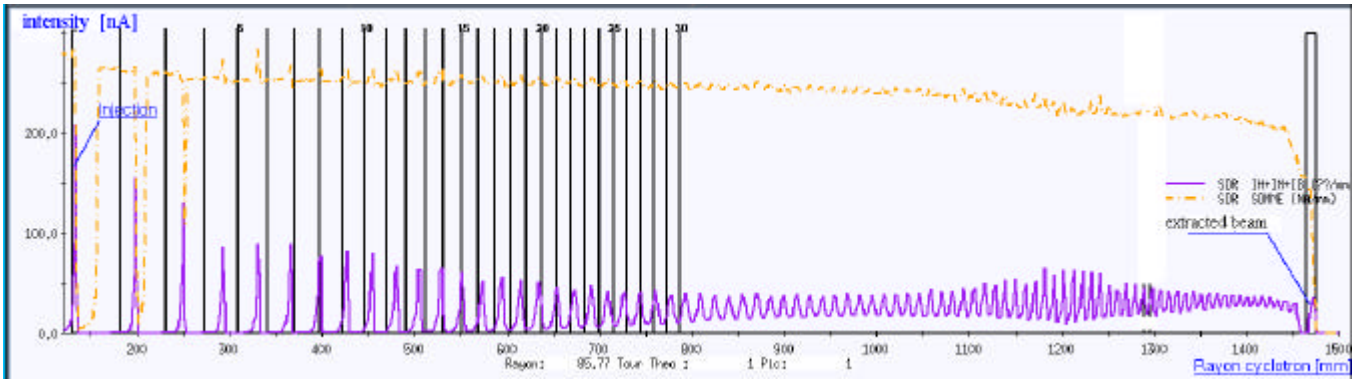

Figure 6 : Beam turn measured in harmonic 6 in CIME

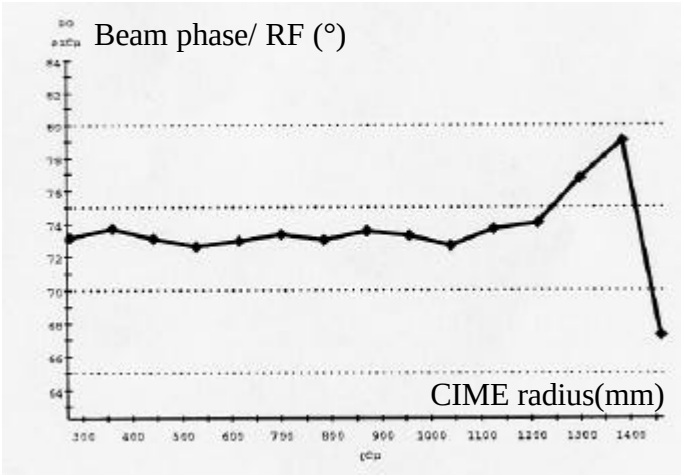

Figure 7 : Isochronism plot measured in CIME in harmonic 6.

15N2+ at 1.4 MeV/A and H6

Transport efficiency from the source to the analyse point decreases due to the space charge effect in the beam at low platform voltage (below 10 kV). An émittance dilution is induced, increasing the beam envelopes. The acceptance of the beamline is then not enough to transport the beam without loss.

The efficiency are around 10% but with closed émittance slits. With opened slits, the transport efficiency in the injection beam line is reduced by a factor 2.

4. Conclusions

The acceleration of an ion beam at low energy with the harmonic 6 is feasible.

The energies studied are the following :

- 1.2 MeV/A with $^{15}N^{1+}$
- 1.74 MeV/A with $^{15}N^{2+}$
- 1.4 MeV/A with $^{15}N^{2+}$
- 1.2 MeV/A with $^{15}N^{2+}$

The injection inflector is designed to inject the beam at a radius of 45 mm in the cyclotron CIME. This centre, as shown in Figure 8, allows to stay above the 10 kV source extraction voltage for charge over mass ratio (Q/m) above 0.1. The space charge effect is contained. For the harmonic 6, one a part of the working diagram at low CIME field level is below the 10 kV limit under space charge regime. Experimentally, the space charge effect have been seen through the important beam loss along the low energy beamline due to the emittance dilution and consequently large beam envelope. To avoid such a beam losses (factor 2 at least), one has to :

- work at high CIME field for 0.06 < Q/m < 0.1 (Figure 8) For example, from the available spiral beam (in theGANIL website), The ^{17}Ne and heavier beams could beam accelerated down to 1.21 MeV/A with respect to the Q/m condition. On the other hand, the following radioactive ions, ^{6}He, ^{8}He, ^{13}N, ^{14}O and ^{15}O can not be accelerated at 1.21 MeV/A

Or

- design a new injection centre for CIME to bring the beam at higher energy meaning higher radius (60 mm) for example. This study should decide to replace or not the cavity extremities

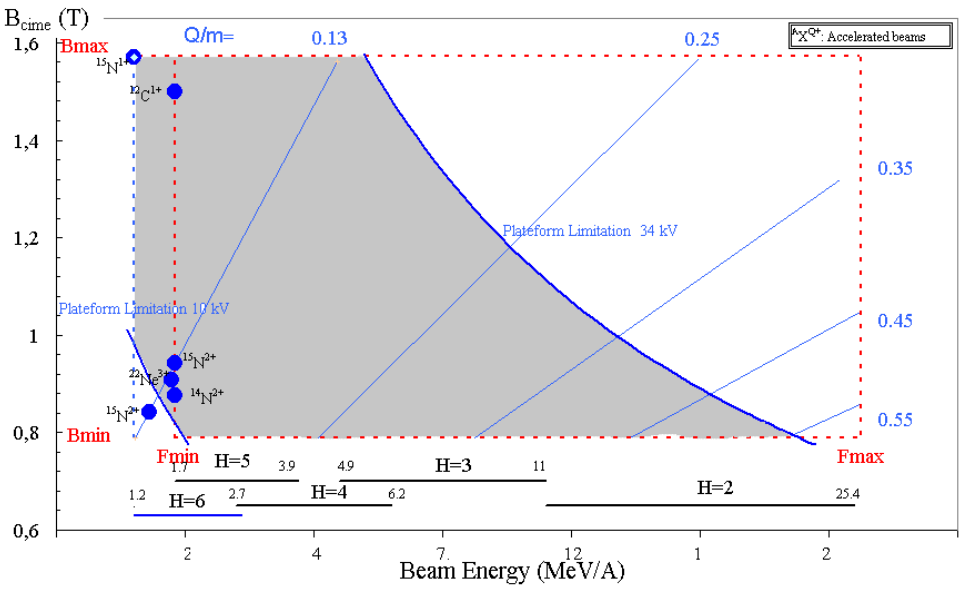

Figure 8 : New working diagram limits with the spiral inflector for the harmonic 4, 5.

3
TECHNICAL DEVELOPMENTS

The CICS Project (Irradiation Control of the Spiral Target)

P.Anger

Abstract : *The CICS project aims at optimizing the Spiral facility experiments schedule as well as the exploitation costs, by controlling the maximum dose (maximum number of ions stopped in the Spiral Target), a new safety criterion.*

1. Introduction

The SPIRAL unit generates a radioactive ion beam by irradiating an ECS "Ensemble Cible-Source" *(Target- Ion Source)* with a high energy ion beam. GANIL is a facility submitted to approval , and the irradiation mode of targets is regulated by the safety authorities. At present, the target irradiation is limited by a safety criterion of 15 days of use , independently of the irradiating beam characteristics(ion species, power and risks linked to the operation of the accelerators). A request for modification of this criterion has been formulated to the safety authorities. It does not impair the safety level of SPIRAL. The maximum irradiation time authorised should depend on the irradiating beam type and of its intensity, the new criterion being that the total number of ions received by the target (integrated flux) should not exceed a certain level, function of the radiological risk. The target irradiation time will nevertheless remain linked to the operation schedule of the accelerators (6 to 10 weeksperiods).

In order to control this new criterion, the CICS project (**C**ontrôle de l'**I**rradiation de la **C**ible de **S**PIRAL) *(Irradiation Control of the SPIRAL Target)* has beenissued: it will require a measurement system and a reliable control of the beam intensity which will, at any time, show both the instantaneous and the integrated beam intensity for each target. The intensity means the number of ions per second.

2. Description of the system

The system (fig.1) consists of two sensors measuring the intensity of the primary beam irradiating the ECS *(Target- Ion Source)* and returning an electric signal proportional to the intensity. A dedicated chain of measurement will handle the signal of each sensor so that they can be digitized by a computing system. This dedicated and autonomous computing system will be able to test the two instrumentations and handle any malfunctions. Using an user interface, this computing system will receive the necessary information from the primary beam, the identification of the ECS and the maximum authorized number of incident ions in order to measure the intensity of the beam, calculate the number of particles per second and integrate the number of ions stopping in the target. The computing system records the data related to the irradiation of each ECS on two reliable and permanent data carriers. It cuts off the beam either when a malfunction occurs or when the target has received the maximum dose (new safety criterion). Via an interface, the system will keep users informed of its configuration and of the operating data.

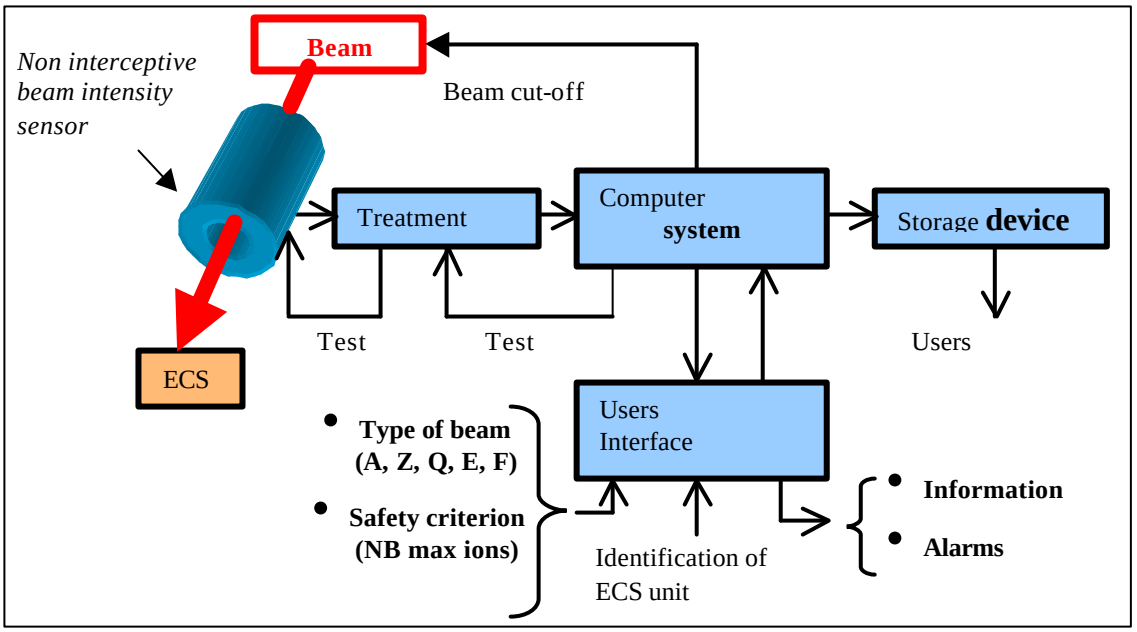

Figure 1 : block diagram

3. Principle of the measurement of the beam intensity

The beam intensity is obtained by measuring the magnetic field generated by the pulsed beam (fig.2) with a Fast Current Transformer.

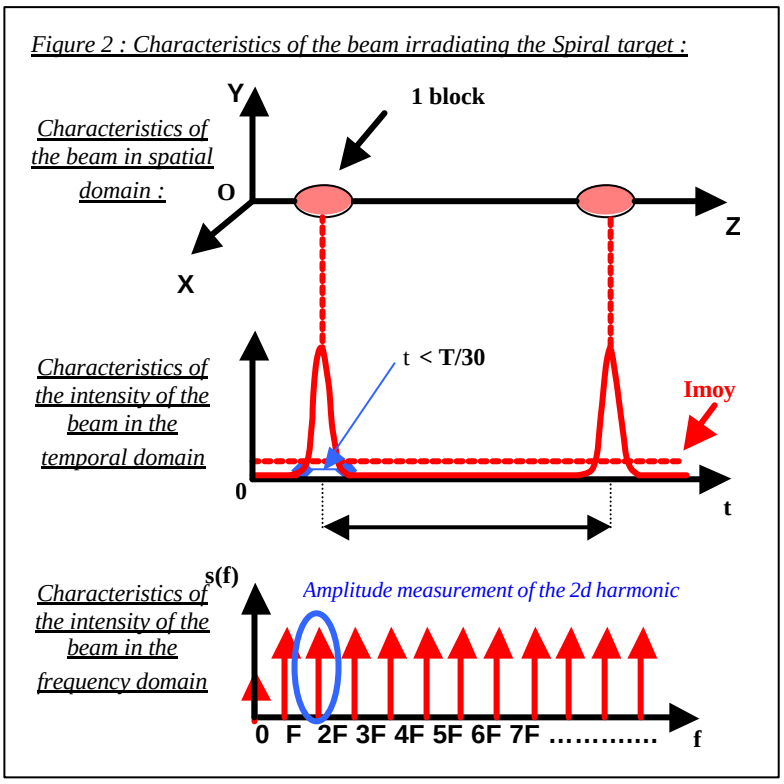

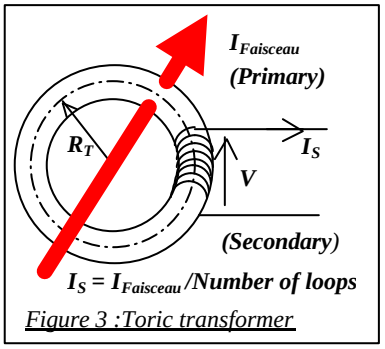

Figure 3 :Toric transformer

Figure 4 : Picture of 2 Fast Current Transformers

The current transformer (fig.3) generates an image signal of the beam intensity to a treatment chain ; then, the amplitude of the second harmonic of the signal is detected by a Lock-in Amplifier. The average value of the intensity is calculated through the relation between the 2d harmonic amplitude and the average value in the Fourier expansion :

$$a_0 = \frac{a_2}{\left(2\frac{\cos(2pFt)}{1-(4Ft)^2}\right)} \cong \frac{a_2}{2} \quad \text{if } t << \frac{1}{F}$$

This measuring equipment is doubled (fig.4) in order to ensure an active redundancy which guaranteed the validity of the measurement. The measuring equipments are calibrated in order to establish the global accuracy of the measurement and therefore to deliberatly overestimate, by programming, the calculated intensity.

4. Mechanical integration

The sensor (fig.5) is installed in the L4 beam line a few meters before the SPIRAL target (fig.6).

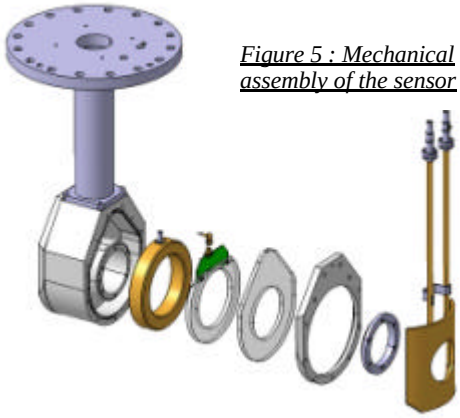

Figure 5 : Mechanical assembly of the sensor

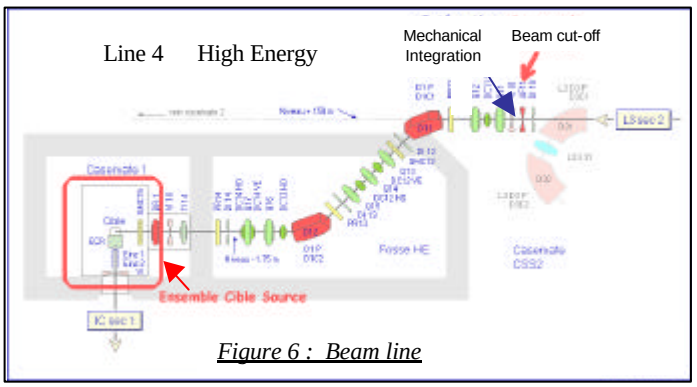

Figure 6 : Beam line

5. Description of the computing system

It is basically composed of a real time industrial controller of the Compact Fieldpoint type (fig.7). It is autonomous, has its own operation system and is programmed under Labview. The system must obtain the detected intensity of the beam, calculate the particle fluency, stop the beam with a beam stopper block if the level is exceeded or in case of malfunction. It will record the irradiation history on a local memory and provide a link to the PC user. The system will also have a user interface in order to configure the system and to keep the users informed (fig.8).

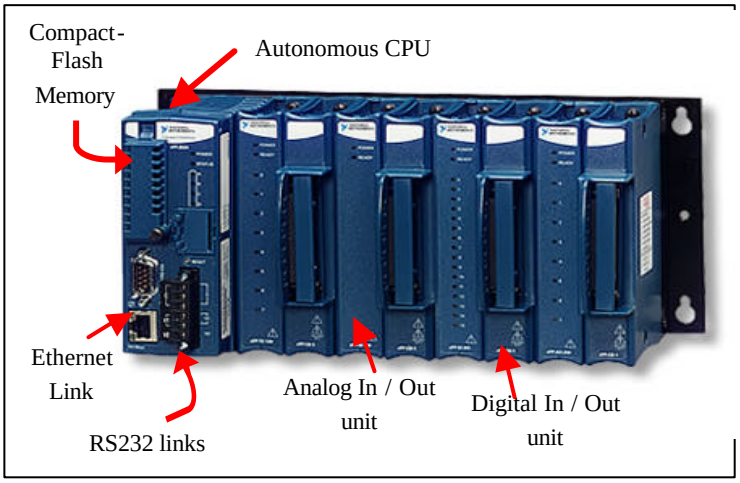

Figure 7 : Compact Field Controller

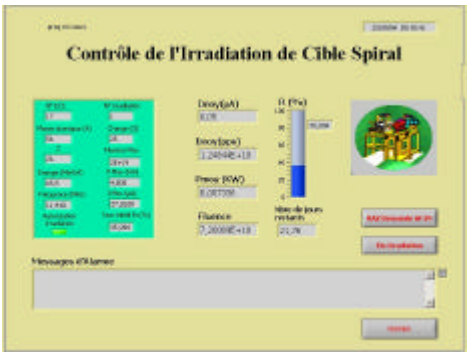

Figure 8 : User Interface

6. Quality Assurance

The study, implementation and operation of this system need to satisfy quality requirements in order to control the new safety criterion. The intensity measurement veracity, the malfunction management and the overall reliability were taken into account from the beginning. For example, the uncertainty of the measurement chain will be treated whatever the beam frequency, the pulse length, the operating temperature of the subsets, and also whichever units or refill installed.

7. Conclusion

This project is nearly completed ; it is awaiting starting-up authorisations for the validation of the concept (control system of the new safety criterion) by the safety authorities. It will greatly improve the production tool that SPIRAL represents. It will allow a better management of target irradiation by lowering the number of ECS *(Target- Ion Source)* used every year. This should decrease SPIRAL's production costs and provide a better response to the physicists' demands for beam scheduling as well as a reduction of the amount of generated waste.

References :

[1] S.Faure, *« Limite d'irradiation d'un ECS de SPIRAL »*, internal document 2003, SPR213B

[2] F.Loyer, *« Cahier des charges fonctionnel du projet CICS »*, internal document 2003, P-CICS-01-A CdCF

[3] P.Anger, *« Plan de développement du projet CICS »* internal document 2003, P-CICS-002-PDD-A plan de développement

[4] P.Anger and the Project Team : C.Doutressoulles, M.Ozille, JF.Rozé, B.Jacquot, M.Dubois, S.Faure, F.Bucaille, C.Mauger, JC.Deroy, *« Cahier des Charges et des Clauses Techniques du projet CICS »* internal document 2003, P-CICS-043-CdCCT-A.

Improvement of the mass separation power of a cyclotron by using the vertical selection method

P. Bertrand, F. Daudin, M. Di Giacomo, B. Ducoudret and M. Duval

Abstract

It is well known that cyclotrons are very good mass separators, specially when the number of turns in the machine is large. This property is particularly interesting if the cyclotron unavoidably accelerates multiple species of radioactive beams simultaneously, which is the case for the cyclotron CIME at GANIL. We propose to improve the natural mass separation power by using a vertical resonance effect: it consists of putting two small electrodes between the poles, which provide a vertical electric field operating at two frequencies close to twice the RF frequency and which are tuned with respect to the vertical betatron oscillation. A prototype has been designed and built at GANIL, and tested successfully in the cyclotron CIME during 2004.

INTRODUCTION

In what follows, we will present successively the theory, the particle simulation, the prototype design, the first experiments and recent and future improvements.

THEORY

Let's consider the vertical motion of a particle (q,m) in a cyclotron, where two electrodes are installed above and below the median plane, between the radii r_1 and r_2 near the extraction radius and with an angular extent Dq (variable potential V, gap g). Introducing the vertical betatron oscillation parameter n, the Dirac function d, the angular pulsation ω, the azimuthal second derivative z", the RF harmonic h and the phase $Df = hDq$, we can write the equation:

$$z'' + n^2 z = a\, d \qquad (1)$$

$$a(t) = \frac{qV(t)}{gmw^2}\Delta q = \frac{V(t)}{g}\frac{\Delta f}{2pf_{hf}B_z} \qquad (2)$$

In order to simplify the equations, let's consider the case n=1/4 and introduce the constant one-turn transfer matrix T and the variable one-turn vertical "kick" matrices B_i :

$$T = \begin{bmatrix} 0 & 4 \\ -1/4 & 0 \end{bmatrix} \quad ; \quad B_i = \begin{bmatrix} 0 \\ a_i \end{bmatrix} \qquad (3)$$

A particle with the initial conditions $u_0=(z_0,z'_0)$ will have the following turn-by-turn transformation :

$$u_1 = Tu_0 + B_1$$

$$u_2 = Tu_1 + B_2 = -u_0 + TB_1 + B_2$$

$$u_3 = Tu_2 + B_3 = -Tu_0 - B_1 + TB_2 + B_3$$

$$u_4 = Tu_3 + B_4 = u_0 - TB_1 - B_2 + TB_3 + B_4$$

Due to the particular choice of n, we see that the particle comes back to the initial conditions after 4 turns, if the vertical kicks are all equal. However, if we choose the successive kicks judiciously with respect to the natural oscillation of the particle, it is possible to make a powerful vertical resonance appear. Let's choose:

$$q_i = 2pi$$

$$a_i = a\sin(nq_i + j) = a\sin(\frac{p}{2}i + j) \qquad (4)$$

After $4n$ turns, we obtain:

$$u_{4n} = u_0 + 8a\,n\begin{bmatrix} -\cos(j) \\ \sin(j) \\ \hline 4 \end{bmatrix} \qquad (5)$$

which shows that the vertical amplitude of the particle oscillation increases linearly with the number of turns. If $1/n$ is not equal to 4 (or not integer), the demonstration is more sophisticated but the effect remains the same. Moreover, we can show that this resonance occurs for the particles having different initial conditions. In fact, this linear effect does not affect the emittance of the bunch.

Having in mind that we want to preserve the acceleration of the reference beam (well isochronised), and to deflect the other species (shifted in phase) verticaly, the best would be to multiply the time-dependant potential signal corresponding to (4) by a normalised square wave (stepped or not), denoted by $H(t)$:

$$V_{ideal}(t) = V_{\max}\sin(\frac{n}{h}w_{hf}t)\,H(t) \qquad (6)$$

However, it is not technically straightforward to generate such a signal, so that for our prototype, we have replaced it by a sinusoidal one, with a frequency equal to $2f_{hf}$, in order to increase the efficiency at 45° instead of 90°, and with a tunable phase y (see also figure 1):

$$V(t) = V_{\max} \sin(\frac{n}{h} w_{hf} t) \sin(2 w_{hf} t + y) \qquad (7)$$

$$= \frac{V_{\max}}{2} \left(\sin(w_1 t + y + \frac{p}{2}) + \sin(w_2 t + y - \frac{p}{2}) \right)$$

$$w_1 = 2w_{hf}(1 - \frac{n}{2h}) \quad ; \quad w_2 = 2w_{hf}(1 + \frac{n}{2h})$$

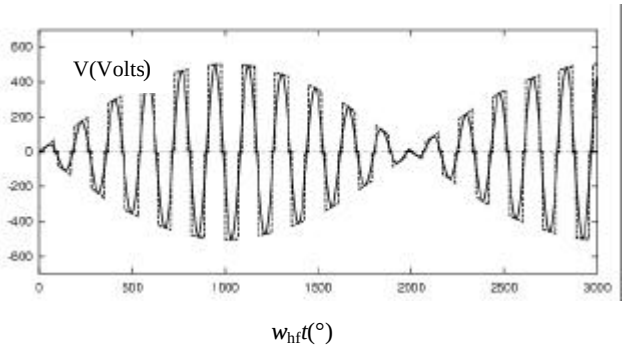

Figure 1: Ideal and realistic potential signals $V(w_{hf})$.

We conclude that two signals with frequencies close to $2f_{hf}$ and with the same amplitude must be generated on one of the electrodes, which requires a large bandwidth. Considering that the excited species are stopped on two horizontal slits separated by a gap g, we can also deduce an estimation of the potential needed:

$$V_{\max} = K.2pn \frac{g^2 f_{hf} B_z}{h \Delta q} \frac{1}{n} \qquad K \approx 1.15 \qquad (8)$$

PARTICLE SIMULATIONS

In order to check the theory, we have simulated the partical behaviour with our code LIONS [1]. We have chosen one of the available measured magnetic maps (B_z=1.5T, n=0.269) and f_{hf}=11Mhz using the harmonic h=3. The results are in very good agreement with the equation (8) , so that we have fixed the objective of the prototype to V_{max}=500 V in order to preserve some margin. (figure 2).

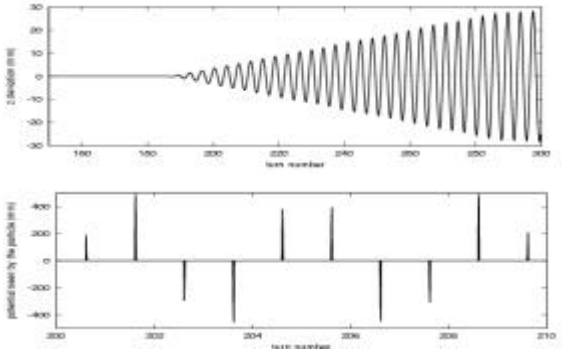

Figure 2: Typical vertical resonance trajectory (top) and applied potential between turns 200-210 (below).

PROTOTYPE DESIGN

Mechanics

The electrodes consist of two copper sheets (length=250mm, angle=5°, gap=18mm) mounted inside an open-ended aluminum box extended by a cylinder towards the vacuum-chamber flange (figure 3). The upper electrode is connected to the box, which is grounded and protects against exterior perturbations. The electrode below receives the RF signal from a 1.2mm wire, left at a constant distance from the ground box in order to keep the caracteristic impedance fixed (Z_c=240Ω, L=60cm). Two insulated copper plates at the entrance allow us to measure beam current losses. The whole device is installed in the hill gap of one cyclotron sector.

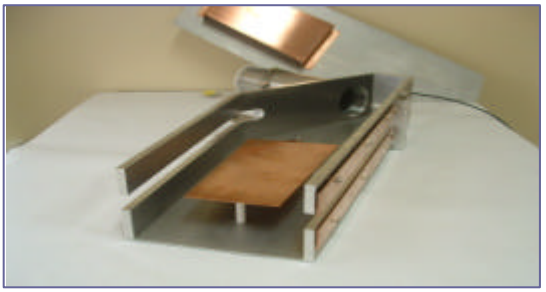

Figure 3: View of the prototype device with the upper part and electrode lifted off.

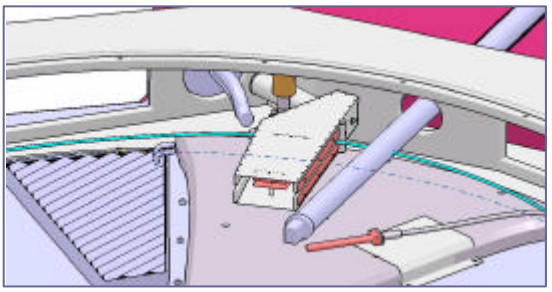

Figure 4: View of the prototype device installed into the cyclotron CIME.

Signal generation and power circuits

In order to obtain the desired electric field between the electrodes, we have designed and installed a power circuit as indicated in figure 5: the driving signal is generated in the control room, by mixing the second harmonic of the CIME RF signal (carrier port) and a frequency generator signal tuned at the "?/2h" value (local oscillator port). The center frequency rejection is better then 40 dB and the two needed frequencies have identical levels.

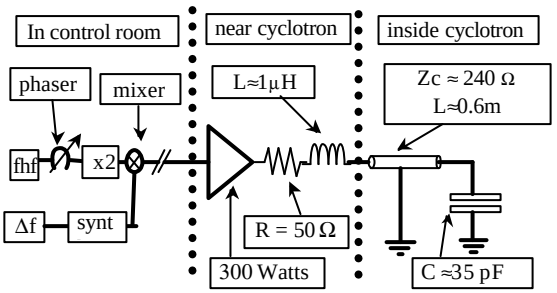

Figure 5: Power circuit and the electrodes.

As a high voltage and a large bandwidth are required, a resonant circuit with a low Q is necessary. Moreover, we need a solution with low losses inside the vacuum chamber, so that cooling is not necessary. The power circuit design is based on the series resonance of a quarter-wave resonant line loaded with the equivalent electrode capacitance (figure 5).

The transmission line is split into two sections in order to avoid some obstacles present in the vacuum chamber, and its length is shortened by a lumped inductance to use the vacuum feedthrough in a very low impedance region, already insensible to the characteristic impedance change.

Outside the vacuum chamber a second inductance is used for fine tuning and a 50 Ω series resistor ensures the Q dumping and the impedance matching to the amplifier. The fine tuning is important to amplify the two signal components equally and to avoid distortion effects.

FIRST BEAM TESTS

We achieved the first beam test with our prototype in september 2004. Due to a lack of available time, it was not possible to tune the machine with 2 simultaneous ion species close one to the other. The accelerated stable beam was $^{16}O^{5+}$ with F_{hf} =11.326Mhz, B_0=1.46 , h=2. The procedure to induce and optimise the vertical resonance effect was very simple an was less than 15 minutes long, the beam having been previously isochronised and extracted. We chose Δf=1.52Mhz, corresponding to the estimated n_z=0.269. Then we shifted the phase of the signal between –90°and 90° in order for the loss peaks to appear (-45° and +45°), measuring them with the beam current probes. Then we tuned the phase to 45° and reoptimized the *Df*. Once the resonance was obtained, we returned the phase to 0°, and checked that the beam passed correctly through the device and through extraction. In order to simulate the presence of another beam, we applied a slight *DB/B* variation and checked that the beam was vertically deflected and stopped by the slits.

Figures 6 and 7 show that the resonance effect occurs efficiently and that the desired beam is not disturbed. In fact the main difficulty was to minimize the phase width of the beam itself, and reduce an unexpected precession probably due to rather approximate knowledge of the acceleration parameters (e.g. angle at injection). The direct consequence was that we needed more potential than expected to make the beam vanish vertically (around 500 Volts instead of 300).

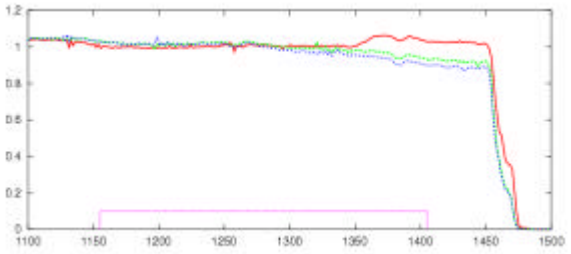

Figure 6: Normalised beam current as a function of the radius (isochronised) : red = no voltage, green ≈ 370V, blue ≈ 500 V, pink=position of electrodes.

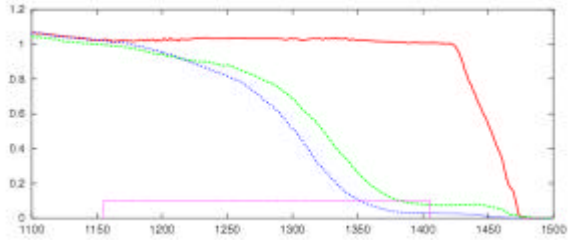

Figure 7: Normalised beam current as a function of the radius for a beam phase shift of 40° : red = no voltage, green ≈ 370V ,blue ≈ 500 V.

Another set of tests were performed in november 2004. The aim was to check that the device works correctly by using the harmonics 4 and 6, in particular at very low energy, and to use our exotic diagnostics at very low current, in order to prove that we can suppress pollutants in the case of a realistic situation (very low beam current).

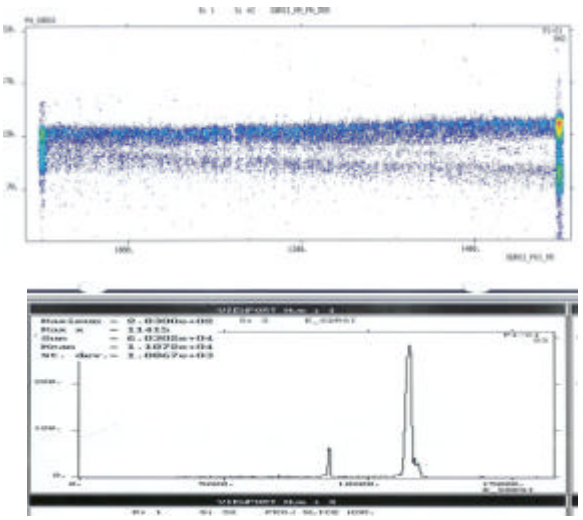

Figures 8: Measurement of Oxygen (majoritary) and Carbon using the Silicium beam diagnostic inside CIME. The separation is about 45° at the extraction.

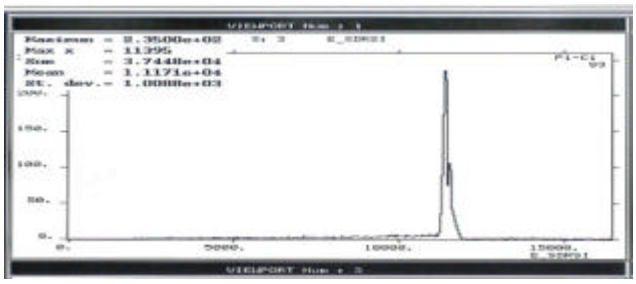

Figure 9: Total mass measurement. Using the VMS, the carbon is completely eliminated

As an example, Figures 8 shows Oxygen and Carbon simultaneously accelerated in the machine, and Figure 9 shows how the Carbon pollutant is eliminated using the Vertical Mass Separator (VMS).

RECENT AND FUTURE IMPROVEMENTS

The tests performed in 2004 have suggested several improvements:

A capacitive pickup on the electrodes, installed in January 2005, will allow us to tune the resonant circuit, in order to obtain equal peaks on both signals and avoid losses of the beam of interest.

A 25 Ω resistor able to accept 500 watts will give a better circuit gain (proportional to 1/R) and allow us to use a more powerful amplifier, if necessary. We checked in January 2005 that the signal generated at the electrodes when using a 25 Ω resistor, was greater in amplitude and not deformed, and that the reflected power was acceptable.

Adjustable vertical slits could be a very power tool : by tuning their gap according to the pollutant masses, we could choose the separation efficency on line, according to the physics requirements.

CONCLUSION

We have proved experimentally that the Vertical Mass Separator concept works without any major difficulty, provided that the beam is tuned correctly.

We are convinced that with the improvements suggested and in the frame of SPIRAL 2, we could reach a mass separation of about 6.10^{-5} and eliminate a significant part of the isobaric pollutants.

One question could be: *what is the theoretical limit ?* In the ideal case of a "round beam" cyclotron, for which the "natural" mass separation could be 3.10^{-4} (as in CIME) and the phase extension of the beam could be ±2 degrees (as at PSI), the mass separation would be less than 2.10^{-5} by using adjustable vertical slits. Note that the "round beam" concept can work for low intensity beams (e.g. RIBs) as proved in [2].

acknowledgments

We would like to thank all those who helped us during the device installation and the first beam tests, in particular : F. Chautard, M. Desmons, M. Gallardo, C. Galard, A. Lemarié, M.H. Moscatello and A. Savalle.

REFERENCES

[1] P. Bertrand: "LIONS: a new set of Fortran 90 codes for the SPIRAL project at GANIL". 4th ICCPO, Japan, (1994).

[2] P.Bertrand, Ch. Ricaud: "Specific cyclotron correlations under space charge effects in the case of a spherical beam". 16th Internat. Conf. on Cyclotrons and their applications. (2001).

[3] P. Bertrand, F. Daudin, M. Di Giacomo, B. Ducoudret, M. Duval: "Improvement of the mass separation power of a cyclotron by using the vertical selection method". 17th Internat. Conf. on Cyclotrons and their applications. Tokyo (2004).

Improvements on stable beams from ECRIS

P.Lehérissier, F.Lemagnen, C.Canet, C.Barué, JL.Flambard, M.Dupuis

L'année 2003 fût marquée par la mise en œuvre de la technique de recyclage par SF_6, pour la fourniture d'un faisceau intense de germanium. La mise au point d'un four haute température (High-Temperature Oven – HTO) destiné à l'augmentation de l'intensité du faisceau d'uranium, s'est poursuivie. Un premier essai en Vanadium a été effectué sur la source d'ions ; Parallèlement la méthode de sputtering a donné un faisceau stable U^{31+} de 0.5 eμA. En 2004, la poursuite du développement du HTO a été différée et la priorité mise sur les essais en ligne du four à grande capacité (Large Capacity Oven - LCO). L'objectif est l'augmentation des intensités des faisceaux de Ca, Pb, Sn et Mg. Par ailleurs, la méthode « MIVOC » a été utilisée avec succès pour la production de faisceau de haute intensité à partir du magnésocène ($24Mg^{5+}$ ~ 110 eμA) et aussi pour des faisceaux de Fer et de Nickel issus de composés organométalliques synthétisés par un laboratoire de l'université de Caen .

In the year 2003 we used for the first time the recycling effect of SF_6 for the production of a high intensity beam of germanium. The development of the High-Temperature Oven (HTO), with the aim of about 10 eμA of U^{25+} beam production, was continued. A preliminary test with vanadium was achieved on the ion source. In the mean time the sputtering method was used and gave a stable beam of U^{31+} of 0.5 eμA. In 2004, the development of the HTO was delayed. The main priority was the test on-line of the Large-Capacity Oven (LCO) for the increase of the calcium, lead, tin and magnesium beam intensities. We have also succeeded with the "MIVOC" method for the production of high intensity beam of magnesium ($24Mg^{5+}$ ~ 110 eμA), and for iron and nickel beams from "home-made" organometallic compounds synthesised by a laboratory of the University of Caen.

I - Recycling of Germanium with SF_6 gas

The recycling effect of germanium with SF_6 gas **[1]** on an ECRIS, observed in 2001, has been studied, then used as beam for research of superheavy elements at the end of 2003 ($^{76}Ge + {}^{208}Pb \rightarrow {}^{283}114 + n$). A beam of 1pμA was delivered to the experiment. First, three loads of GeO_2 were evaporated into the source using the micro-oven and with helium as support gas. For 4 days, 150 mg of ^{76}Ge were consumed and the ionisation efficiency for Ge was around 4%. Then a very stable beam of $^{76}Ge^{10+}$ with an average intensity of 35 eμA, was produced for 17 days, using SF_6 as support gas (Fig. 1).

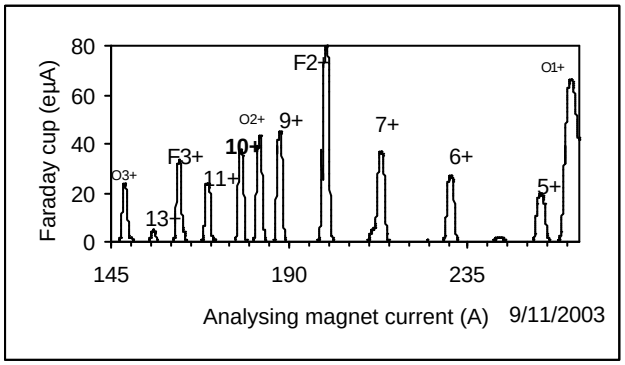

Figure 1: Germanium spectrum – recycling with SF6 gas.

Fluorine coming from dissociated SF_6 gas in the plasma reacts gradually with thin layers of germanium or germanium oxide deposited on the walls. A germanium tetrafluoride (GeF_4) vapour is directly produced in the plasma chamber and ionised as a gas, leading to a high ionisation efficiency of 38%. The intensity and the request charge state can be adjusted by varying the RF power and the SF_6 flow rate. The easy tuning of the source, the stability, the very small background noise of the beam, the high intensity and the ionization efficiency confirm that the source behaves as well as with a gas. The main source parameters were: RF power 60 W, high voltage 66 kV/1.3 mA. Previous tests on $^{76}Ge^{13+}$ beam gave us 35 eμA with a RF power at 230 W.

II - High-Temperature Oven

A High-Temperature Oven **[2]** able to reach 1900°C was designed and built for the production of an intense uranium beam (10 to 20 eμA of U^{25+}). This high operating temperature prohibited the use of any ceramic, which is a limitation for the present micro-oven. The HTO has a coaxial geometry (Fig. 2).

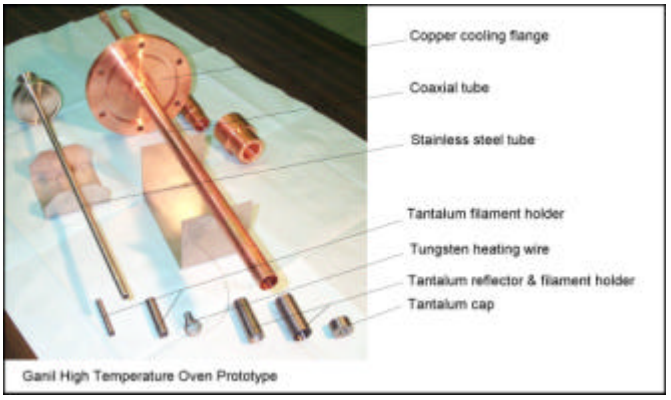

Figure 2: HTO components and coaxial tube.

Two external coaxial tantalum cylinders – used as reflectors – and a filament holder, are fitted together into a copper tube which is also the RF coaxial line. The copper tube is welded to a water-cooling flange. The inner part is made of two coaxial tantalum cylinders used as a filament holder and fitted together into a stainless steel tube which allows the introduction of either a movable crucible or gaseous compounds. The tungsten filament (ϕ 0.5 mm) has a conical shape, giving a better mechanical stability, and joins the tantalum cylinders. The crucible (ϕ 5 mm, length

15 mm), made of a refractory material suitable for the required compound, is movable and can be refilled without breaking the vacuum in the source. A temperature of 1800°C has been measured for an electrical power of 310 W (18 V / 17 A),with the off-line prototype. A temperature higher than 1700°C has been maintained for 50 hours. First evaporation tests with vanadium (vapour pressure: 10^{-2} mbar at 1850°C) into a tantalum crucible were successful (1 mg/h at 200 W for 20 hours). However, the next tests with melted metallic uranium or solid uranium oxide failed. A chemical reaction with the melted uranium destroyed the tantalum crucible.

A on-line version, with a longer copper tube, was built for tests with the ECR 4M source. Despite increasing the DC heating current up to 18 A, we do not observe any constraints on the filament located near the maximum magnetic field of the source.

First tests with lead at low temperatures gave the same performance as those obtained with the standard micro-oven and validated the increase of the diameter of the coaxial tube up to 18 mm. However, tests with vanadium at high temperature failed. Copper peaks appeared in the spectrum. The appearance of the copper tube close to the tantalum reflectors was observed to have changed. Thermal simulations, without RF power, showed that this part of the copper tube could reach up to 840°C. This could explain the difficulties encountered with the tuning of the vanadium beam. Modifications have to be made to increase the cooling of the copper tube. Although the mechanical concept of the heating part has been successfully tested, some improvements are necessary to adapt the oven to the ion source.

III - Uranium beam by sputtering method

The sputtering method has been tested for the production of a uranium beam with a high charge state, i.e. U^{31+} **[2]**. Previous runs using neon as support gas for producing U^{25+} and U^{28+} gave intensities of 2 eμA and 0.8 eμA respectively, but with a high consumption rate, around 7 mg/h. This time the ECR 4M source was tuned for U^{31+} with oxygen as support gas, and could deliver a beam up to 0.5 eμA. The uranium sample (ϕ 5 mm, length 8 mm) was fixed via a copper support at the end of a cooling stainless steel tube. An alumina tube insulated it and centred it in the coaxial tube (Fig. 3).

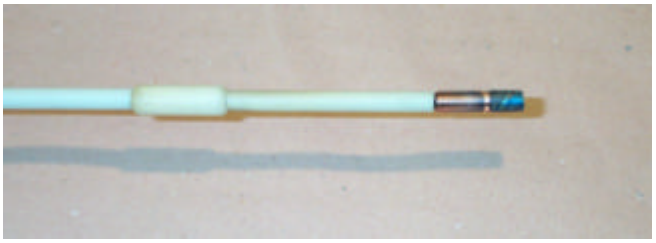

Figure 3: Uranium sample after sputtering with O_2.

A low consumption rate of 0.33 mg/h was measured. However, the ionization efficiency still remained at a low value of about 1%. The main parameters of the source were an RF power of 210 W, an extracted current of 1.1 mA at 16 kV, and 1 kV / 0.76 mA as sputtering values.

Some short tests were done with SF_6 as support gas instead of O_2. The charge state distribution in the spectrum (Fig. 4) then shifted from U^{28+} (800 enA) to U^{24+} (3.5 eμA) but with only 150 W of RF power, and 150 V / 0.5 mA for sputtering parameters. Possibly a process other than sputtering occurred. It could be the formation of UF_6 gas by chemical reaction between uranium and dissociated fluorine. However this effect was not enough to indicate any clear improvement in the uranium intensity.

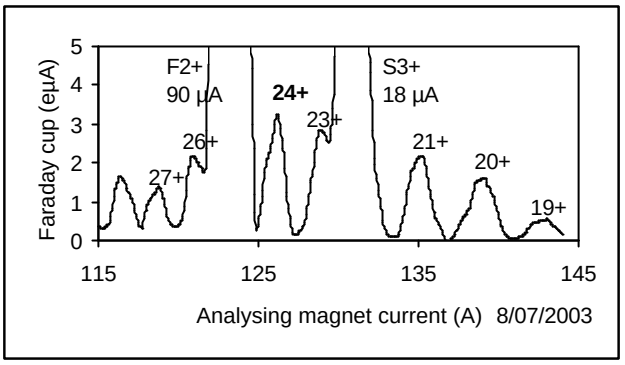

Figure 4: Uranium spectrum optimised on U^{24+}, sputtering with SF6

IV - Large Capacity Oven

A Large Capacity Oven **[2]** has been developed in order to replace the micro-oven used at GANIL since 1985. The same concept is applied with an external diameter of 10 mm (Fig. 5) instead of 5 mm.

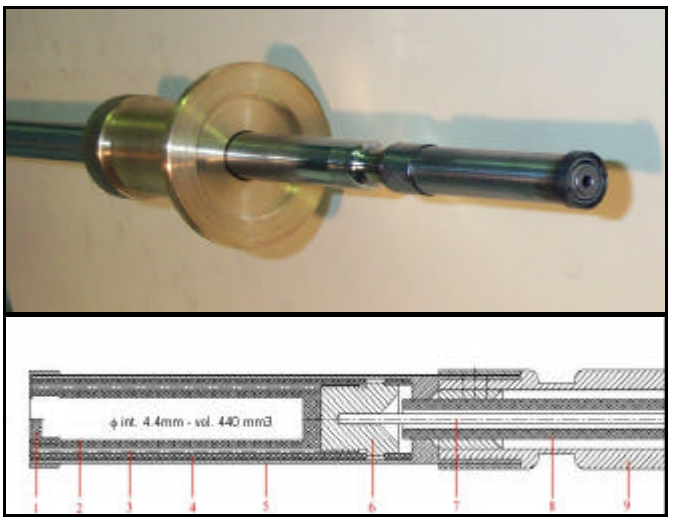

Figure 5: Large-capacity oven.

The bigger capacity allows a longer lifetime, particularly with low-density materials, easier filling of the alumina container, the possibility of safe working with molten materials, owing to a movable cap over the opening. The reliability is also increased, with bigger dimensions of all components. The sample or the tantalum container, when running with enriched metallic ^{48}Ca, is introduced inside an alumina container. The coaxial tube diameter has been increased up to 12 mm, with a minor decrease in the gaseous performance. Characteristics are given in table 1.

	Micro-oven – ϕ 5mm		LCO – ϕ 10 mm	
Container ϕ int. Volume Aperture	1.5 mm 45 mm^3 1.8 mm^2	Al_2O_3	4.4 mm up to 400 mm^3 0.8 to 12.5 mm^2	any material movable cap
Current feed line	1 mm^2	Mo	2 mm^2	Mo
Filament W	ϕ 0.2 mm	Pitch 1 mm	ϕ 0.3 mm	pitch 1 mm
T° max	1500°C	50 w (2.7 A)	1600°C	140 w (6 A)

Table 1: Comparison between the micro-oven and the large capacity oven.

A temperature higher than 1500°C has been maintained for 5 days without any damage (Fig .6). The beginnings of fusion of the alumina container were observed after 12 hours at 1700°C.

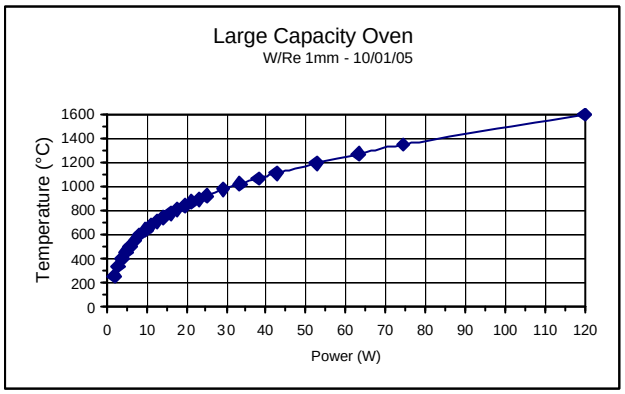

Figure 6: LCO – Temperature versus heating power

Off-line evaporation with calcium, lead, tin and magnesium has been done to measure the evaporation flux rate as a function of the container aperture, of the heating power and of the surface of the sample. In the range of 0.1 to 4 mg/h, the crucible geometry did not disturb the evaporation flux according to the vapour pressure tables. A measurement at the same temperature with an initial weight of lead of 90 mg instead of 30 mg increased the rate of consumption by a factor of about 2, which correlates with the increase of the surface area of the spherical molten lead droplet in the crucible. This surface effect was also roughly verified with a calcium sample. We can thus decrease the operating temperature compared to the micro-oven and also the container aperture could be used to decrease the interaction with the plasma heating.

On-line tests have been successful with lead, calcium, tin and magnesium beams **[3].** With the ECR4 ion source, located on the modified high-voltage platform, **[4]** the beam extracted at 24 kV from the source, is first analysed on the platform, then accelerated to 55 kV and measured after a second bending magnet (transmission from 55% up to 65%). With the ECR 4M source, tuned at 20 kV, the beam intensity is measured in a Faraday cup after the analysing magnet (transmission around 50%). A hot screen was tested to achieve a recycling effect for the elements with a high vapour pressure, like calcium and magnesium, if the RF power is high enough to provide the necessary temperature at the screen. It consists of a 0.2 mm thick tantalum cylinder placed with a 0.5 mm gap from the wall of the plasma chamber. Oven positions into the coaxial tube are given as the distances the back of the plasma chamber. Ionization efficiencies are corrected with the beam line transmission.

Ca beam

On the ECR 4M source, tests have been made with the alumina container (aperture ϕ 2mm), without a hot screen, and then with a tantalum container (ϕ int. 2mm) and a tantalum hot screen in the plasma chamber. The oven heating power was low (< 2 W), and the consumption of calcium of 0.6 to 1.2 mg/h was rather high, indicating a strong interaction with the plasma heating. A stable beam of $^{40}Ca^{9+}$ ~ 30 eμA (Fig. 7) is now available using this new oven.

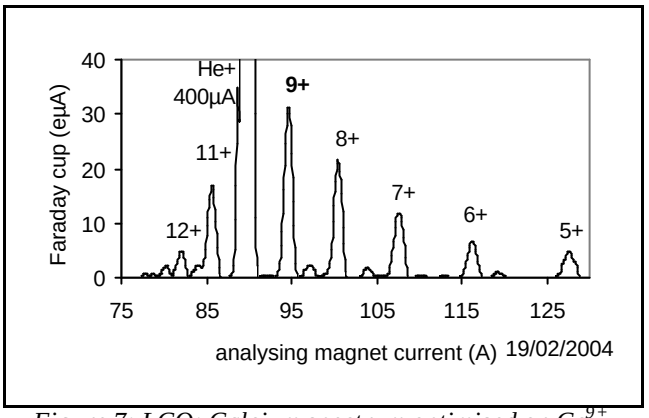

Figure 7: LCO: Calcium spectrum optimised on Ca^{9+}

More tests are needed to reach a ionisation efficiency better than 4% (average intensity 18 eμA) and the oven position should be moved back. On ECR 4, the oven power (6 W) and the consumption rate of 0.2 mg/h indicated a small interaction with the plasma. This led to an ionization efficiency of 8% (average intensity 10 eμA).

In both cases the ovens were positioned at 0 mm, and the RF power of 160 W was too low to obtain the temperature needed on the hot screen to get a recycling effect.

Mg Beam

For Mg beams, the alumina container is filled with 90 mg of natural metallic magnesium and closed with a stainless steel cap (aperture ϕ 1mm). The metal must be silvery-white, without impurities on its surface, to achieve the expected evaporation rate according to the vapour pressure tables. ECR 4M was equipped with a hot screen, and a very

high ionization efficiency of 14% was achieved with an average beam intensity of 48 eμA for $^{24}Mg^{5+}$ (Fig. 8).

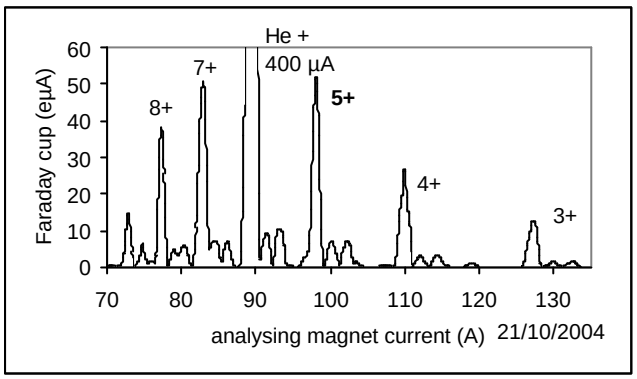

Figure 8: LCO: Magnesium spectrum optimised on Mg^{5+}

Nevertheless, the increase of the efficiency due to the hot screen could not be established clearly. The RF power was 230 W, the oven power heating 0.6 W and the magnesium consumption 0.75 mg/h. It seems that the back position of the oven, i.e. at -20 mm, allows better control of the evaporation rate.

Tin beam

Taking into account the low vapour pressure of tin, the position of the oven in the ECR 4M ion source was chosen to be closer to the plasma, i.e. +7mm, and the aperture of the alumina container enlarged up to 9 mm^2. This tantalum half-cap retained the 150 mg of natural metallic tin melted in the container. A stable beam of $^{120}Sn^{21+}$ of 3 eμA remained for 4 days at 20 W oven power, and was then increased up to 8 eμA (Fig. 9) for 3 days, when the oven power was increased from 25 W to 34 W. A high ionization efficiency of 14% was measured during the first period. The RF power was 275 W and the magnesium consumption 0.11 mg/h. From a filament current of 2.5 A, the filament resistance dropped slowly, and then faster and faster. At the end of the experiment many of the filament turns were short-circuited. These were located at the front of the oven where the axial magnetic field is a maximum, about 12000 gauss. The electromagnetic forces on the filament are lower in the back of the oven where the axial magnetic field is only 5200 gauss . Above a certain value this leads to deformation of the coil turns. A first test using a current power supply at 400 Hz showed that this could be a solution..

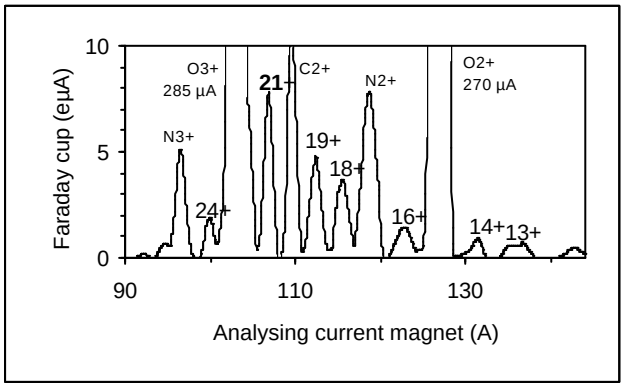

Figure 9: LCO: Tin spectrum optimised on $^{120}Sn^{21+}$

Lead beam

Tests have been made with the ECR 4M ion source, using an alumina container (aperture ϕ 2mm), filled with 30 mg of ^{208}Pb isotope. The RF power was 210 W, the oven heating power 4 W and the lead consumption 0.17 mg/h. An average beam of $^{208}Pb^{24+}$ ~ 8 eμA, has been obtained with an ionisation efficiency of 14%, although with a very advanced position of the oven, i.e. +18 mm (Fig. 10).

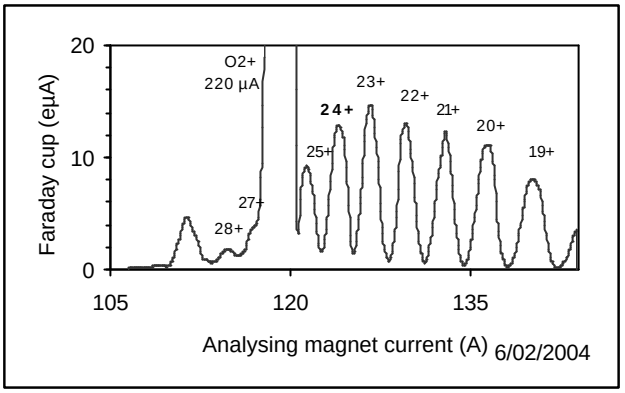

Figure 10: LCO: Lead spectrum optimised on $^{208}Pb^{24+}$

IV - MIVOC Method

In collaborating with chemistry department of the university, LCMT–ENSI Caen **[5]**, the synthesis of ferrocene and nickelocene with enriched isotopes has now been made available for GANIL's users. The chemical transformation yield should be greater than 80%. The synthesis of magnesocene is being studied.

A $^{24}Mg^{5+}$ beam was produced from natural commercial magnesocene, $Mg(C_5H_5)_2$, in the following manner. About 840 mg of compound was placed in the MIVOC chamber using an argon-filled box to avoid contact with air and moisture. The argon filled box is recommended with nickelocene, but indispensable with magnesocene. The compound was outgassed for one hour at a residual gas analyser until the Mg (mass=24), $Mg(C_5H_5)$ (mass=89), and $Mg(C_5H_5)_2$ (mass=154) peaks became greater than impurities like C_5H_5 (mass=65). If not, the appearance of the magnesium beam could take even longer than the two hours necessary to obtain a stable beam.

On ECR 4M ion source at 20 kV, the test time was only 2 days, nevertheless an easy tuning of the source and a very high ionisation efficiency, 24%, were achieved. The average consumption rate of $Mg(C_5H_5)_2$ was 3 mg/h with an average beam intensities of $^{24}Mg^{5+}$ and $^{24}Mg^{7+}$ of 48 eμA and 32 eμA, respectively.

On ECR 4 ion source on the new high voltage platform at 79 kV, the Mg beam gave the following results :

$^{24}Mg^{5+}$ = 105 eμA , $^{24}Mg^{7+}$ = 50 eμA without hot screen ($Mg(C_5H_5)_2$: 4 mg/h) [see spectrum page 57]

$^{24}Mg^{5+}$ = 110eμA , $^{24}Mg^{7+}$ = 40 eμA with hot screen ($Mg(C_5H_5)_2$: 3.6 mg/h)

As with the LCO, the increase of the efficiency due to the hot screen was not measured, although less deposits were observed on the hot screen than on the plasma chamber wall. Nevertheless the production of magnesium beam seems to be easier to do with the MIVOC method than with the oven .

[1]-P.Lehérissier et al., Nucl. Instrum. Meth. Phys. Res. A 211/2 (2003) 274.
[2]-P.Lehérissier et al., Rev. Sci. Instrum. 75 (2004) 1488.
[3]-P.Lehérissier, C.Canet and F.Lemagnen - GANIL-SDA-GPI-259 (2004).
[4]-C.Barué et al., – This report.
[5]-P.A.Jaffres - see http://lcmt.ensicaen.fr.

Linux migration of the Ganil control system

Groupe Informatique Machine

Abstract

For almost ten years, the Ganil control system has been based on VMS workstations and Camac/Vme crates running Vaxeln on RtVax controllers, with Ada as common language, and Ingres as the relational database management system.
When Digital Equipment (now HP-Compaq) gave up with RtVax processors, we decided to move to Vme crates with PowerPC controllers running VxWorks.
The last rejuvenation of the system was the migration to Linux, providing a commonly used environment and also allowing us to use some free software tools that weren't very powerful in a Vms/Motif environment.

This paper describes the milestones we performed :

- Graphical user interfaces using Motif with XRT widgets
- Database access with Ada / SQL requests
- TCP/IP communication with VxWorks real time crates

1 The legacy control system

When it was defined in the early nineties, the control system was based on Vax workstations and VMS servers, programmed in Ada.
The front-end level was made with Camac crates using RtVax microprocessors.

When Dec decided to stop the Vax family, we began to replace the Camac crates by Vme with PowerPc processors, and we moved from VaxEln system to VxWorks, using Ada95 (object oriented) instead of Ada83.
At this time the network, which was a 10B2 daisy chain, was replaced by a 10BT structure, with bandwidth switching at 10 Mb/s speed linked to the external national research network.

1.1 Software

The control system is built upon several levels :

- The graphical user interfaces, used for the beam tuning programs are Motif based with XRT commercial widgets and the algorithms are written in Ada,
- The relational data base Ingres, used by all the programs accessing to the parameters of the beams and to the characteristics of the 4500 devices involved into the accelerator control,
- The network communications using TCP/IP sockets, between the operator consoles and the real time crates, with a client mode on the workstations and a server mode on the crates,
- The drivers for the devices on the Vxworks crates, also programmed in Ada.

1.2 Development tools

The Ada programs were developed on a Vms server, with an X terminal for each programmer.
Concerning the real time tools, the Aonix Ada cross compiler was running on Windows PCs.
The offline programs for beam parameters calculations were written in Fortran.

2 Evaluations

The aim of this upgrade was to install a solution with new technologies, that can easily evolve in future and to have cheaper operator consoles than the commercial workstations, which means to choose PCs.
Concerning the operating system, the choice was between Linux and Windows. Linux was chosen for the accelerators controls because of reliability reasons and its wide use among the accelerator control community. It was also easier to move the control programs, keeping the same Motif graphical interfaces. Another reason was the compatibility with Epics, which is a possibility for the Spiral2 project.

Windows was reserved for the supervision interfaces of the Programmable Logic Controllers, with Panorama, commercial software widely used in Ganil, only available on Windows.

3 Hardware upgrades

3.1 Client server architecture

The new control system is built over a cluster server for common services, and PCs clients are used for the beam tuning in the main or auxiliary control rooms.
Several links have been established with the office desktops and the Intranet, so that all the measurements from the accelerator devices, which are archived on the server, could also be read by Windows clients and displayed on the Intranet with all the accelerators information.

The development software is made on other PCs, Linux or Windows.

The Vme crates were kept as before, but the Aonix cross compiler was changed for the Gnat compiler and the upgrade of the processors towards a new generation will be evaluated later.

3.2 The cluster server

To provide high availability capabilities on the server, a failover cluster architecture has been configured based with the HP Service Guard package beside of the Red Hat Linux toolkit.
So the main server is set up with two similar nodes, working in this cluster mode.

If one of them stops, the services running on it can move to the other server.

To get more reliability, the disks are in an external cabinet, connected through two optical switches, so that both of the servers can use these disks.

To make sure that the redundancy is effective, all the links are always dual, even for the switch and the disk controller. In case of failure, the second link will be automatically activated and the disks will still remain available.

These disks are mirrored in two different racks, so that a disk failure won't have any consequence on the data integrity. Two other racks are planned in the same cabinet to be connected to a future Windows cluster for the office work.

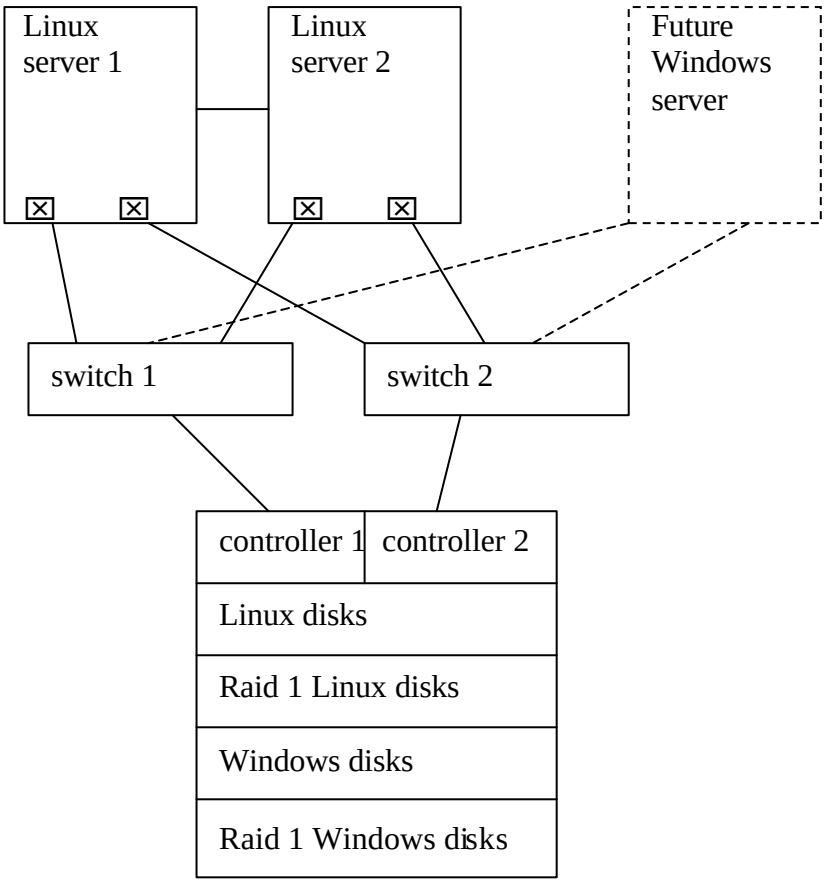

3.3 The operators PCs

New dial boxes with shaft encoders have been studied and produced for the operator PCs. They have the same function as the old ones, but with an USB output, so they can be connected to laptop PCs or to new PCs without any serial port.
All these PCs are strictly the same, each of them with a dual channel graphic card, one VGA and one DVI, to drive either two flat TFT screens, either both one CRT and one TFT.
On the new flat screens, the pixel definition is linked to the size of the screen, so if the definition is decreased to obtain large windows, the graphical aspect is worse.

21" TFT screens with 1600x1200 pixels will display smaller windows than 19" with 1280x1024 pixels. So the screens in the control room are TFT 19", until the availability of a new generation or changes in our graphical software to display larger windows on any screen.

3.4 Development PCs

Each member of the Computer group and of the Beam tuning group, working on Windows PCs, also needs to use the Linux server for parameters calculations or Ada compilations.
An X emulator on Windows was tried to make connections to the Linux server with graphical display, but a problem appeared : the XDM server on the cluster prevented to perform the switch of the NFS package from one node to another.

So the PCs with the X emulator Cygwin are now connected to an X server on a front node, with SSH access to the cluster. So there isn't any X server blocking the NFS package as described above.

For simple commands, the so-called Putty utility on Windows allows to open a terminal window with a secure protocol. It could also be used during external interventions through ADSL connections.

3.5 Network

The network has been separated in two different TCP/IP subnets : one is public for the office work while the other specific for the control is hidden from the Internet networks.
The control network is based over two main and three remote Gigabit switches (one for the injector area, one for the Spiral area and one for the instrumentation gallery).

In the control room, the Linux servers and PCs are plugged on the main switches, with unshielded twisted pairs (UTP). In the remote areas the Vme crates can be connected with 100 Mb/s UTP links while deported PCs are reached through UTP Gigabit links. Lastly, office and control networks are connected to the other Ganil networks by a Gigabit optical fiber link.

4 Software upgrades

4.1 Common services

The cluster is used for two main functions : the control of the accelerator and off line services such as the development of the Ada programs, the Intranet server, the printing server and the file access from the windows clients. So each server runs a separate database system, one for the control and the other one for the development.
Except the databases that have direct access to the disks, the other services perform disks access as clients of a central NFS service on the development server.
On the control server, common services are always running and restart in case of failure :

- Ingres database server for the requests from the control programs, the alarm server …
- Alarms display, sent by the Vme crates or the tuning programs
- Several data collectors, which read a list of devices on the Vme crates and keep the measurements in memory. So the different requests issued by all the clients won't create as many network connections as applications having to reach those devices
- Data collectors dedicated to external clients from the control system, such as the acquisition process for the identification of exotic ions, or the standalone irradiation target control
- Periodical archiving of measures on most of devices of the accelerator, so that they can be displayed on Windows PCs later
- Downloads of the front-end databases with the devices characteristics, needed by the Vme crates
- On-line display of the accelerator status, generated by HTML sheets and broadcasted by a web browser and a video network

On the development server, off-line services are running :

- Ingres development database (preparation of the beams to be accelerated, beam statistics, …)
- Cups printer server
- Apache web server
- Samba server to give file access for the Windows PCs
- Nfs server for remote access from the Linux control PCs
- Gnat compiler, with the GPS graphical tools

All these services can move from one node to the other, if the first node stops or shutdowns.

4.2 Databases

The Ingres relational database management system is involved into the whole control system so being the core of the system. It deals with the front-end real-time crates configuration, the pieces of equipment definition and specification, the alarms archiving system, an electronic log-book for the machine operation, the on-line configuration of the machine status, the dynamic beam parameters management, the beam optics definition and the links with the off-line computing programs.
The Ingres software has been configured to be fully integrated into the cluster environment adopted for the servers. Therefore, two different Ingres installations are running at the same time ; a first one is used in an off-line mode for the beams preparation or the pieces of equipment configuration while the second one is devoted to the on-line control of the accelerators. Each of these two Ingres servers is normally run on each of the two nodes but in case of failure they are able to be executed simultaneously on the same node.

In addition, the Ada / Sql gateway between the beam tuning programs and the Ingres database has been migrated from the Ada 83 Vms compiler to the Gnat Ada 95 environment within the Linux operating system, so being able to keep most of the existing code (more than 200 Ada / Sql procedures have been developed previously).

Applications written in alphanumeric mode (such as the uploading procedure for the output data from the off-line computing program or the preparation of the set of beams to be accelerated) have been migrated into this new environment. Specific graphic applications developed within the OpenRoad environment are also available into this new context, allowing people to configure any piece of equipment, to retrieve archived alarms according to various criteria or to update the on-line machine operation logbook. Lastly, Intranet access using a PHP gateway gives users the ability to access the beam parameters database or to manage the list of the specific recommendations or warnings for the daily accelerator operation.

4.3 Tuning beam programs

On Vms the fifty beam tuning programs were developed with the Motif graphical user interface, so that they could have been moved to Linux with few changes inside their source code, only in a year instead of several if all of them had to be rewritten completely.
Later, this library could be replaced, because of the lack of evolutions and functions only available in newer standards such as GTK, which will be necessary for new projects.
The Vms system procedures calls which were already embedded in Ada packages have been modified to fit to the Linux run-time.
The Gnat compiler includes a project manager, source oriented, that needed to reorganize the tree structure of all the program files, including binaries or data associated with each of them.

4.4 Off line parameters

Some of the beam parameters calculations are made off-line by Fortran programs such as Galop or Param. A reduced release of Galop has been moved to Linux, without the Cern and Nag libraries. This program is running fine, and the next milestone is to install a full size development workbench including the Cern libraries on the development server.
The Param program, based on a lot of different generations and writers procedures, has been moved without any change, keeping data access through flat files instead of migrating them into the Ingres database.

4.5 Epics binding

In the Spiral2 project, several Vme crates running Epics are planned to be installed by the Dapnia, for the primary beam control.
Within this context, Epics, which was developed by a community of American laboratories, is built over VME front-end controllers (IOC) with I/O slots embedded into Vxworks crates and graphical interfaces (OPI) on Linux PCs.

The procedures available to get access to the devices (Channel Access) are written in “C”. An Ada binding has been developed to interface these Epics client procedures. So it will be possible, from the current control system, to get access to the Epics Vme crates running an Epics server for specific devices control such as the RFQ or the ion sources. For the exotic beam lines, the Ada control system used for the Cime cyclotron will be extended and the Epics binding described above won’t be necessary.

A training PC for has been installed by the Dapnia/SIS team and an initiation class was performed.
If more specific tests are needed, the graphical Epics tools (MEDM) will have to be used and learned by the Ganil programmers, although based on Motif. Also, according to the size of the Spiral2 project, a relational database will have to be considered and designed later in this Epics system.

4.6 Real time

The real time programs, running on the front end crates, have also been changed, to follow the new beam tuning interfaces and central services (alarms and database downloads).
A new Ada cross compiler for Vxworks, GnatPro, was installed on Windows, with a project oriented manager GPS providing the same environment as the native Linux one. So the communication packages and the interrupt handling have been modified to fit this new system surrounding. Later a new release of Vxworks and associated tools will allow the programmers to develop either from Windows or from Linux.

5 Conclusion

The basic access to the accelerator devices were tested during the last run of year 2004 with a Linux console operated among the existing Vms environment. So during the winter shutdown period, the servers were set up, and the 30 operators PCs were installed and connected to the network. As the algorithms had not been changed, the beam tuning programs were all tested in the first two weeks of accelerator restart in early 2005.
From the operation point of view, the functionalities have been kept and the operator interface is the same as in the previous control system ; one major feature to be noticed is the response time improvement, mainly for the database access for all the beam parameters management.

The total cost of the project has been kept to, and the complete move to Linux has been achieved one year sooner than expected. This year will be useful for the primary tests of instrumentation over the Spiral2 project, concerning first the R-F amplifiers, and larger tests with the Epics binding if necessary.

With this new Linux control system, it becomes easier to add other control PCs in remote control rooms, dedicated to specific beam lines. Recently two auxiliary control rooms were added for the low energy beams (Irrsud for stable beams and Lirat for exotic beams) and linked to the main control system.
The next step will be the control of the Spiral2 project and its integration with the existing control system.

4

EVOLUTION OF THE FACILITY

The new high-voltage platform of the injector C01

PFI1 project

contact person : barue@ganil.fr

1) The reasons for a high voltage platform

The high-voltage platform used to inject the beam into the injector cyclotron C01 has been built in order to increase the primary beam intensities (operation O.A.I.). The beam extraction at 100 kV from the source leads to a beam emittance a factor of two lower compared to that of the injector C02 where the beam is extracted at 25 kV. Therefore the transmission through the cyclotron C01 is improved, with typically 50% transmission for C01 and 25% for C02.

2) Description of the old platform

At such a high potential, all source equipments must be placed on a high-voltage platform as represented in Fig.1.

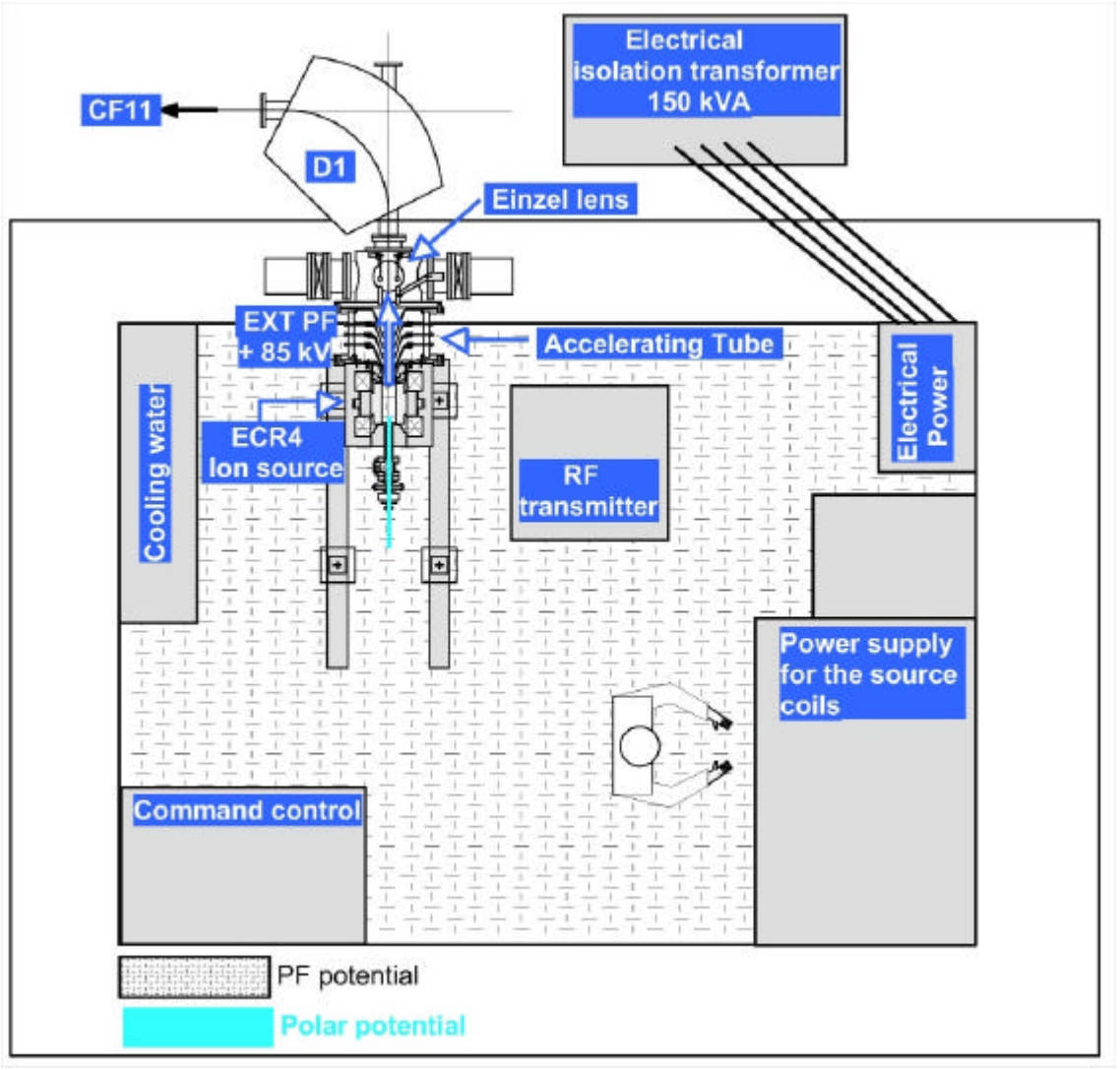

Fig 1. The old platform.

The accelerating tube has 4 electrodes polarized with the help of one 100 kV power supply and a set of resistances. All charge states escaping from the plasma source are accelerated by the tube. The required charge state for acceleration is selected by the dipole magnet D1 at ground potential. The einzel lens is necessary to allow the beam to pass through the dipole D1 with minimum losses. The typical transport efficiency from the source to CF11 is 80%.

3) Performance limitation with the old platform

Despite destructive sparking at the beginning inside the accelerator tube, the platform had been made reliable and operational, but with some limitations.

Due to the numerous (and useless) charge states in the accelerating tube, the total current from the source had to be limited to 2.5 mA. At this level, uncontrollable discharges occur in the tube and lead to a strong defocusing of the beam making the beam unsuitable for the physicists. For similar reasons, the platform potential had to be limited to 85 kV.

- **The limitation at 85 kV**: higher charge states are required for acceleration. For example, charge state 10+ is required to accelerate an ^{36}Ar beam to the maximum energy whereas charge state 9+ (with twice the intensity from the source) is required at 100 kV.
This is also the case for ^{36}S : twice the intensity from the source at 100 kV (q=8) compared to 85 kV (q=10).
For some elements, increasing the extraction voltage does not improve the beam intensity. This is the case for accelerating a ^{48}Ca beam to the maximum energy : q=10 was required with the old platform, and was the optimum charge state produced by the source.

- **The limitation of the total source current at 2.5 mA**: impossible to increase the beam intensity further for some elements. This is the case for metallic beams produced by the MIVOC method where the total source current could reach 5 mA.

4) The new platform

In order to overcome these limitations, different solutions have been investigated :

(1) placing a solenoid between the source and the accelerating tube, in order to decrease the total beam intensity accelerated by the tube.

(2) placing a dipole upstream the accelerating tube, in order to accelerate only the required charge state.

As the total beam intensity sent into the accelerating tube is much reduced in the second configuration, this second solution has been approved.

The new platform is shown in Fig. 2. All charge states are extracted from the ion source at 25 kV and a solenoid (SOL0) focuses the required charge state at the focal point of a double focusing magnet (D0). At the faraday cup CF0, the beam has an energy of 25 keV/q. The selected charge state is then extracted from the platform at 75 kV by the existing accelerating tube (EXT PF). At the position of the faraday cup CF11, the beam has therefore an energy of (25+75) keV/q.

The limited place available on the platform (3m x 4.2m) was the major constraint for the feasibility of the modification. A solution has been found by using "switch mode" power supplies. Their compact size made the modification possible:

- injection coil of the source : 1300 A / 65 V / 84.5 kW (60 cm width)
- extraction coil of the source : 1300 A / 65 V / 84.5 kW (60 cm width)
- dipole and solenoid : 250 A / 40 V / 10 kW and 400 A / 50 V / 20 kW (60 cm width)

For the same reason, the dipole D0 had to be made more compact. It has been designed with a radius of only 20 cm. The resulting low A/q resolution of the dipole only permits us to make A/q-resolved spectra for elements slighter than argon. For heavier elements, the analysis must be done at the CF11 position to separate the different A/q values.

The Faraday cup CF0 and a set of slits are located in a movable diagnostic box allowing easy access inside the accelerating tube. It allows a quick change of the two first electrodes of the tube, for example to investigate the best shape and size of the electrodes.

The electrical power has been increased by a factor of two. A new 300-kVA isolation transformer has been installed. This change was justified by the electrical power needed for the dipole and the solenoid : the 150-kVA power of the old transformer was too low. Moreover, the higher available power will make possible the use of more powerful sources, such as "Supershypie" developed at GANIL.

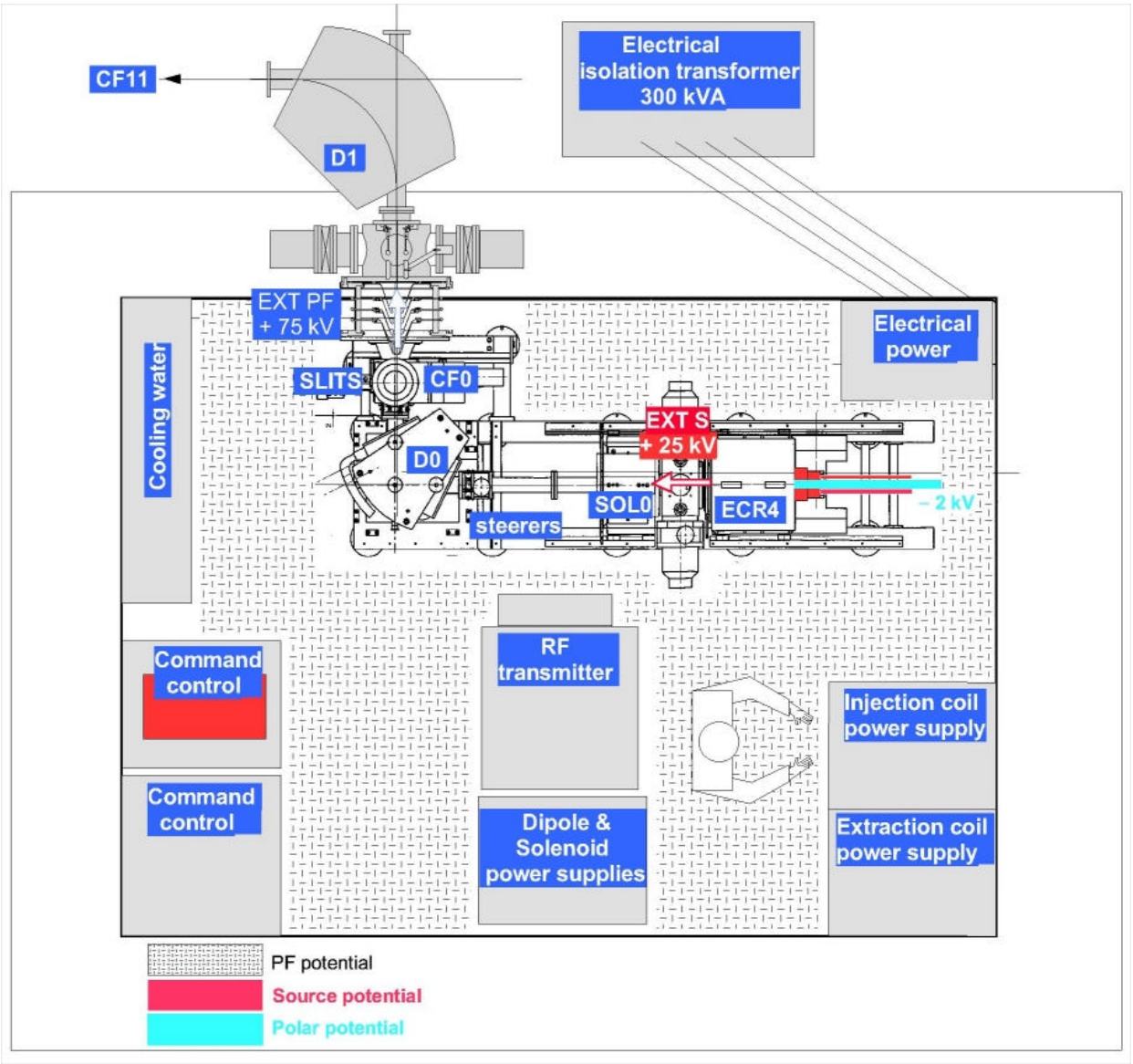

Fig. 2 The new platform.

A brief history of the high voltage platform of the injector C01:

– November 1989 : start of the construction of the old platform
– March 1991 : first available beam with the old platform
– March 2001 : solution 2 approved for the new platform
– January 2003 : modification delayed 1 year due to the unavailability of the injector C02 (replacement of the cavity of the cyclotron C02)
– January 2004 : start of the modification
– June 2004 : first available beam with the new platform (^{48}Ca)

Some pictures of the modifications:

Top Left: the platform after removing all equipment; **Top Right**: laying of the ground plates
Bottom Left: installation of the beam line; **Bottom Right** : the platform after installing all equipment.

5) First results

An intensity of 160 µA for Ar^{9+} has easily been obtained after only a few days operating the new platform, but with low transmission (60%) between CF0 and CF11. Due to the scheduled planning, we had to stop investigations and to make the platform available for physics. Despite the low transmission, the new platform provided the first beam (^{48}Ca) for physics in June 2004.

The next beam was ^{13}C for SPIRAL. After three weeks of operation with ^{13}C, we have observed visible sputtering impacts on the first electrode of the accelerating tube (see picture below).

Sputtering impacts on the first electrode of the accelerating tube.

No clear conclusion could be drawn, but obviously the beam did not fit well within the 10mm hole of the first electrode. Placing a $Si0_2$ target at this location and looking with a CCD camera could help with understanding the problem. It has therefore been decided to replace the two first electrodes of the accelerating tube by two bigger electrodes: the hole diameters increased from (10 mm, 13 mm) to (15 mm, 20 mm). With this new geometry the transmission of Ar^{9+} from CF0 to CF11 has been increased from 60% to 80%.

Three steerers have been placed between the solenoid and the first dipole, in order to compensate for steering effect on the beam.

The solenoid position has been investigated briefly, and it seems that the best position is close to the extraction source.

It should be mentioned that the einzel lens is no longer necessary to transport the beam up to CF11.

6) Results for calcium

The beam intensity and ^{48}Ca consumption obtained during the run were similar to those obtained with the old platform. No gain in intensity was expected for this beam (see chapter 2).

It should be mentioned that excellent beam transmissions have been measured as shown in Fig. 3.

	16 keV/u	C01	0.65 MeV/u	CSS1	9.1 MeV/u (stripper)	CSS2	60.3 MeV/u
June 17th, 2004		62%	84%	98%	43%	95%	=> 21%
48Ca 10 + 19 + 60.3 MeV/u	11.6 µA	7.2 µA	6.05 µA	5.9 µA	4.86 µA		4.6 µA
48Ca 65% enriched							0.24 pµA
HT_S = 24 kV , HT_PF = 52 kV							1.45E+12 pps
=> 76 kV							701 W

Fig. 3: Best ^{48}Ca transmissions measured with the new platform.

7) Results for carbon

An intensity of 90 µA for $^{13}C^{3+}$ has been easily obtained on CF11 with a good stability. A beam power of 4.3 kW has been obtained (the mean power was limited to 3 kW for safety reasons). No time was left to investigate further the maximum intensity possible from the source. We have noticed a lower transmission compared to argon: ~ 70 % from CF0 to CF11.

8) Best results for argon

An intensity of 253 µA for charge state 9+ has been obtained at the CF11 position. Compared to the old platform (100 µA Ar^{10+}), the available intensity from the source is 2.5 times higher.

Although this intensity is too high to be sent in the accelerator, the beam from the source could be reduced in emittance by a set of slits in order to minimize the losses in the accelerator : 100 µA corresponds to a 6-kW beam (36Ar at 95 MeV/u).

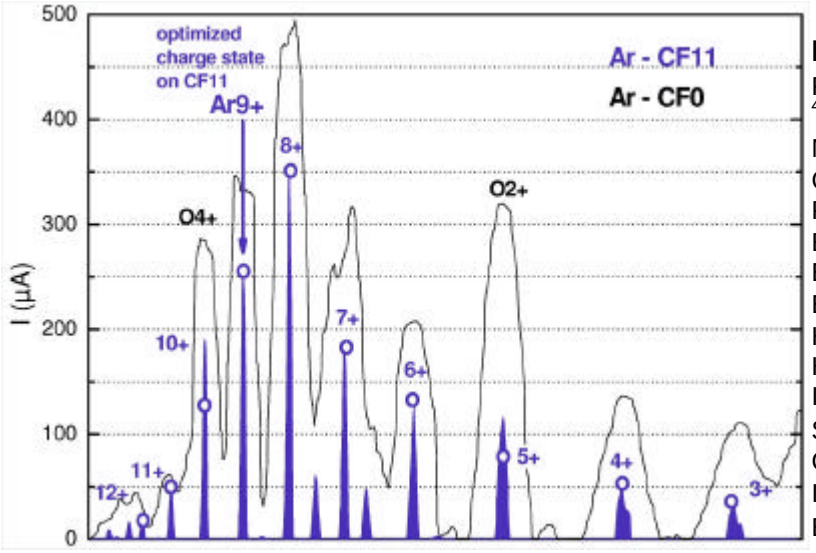

Fig. 4 Best result for $^{40}Ar^{9+}$

February 16th, 2005

$^{40}Ar^{9+}$	: **253 µA CF11**
Mixing gas	: O_2
CF0 & CF11	: – 300 V
PHF	: 600 W
Binj	: 1090 A
Bext	: 1000 A
Biased tub	: – 140 V / 0.60 mA
HV Source	: 24 kV
HV Platform	: 55 kV
IHT source	: 3.3 mA
Source -> CF0	: 73 % (Σq)
CF0 -> CF11	: 73 % (9+)
Injection	: 9 10^{-6} mbar
Extraction	: 2 10^{-7} mbar

Both spectra at CF0 and CF11 location are represented in Fig. 4. The low resolution spectrum obtained at CF0 is evident.

It should be mentioned that this spectrum was obtained with a tantalum screen inside the plasma chamber, after a few days of operation with magnesocene.

9) Best results for krypton

	18 keV/u	C01	0.75 MeV/u	CSS1	10.4 MeV/u (stripper)	CSS2	70.4 MeV/u
October 3rd, 2004		51%	67%	96%	40%	90% =>	12%
78Kr 15 + 33 + 70.4 MeV/u	30 µA	15.2 µA	10.2 µA	9.8 µA	8.6 µA		7.7 µA
78Kr 99% enriched							0.23 pµA
HT_S = 25 kV , HT_PF = 70 kV							1.40E+12 pps
=> 95 kV							1281 W

Fig. 5: Best ^{78}Kr transmissions measured with the new platform.

The maximum beam power produced with the old platform was ~ 800 W at 68 MeV/u. The charge state required for acceleration was 15+. With the new platform the beam power has been increased up to 1280 W, and at higher energy.

10) Best results for magnesium

A magnesium-24 beam has been produced using the MIVOC method (using $Mg(C_5H_5)_2$). Natural magnesium was used (79% 24Mg). The best intensity on CF11 was 105 µA for $^{24}Mg^{5+}$ and 50 µA for $^{24}Mg^{7+}$. Spectra are shown in Figs. 6 and 7.

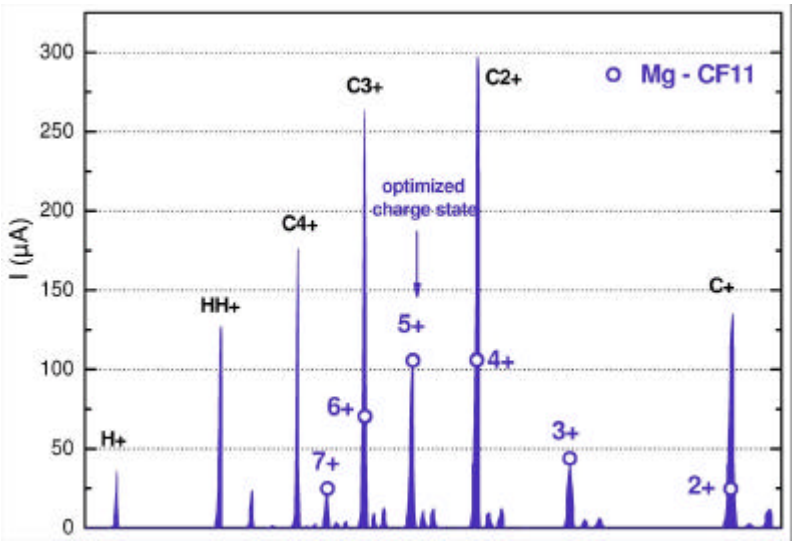

Fig. 6 Best result for $^{24}Mg^{5+}$
January 26th, 2005

$^{24}Mg^{5+}$	: **105 µA CF11**
CF0 & CF11	: – 300 V
PHF	: 160 W
Binj	: 1050 A
Bext	: 1000 A
Mivoc valve	: ~ 300 mbar L/s
Biased tube	: – 56 V / 0.0 mA
HV Source	: 24 kV
HV Platform	: 55 kV
IHT source	: 3.8 mA (Σq)
CF0 -> CF11	: 70% (5+)
Injection	: 4.2 10^{-6} mbar
Extraction	: 2.2 10^{-7} mbar

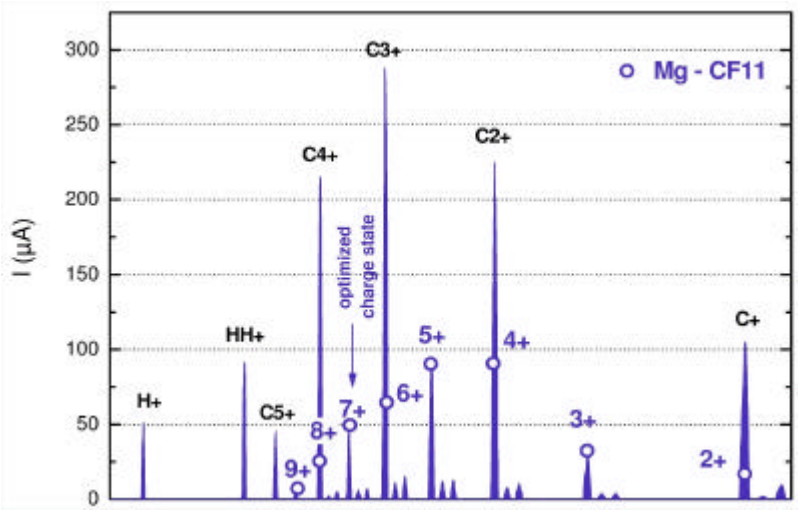

Fig. 7 Best result for $^{24}Mg^{7+}$
January 28th, 2005

$^{24}Mg^{7+}$	: **50 µA CF11**
CF0 & CF11	: – 300 V
PHF	: 300 W
Binj	: 1050 A
Bext	: 1000 A
Mivoc valve	: ~ 200 mbar L/s
Biased tube	: – 105 V / 0.0 mA
HV Source	: 24 kV
HV Platform	: 55 kV
IHT source	: 3.1 mA
Source -> CF0	: 58% (Σ q)
CF0 -> CF11	: 77% (7+)
Injection	: 2.8 10^{-6} mbar
Extraction	: 1.9 10^{-7} mbar

These intensities are similar to those obtained with the ECR4M ion source of injector C02 at the CF2 position. With the new platform it will be now possible to use the source at high total current (~ 4 mA) and the expected gain in intensity for the accelerated primary beam is a factor two. This has still to be measured. For details about the magnesium beam developments see, the article "improvements on stable beams from ECRIS" in this report.

11) Best results for sulphur

An intensity of 42 µA for $^{36}S^{8+}$ ($^{36}SF_6$ 65% enriched) has been obtained at CF11. This beam has been accelerated at 77.5 MeV/u and a beam power of 3.2 kW has been obtained. It represents a gain intensity of 2.1 compared to the old platform.

The stability was very good as can be seen in Fig. 8.

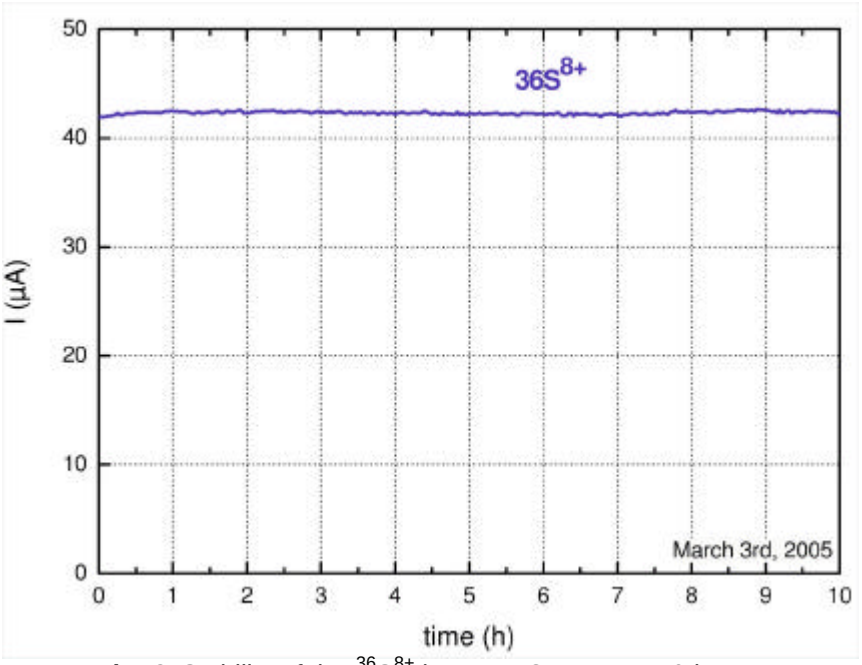

Fig. 8: Stability of the $^{36}S^{8+}$ beam at CF11 over 10 hours.

	20 keV/u	C01	0.82 MeV/u	CSS1	11.4 MeV/u (stripper)	CSS2	77.5MeV/u
March 7th, 2005		50%	67%	95%	79%	94%	=> 24%
36S 8 + 16 + 77.5MeV/u	38.4 µA	19.3µA	12.9µA	12.3µA	19.4µA		18.2 µA
36S 65% enriched							1.14 pµA
HT_S = 25 kV , HT_PF = 64 kV							6.83E+12 pps
=> 89 kV							3174 W

Fig. 9 Best ^{36}S transmissions measured with the new platform.

12) Conclusion

The discharges in the accelerating tube have completely disappeared with the new platform. It is now possible to increase the source intensity above the old limit of 2 mA. It should be a great benefit for metallic beams produced by the MIVOC method where the total source current could reach 5 mA. Results are not yet available, as the platform is in constant use for operation. A gain in intensity of a factor 2 is expected for these elements. For example, it should be possible to reach a beam power of 3 kW for magnesium.

Krypton and sulphur beams have been accelerated to 70 MeV/u and 77 MeV/u respectively. Compared to the old platform, the gain in intensity is 1.6 (at 1.3 kW) for krypton and 2.1 (at 3.2 kW) for sulphur.

Since the ion source can be isolated from the accelerating tube by a vacuum valve, the time needed to make the source operational after a plasma chamber replacement is reduced by a factor 2 compared to the old platform, needing just one day instead of two.

Almost all groups of the SDA (accelerator sector) and SST (technical sector) have participated in the modification of the high-voltage platform. The project leader thanks all those involved in the project for the work performed.

LIRAT
A VERY LOW ENERGY BEAM LINE FOR RADIOACTIVE IONS

F. Varenne

The availability to produce radioactive species with SPIRAL since 2001 opened a new field of investigation at GANIL for an interdisciplinary scientific community, interested in the use of ions at few keV. The LIRAT project was designed for this purpose. Now a technical reality, LIRAT is ready to produce, next spring, its first radioactive beam.

1. Introduction

Interest in low energy physics with radioactive species at GANIL was first presented by Bertram Blank (CENBG) at the time of the Scientific Council meeting in December 1998. A technical report (R-00-01) and two other presentations to the Scientific Council followed in 2000 and 2001. After receiving positive recommendations, a project team led by Alain Péghaire (GANIL) was set up in February 2001, forming the beginning of the LIRAT project.

The year 2001 produced a first technical proposal. Unfortunately, budget constraint and technical difficulties led the project team to reduce its ambitions drastically, and at the end of 2002, a second simplified technical proposal was accepted by the GANIL authorities.

The LIRAT project, initially foreseen to permit the delivery of all radioactive beams from SPIRAL to various experimental areas was reduced to a 10-metre long beam line coupled with dedicated experimental apparatus, for only four authorized ion species (^{6}He, ^{19}Ne, ^{32}Ar and ^{35}Ar) and one user. The beam line was constructed in 2003 and first beam tests were realized in 2004.

Figure 1 shows the implementation of LIRAT in the SPIRAL basement area.

This document gives a brief technical presentation of the LIRAT facility (beam line and experimental apparatus) and its commissioning starting with stable ions during 2004.

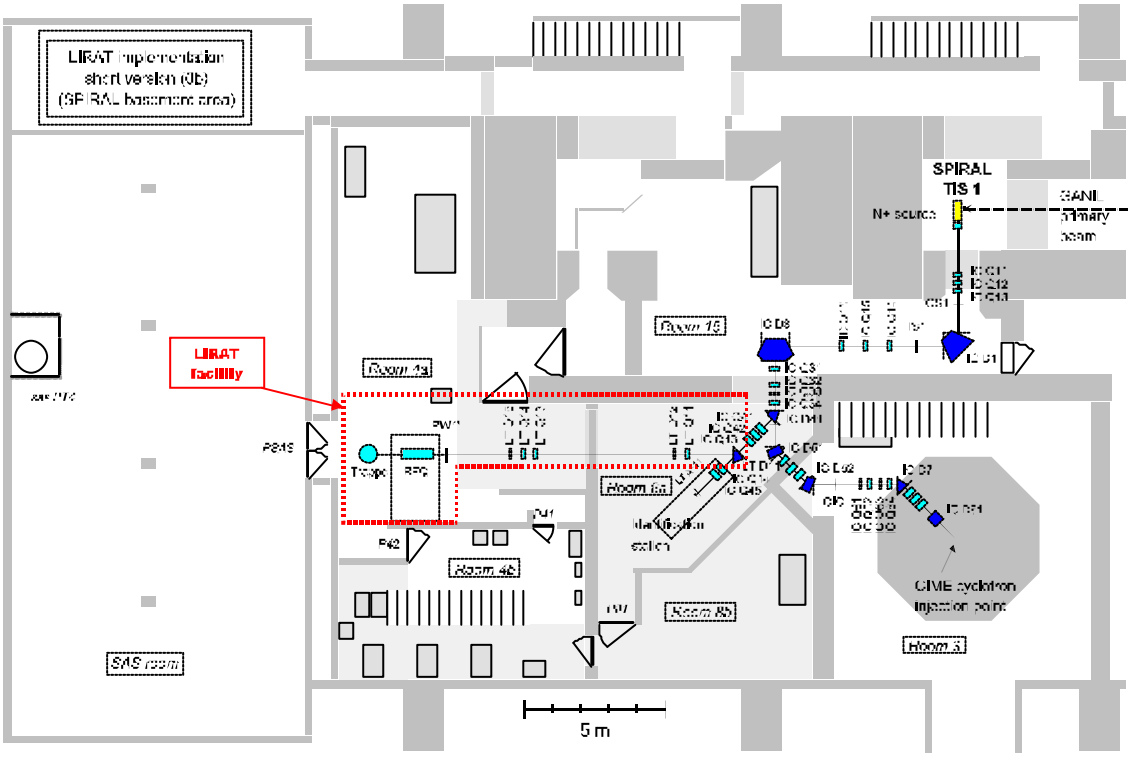

Figure 1 : Scheme of the LIRAT project implantation

2. Technical aspect

2.1. Beam line

The LIRAT beam line is a 10-metre long addition to the very low energy beam line of SPIRAL. Dedicated to low energy ions, its magnetic rigidity has been set at 0.136 Tm to permit singly-charged ion transport. Its contractual acceptance is 80 π.mm.mrad. In the actual configuration (LIRAT phase 1), the beam line makes it possible to deliver a (transversally) round beam of diameter between 14 and 30 mm. Figure 2 shows the complete LIRAT beam line, seen from its end. Its common section with identification line can be seen in the distance.

Figure 2 : LIRAT beam line view

Reduced to just the first section of the complete project proposed, the beam line is not really adapted to tune a large range of optics. Designed initially with the four quadrupoles necessary to obtain long distance optical conditions, a fifth one has been added to provide more flexibility in the downstream beam tuning (at the experimental device entrance).

For reasons of standardization and because it was well adapted, LIRAT utilizes the same technical solutions as SPIRAL. Magnetic devices are designed with equivalent characteristics and are interchangeable to preserve the evolutionary aspect of the project. Vacuum, electrical and operating securities are managed by specific numerical controllers (Siemens S7) which are coupled to their host on the SPIRAL facility.

Vacuum pressures (5.10^{-8} mbar as mean value) are reached with one turbo-molecular (550 l/s) and two cryogenic pumps (2 x 800 l/s), distributed along the line. All extracted pumping flux is guided through the nuclear ventilation system of SPIRAL.

Electrical power necessary for LIRAT operation (phase 1) is around 50 kW but 260 kVA has been installed to permit installation of various experimental physics equipment and to facilitate future expansion of the beam line.

Optically, the LIRAT beam line has been reduced to its minimum. Inserted within the SPIRAL identification line at a reserved location, a magnetic dipole steers the beam to the experimental area. With a similar one already installed (identification dipole), it constitutes an achromatic system. Five quadrupoles realize the beam requirements for physics. Figure 3 shows the standard optics of the actual line, low energy SPIRAL line included. The beam is tuned to meet the RFQ entrance conditions (H/V ± 9 mm).

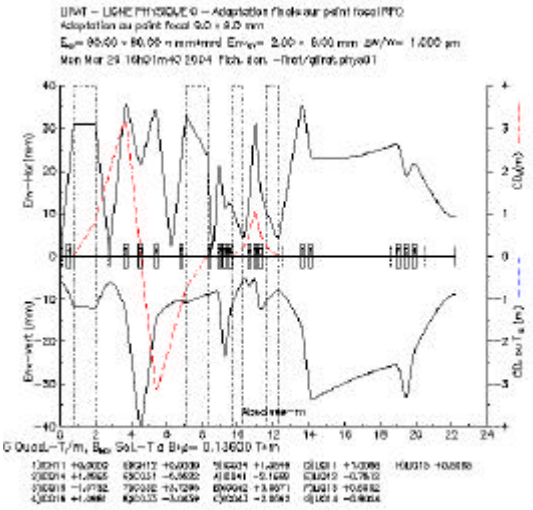

Figure 3 : LIRAT beam line optics
(H-plane above and V-plane below)

Four steering magnets are sufficient to align the beam along the line and the two last are reserved for precise injection into the RFQ of the experimental device. A set of four EMS beam profile monitors is installed to aid the beam fitting.

2.2. Experimental device

The experimental device installed on LIRAT facility (phase 1) have been developed to study the β–ν angular correlation in a pure Gamow-Teller transition of β-decay for various radioactive species.

Figure 4 : LPC CAEN experimental device for LIRAT

As can be observed in figure 4, it consists of two successive Paul traps. The first, situated inside the Faraday cage (left side) is a linear Paul trap, a radio-frequency quadrupole (RFQ) terminated by an electrical trap. Its goal is to catch and focus the desired ions, to cool them to few eV and to bunch them into small RF buckets. To facilitate this, the RFQ is polarized at 1 kV less than the ion source voltage and a

buffer gas (H_2 or He) is confined inside it at 10^{-2} mbar. An important vacuum system comprising five turbo-molecular pumps is necessary to isolate the RFQ chamber from the rest of the installation (~10^{-7} mbar).

The second one is a 3-dimensional Paul trap (right side in figure 4). By a combination of static and RF voltages, it permits one to localize the bunch extracted from the RFQ inside a volume of few mm^3. Around this trap a detection set-up made of a beta telescope and a recoil ion detector is installed in order to record one by one the radioactive decays.

Between these traps, two "pulse-down" electrodes are interfaced to reduce gradually the potential energy of the Faraday cage to 1 keV and finally 20 eV, making possible the injection of ions in the second Paul trap.

Typically, the working diagram of this system uses RF voltages up to 500 Vpp in a frequency range between 0.5 and 2.2 MHz, depending of the ions studied.

3. Safety aspect

As LIRAT is a new area for transport of radioactive ions, some structural modifications of the site were needed. The beam line goes through two existing rooms (room 8 in common with identification station and room 4 in common with LIRAT experimental device). It was thus necessary to divide these rooms in two, separated by a concrete wall, to protect users from the radioactive nature of the transported beam. In normal operation, these rooms are closed. An independent electromechanical system, using electric switches linking beam security system, radiological detector stations and the room status, manages the entry into areas occupied by the beam line.

Biological shielding has been dimensioned for the most demanding ion transported through LIRAT, from radiological point of view, i.e. ^{19}Ne.

A specific nuclear safety report has of course been written for its approval by the DGSNR (the French nuclear safety authority). It is expected that GANIL will receive the authorization to operate LIRAT with radioactive beams from the beginning of 2005.

4. Commissioning

4.1. Beam line

Two beam tests with stable ions have been performed to validate the construction phase of the LIRAT beam line. In June 2004, a short period was devoted to the LIRAT team to verify the technical operation of the project. No critical fault was observed and quite enough beam transmission and quality was obtained. It was somewhat more difficult than expected to inject the beam into the RFQ entrance correctly, in respect of its characteristics on the last EMS beam profiler.

Last December, a second period of beam tuning with stable ions was used to understand and correct these beam optics difficulties. This time, results were good. Having correcting a technical fault on the last EMS diagnostic of the line, the beam was as expected by calculations. Figure 5 shows beam profiles obtained in the LIRAT line with a ^{4}He beam of 15 keV. Transmission was 100% for the nominal acceptance of the beam line.

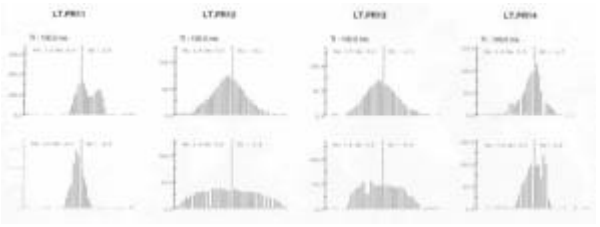

Figure 5 : Beam profiles of ^{4}He on LIRAT beam line (Dec. 8, 2004)

During that period, two different beams were transported to simulate the two first radioactive beams programmed for 2005. A $^4He^{1+}$ beam (pure and then polluted by $^{12}C^{3+}$) was produced to emulate $^6He^{1+}$ (polluted by $^{12}C^{2+}$) experiments and an $^{40}Ar^{1+}$ one to prepare for the first experiment (next April) with a $^{35}Ar^{1+}$ beam.

4.2. Experimental device

Simultaneously with beam line tests, in-situ commissioning of the experimental device was done. Figures 6 and 7 show the signatures of the first SPIRAL stable beam captured by the LPC RFQ. It was an ^{16}O beam and the coupling between the beam line and the experimental system proved to be efficient.

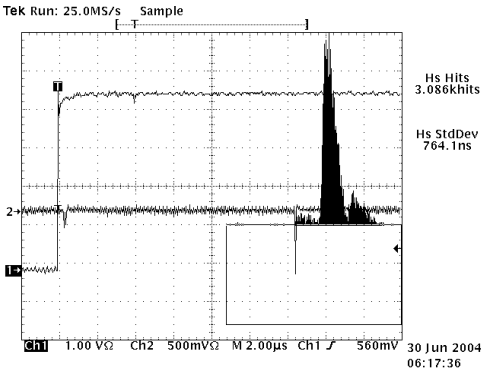

Figure 6 : $^{16}O^{1+}$ ions driving through the RFQ characterized by time-of-flight method

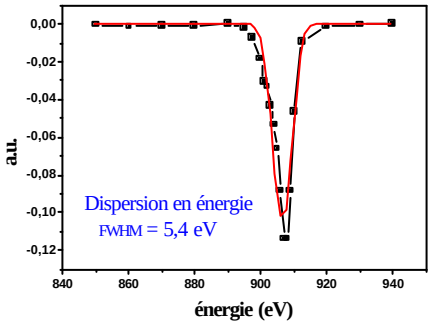

Figure 7 : $^{16}O^{1+}$ ions cooled down by the RFQ at 5.4 eV (FWMH)

Last December, more precise measurements were made with this apparatus. A stable helium beam was cooled down with the expected transmission and the resulting bunches if ions were injected into the Paul trap. For the first time, the integrality of the Lirat device was tested. Typical trapping times measured with this beam have shown that helium ions are properly driven through the system even when the produced beam is polluted by other species (a typical case with ^{6}He beam produced by the ISOL method using a carbon target). At the opposite mass range of SPIRAL beams for LIRAT, tests with argon ions have shown that the RFQ is easily adaptable to various species.

5. Perspectives

In the next two years, we expect to use the LIRAT facility to study the process of radioactive decay of the four specifically authorized radioactive ions. More particularly, the β–ν correlations will be observed in order to test the limits of the Standard Model.

During that period, we will try to obtain from Nuclear Safety Authorities permission to expand the LIRAT operation to all radioactive species produced by SPIRAL. However, a strategic reflection have to be led for the future of the LIRAT facility. If the actual device with the present large beam spot size is acceptable for all types of low energy experiments, no more heavy investment will be necessary for this facility at GA NIL. If on the other hand there may be optical incompatibility between the present beam spot size and some future experiments, this will require LIRAT to evolve to a real beam delivery platform with a dedicated experimental room, as was proposed initially.

It must be recalled that experiments in other domains of low energy physics could be performed with this facility. Static properties of exotic nuclei like mass, spin, parity or quadrupole momentum measurements are, of course, very interesting to be implemented on LIRAT. But experiments on atomic or steady state physics are also possible (impurities inside semi-conductors, material stability for nuclear waste storage, Mossbauer spectroscopy…).

We expect the LIRAT facility to be the first step toward a common SPIRAL 1 / SPIRAL 2 low energy area. Experiments will be able to start with trapping devices and explore new physics. All the results and know-how obtained from the LIRAT beam line will be a great asset for the design of this future area.

6. Conclusion

The LIRAT facility is almost ready to operate with radioactive beams at the beginning of 2005. A few last points have to be finalized. Technically, the security access system has still to be finished and tested. Administratively, the authorization of the Nuclear Safety authorities has yet to be received. It is hoped that these two points will be resolved by March 2005.

The first experiment with LIRAT and radioactive beam (^{35}Ar) is planned to take place at the beginning of April 2005. We wish our users good luck and interesting physics with this new facility at GANIL.

5

APPENDIX #1

EXPERIMENTS CONDUCTED IN NUCLEAR PHYSICS

YEAR 2003

Date	exp #	Duration hours	Title	Spokes person	Beam	Energy	Cave
18-mars	Test	50	Test VAMOS	Savajols	32S	95AMeV	G1
21-mars	Test	16	Test LISE 2000		32S	95AMeV	D3
21-mars	E398	144	High-precision measurements of the decay of ^{21}Mg and ^{25}Si and its mirrors	J.C. Thomas	32S	95AMeV	D6LISE3
1-avr	E314b	24	Nuclear spins and moments of nuclei in the "Island of inversion" around ^{32}Mg	G. Neyens	32S	95AMeV	D6LISE3
2-avr	E421S	24	Deep inelastic collisions induced by neutron rich beams from SPIRAL and in beam gamma spectroscopy using EXOGAM	F. Azaiez	14N	4,75AMeV	G1 EXOGAM
4-avr	E314b	72	Nuclear spins and moments of nuclei in the "Island of inversion" around ^{32}Mg	G. Neyens	36S	78AMeV	D6LISE3
6-avr	E314b	72	Nuclear spins and moments of nuclei in the "Island of inversion" around ^{32}Mg	G. Neyens	36S	78AMeV	LISE2000
9-avr	E421S	16	Deep inelastic collisions induced by neutron rich beams from SPIRAL and in beam gamma spectroscopy using EXOGAM	F. Azaiez	14N	4,75AMeV	G1 EXOGAM
11-avr	E421S	168	Deep inelastic collisions induced by neutron rich beams from SPIRAL and in beam gamma spectroscopy using EXOGAM	F. Azaiez	24Ne	4,75AMeV	G1 EXOGAM
23-avr	E389	24	Study of effective charges at ^{100}Sn via the nuclear level lifetime measurements in ^{96}Pd and ^{98}Cd	H. Mach	78Kr	73AMeV	D6LISE3
24-avr	E344aS	8	Shape coexistence near the N=Z line and collective properties of Kr isotopes investigated by low-energy Coulomb excitation of radioactive ion beams	W. Korten	82Kr	4,4AMeV	G1 EXOGAM
25-avr	E344aS	56	Shape coexistence near the N=Z line and collective properties of Kr isotopes investigated by low-energy Coulomb excitation of radioactive ion beams	W. Korten	74Kr	4,4AMeV	G1 EXOGAM
29-avr	E344aS	4	Shape coexistence near the N=Z line and collective properties of Kr isotopes investigated by low-energy Coulomb excitation of radioactive ion beams	W. Korten	82Kr	2,6AMeV	G1 EXOGAM
29-avr	E344aS	44	Shape coexistence near the N=Z line and collective properties of Kr isotopes investigated by low-energy Coulomb excitation of radioactive ion beams	W. Korten	74Kr	2,6AMeV	G1 EXOGAM
6-mai	E389	144	Study of effective charges at ^{100}Sn via the nuclear level lifetime measurements in ^{96}Pd and ^{98}Cd	H. Mach	112Sn	63,5AMeV	D6LISE3

Date	exp #	Duration hours	Title	Spokes person	Beam	Energy	Cave
9-mai	E435	72	Test of the EXCYT target-ion source assembly	M. Menna	112Sn	63,5AMeV	D2 SIRA
13-mai	E435	72	Test of the EXCYT target-ion source assembly	M. Menna	13C	75AMeV	D2 SIRA
29-mai	Test	28		De Oliveira	13C	75AMeV	D4
31-mai	Test	40		De Oliveira	13C	75AMeV	D4
4-juin	E406S	24	Study of extremly neutron-rich light isotopes with a new technique	H. Savajols	16O	15,4AMeV	G3
6-juin	E406S	136	Study of extremly neutron-rich light isotopes with a new technique	H. Savajols	8He	15,4AMeV	G3
14-juin	E416	24	Search for long lifetime components in the fission of super-heavy elements	M. Morjean	208Pb	4,5AMeV	D5
19-juin	E416	120	Search for long lifetime components in the fission of super-heavy elements	M. Morjean	238U	6,6AMeV	D5
25-juin	E416	16	Search for long lifetime components in the fission of super-heavy elements	M. Morjean	86Kr	6,5AMeV	D5
26-juin	Test	32	Test TIARA		20Ne	12AMeV	G1
27-juin	E371a	96	Data base of signals from silicon detectors - R&D for improvement of mass identification of medium mass nuclei	M.F. Rivet	86Kr	43,1AMeV	D4
2-juil	Test	30	Test TIARA		20Ne	12AMeV	G1
3-juil	E416	88	Search for long lifetime components in the fission of super-heavy elements	M. Morjean	238U	6,6AMeV	D5
7-juil	E401S	28	Study of ^{9}He via the d(^{8}He,p) reaction	S. Fortier	16O	15,4AMeV	G3
9-juil	E401S	200	Study of ^{9}He via the d(^{8}He,p) reaction	S. Fortier	8He	15,4AMeV	G3
18-juil	E416	16	Search for long lifetime components in the fission of super-heavy elements	M. Morjean	129Xe	7,49AMeV	D5
22-juil	E314b	72	Nuclear spins and moments of nuclei in the "Island of inversion" around ^{32}Mg	G. Neyens	36S	77,5AMeV	D6
25-juil	Test	32	Test TIARA		36S	11AMeV	G1
27-juil	E437	125	From spherical ^{34}Si to deformed ^{32}Mg : study of the ground state magnetic moments of ^{32,33}Al	G. Neyens	36S	77,5AMeV	D6
6-sept	E445S	60	Transfer study of ^{23}F in inverse kinematics	R. Lemmon	14N	10AMeV	G1 VAMOS
6-sept	E436	60	Spectroscopy of the unbound nucleus ^{25}O	W. Mittig	14N	10AMeV	G3 MAYA
10-sept	E445S	168	Transfer study of ^{23}F in inverse kinematics	R. Lemmon	14N	10AMeV	G1 VAMOS
10-sept	E436	168	Spectroscopy of the unbound nucleus ^{25}O	W. Mittig	14N	10AMeV	G3 MAYA
24-sept	E440	39	Synthesis of element Z=114	C. Stodel	40Ar	4,8AMeV	LISE3
27-sept	E440	258	Synthesis of element Z=114	C. Stodel	58Fe	5AMeV	D6LISE3
10-oct	E436	181	Spectroscopy of the unbound nucleus ^{25}O	W. Mittig	36S	77,5AMeV	G3 MAYA

Date	exp #	Duration hours	Title	Spokes person	Beam	Energy	Cave
28-oct	E440	16	Synthesis of element Z=114	C. Stodel	208Pb		D6LISE3
30-oct	E440	448	Synthesis of element Z=114	C. Stodel	76Ge	5AMeV	D6LISE3
19-nov	E406S	36	Study of extremly neutron-rich light isotopes with a new technique	H. Savajols	16O	15,4AMeV	G3
24-nov	E406S	24	Study of extremly neutron-rich light isotopes with a new technique	H. Savajols	16O	15,4AMeV	G3
26-nov	E406S	301	Study of extremly neutron-rich light isotopes with a new technique	H. Savajols	8He	15,4AMeV	G3
10-déc	E375	216	Spectroscopy of transfermium nuclei	C. Theisen	48Ca	4,5AMeV	D6LISE3

EXPERIMENTS CONDUCTED IN NUCLEAR PHYSICS

YEAR 2004

Date	exp #	Duration hours	Title	Spokes person	Beam	Energy	Cave
17-mars	E395	24	Single particle transfer on doubly-magic ^{56}Ni	B. Rubio	58Ni	27AMeV	G1
18-mars	E312c	72	Spectroscopic studies of proton-rich nuclei in the vicinity of ^{45}Fe and ^{48}Ni	B. Blank	56Ni	27AMeV	D6
18-mars	E395	192	Single particle transfer on doubly-magic ^{56}Ni	B. Rubio	56Ni	27AMeV	G1 VAMOS
27-mars	E312c	16	Spectroscopic studies of proton-rich nuclei in the vicinity of ^{45}Fe and ^{48}Ni	B. Blank	56Ni	27AMeV	D6
27-mars	E438	32	Test of MUST II prototype	E. Pollacco	58Ni	74,5AMeV	G3
31-mars	E312c	200	Spectroscopic studies of proton-rich nuclei in the vicinity of 45Fe and ^{48}Ni	B. Blank	45Fe	50AMeV	D6 LISE 3
20-avr	E443S	24	Study of N=16 for neutron rich nuclei with (d,p) transfer	A. Gillibert		10AMeV	G1
22-avr	E443S	16	Study of N=16 for neutron rich nuclei with (d,p) transfer	A. Gillibert	36S	78AMeV	G1
24-avr	E443S	84	Study of N=16 for neutron rich nuclei with (d,p) transfer	A. Gillibert	26Ne	10AMeV	G1
30-avr	E443S	68	Study of N=16 for neutron rich nuclei with (d,p) transfer	A. Gillibert	26Ne	10AMeV	G1
3-mai	E443S	72	Study of N=16 for neutron rich nuclei with (d,p) transfer	A. Gillibert	26Ne	10AMeV	G1
9-mai	E312c	136	Spectroscopic studies of proton-rich nuclei in the vicinity of ^{45}Fe and ^{48}Ni	B. Blank	48Ni	50AMeV	D6
17-mai	E442S	45	Very high resolution spectroscopy of ^{19}Ne for application to astrophysics	F. De Oliveira	15N	1AMeV	D6
3-juin	E447S	24	Determination of ^{44}Ar(n,g)^{45}Ar and ^{46}Ar(n,g)^{47}Ar reaction rates by (d,p) transfer reaction	O. Sorlin	40Ar	10AMeV	G3
7-juin	E447S	28	Determination of ^{44}Ar(n,g)^{45}Ar and ^{46}Ar(n,g)^{47}Ar reaction rates by (d,p) transfer reaction	O. Sorlin	40Ar	10AMeV	G3
9-juin	E447S	32	Determination of ^{44}Ar(n,g)^{45}Ar and ^{46}Ar(n,g)^{47}Ar reaction rates by (d,p) transfer reaction	O. Sorlin	44Ar	10AMeV	G3
11-juin	E447S	128	Determination of ^{44}Ar(n,g)^{45}Ar and ^{46}Ar(n,g)^{47}Ar reaction rates by (d,p) transfer reaction	O. Sorlin	46Ar	10AMeV	G3
19-juin	E377b	48	Search for the 0^{+}_{2} isomeric state in ^{44}S	S. Grévy	44S		D6
3-juil	E408S	24	Competition between octupole and multi-particle excitations in Po-212 and At-213	PM. Walker	16O	3.5AMeV	G1
3-juil	E350aS	24	Isobaric analogue states of 7He and 9He	W. Mittig	16O	3.5AMeV	G3

Date	exp #	Duration hours	Title	Spokes person	Beam	Energy	Cave
5-juil	E408S	88	Competition between octupole and multi-particle excitations in Po-212 and At-213	P. Walker	8He	3.5AMeV	G1
5-juil	E350aS	88	Isobaric analogue states of ^{7}He and ^{9}He	W. Mittig	8He	3.5AMeV	G3
9-juil	E408S	80	Competition between octupole and multi-particle excitations in Po-212 and At-213	P. Walker	8He	3.5AMeV	G1
9-juil	E350aS	80	Isobaric analogue states of ^{7}He and ^{9}He	W. Mittig	8He	3.5AMeV	G3
17-juil	E344aS	74	Shape coexistence near the N=Z line and collective properties of Kr isotopes investigated by low-energy Coulomb excitation of radioactive ion beams	W. Korten	78Kr	73AMeV	D6
20-juil	E410	192	Collective properties and shapes of N=Z nuclei around A=70 investigated by intermediate-energy Coulomb excitation	W. Korten	78Kr	73AMeV	D6
3-sept	E465S	32	Study of 4-neutron system using the d(^{8}He,^{6}Li) and d(^{8}He, d'alpha) reactions	D. Beaumel	16O	15.4AMeV	G3
6-sept	E465S	256	Study of 4-neutron system using the d(^{8}He,^{6}Li) and d(^{8}He, d'alpha) reactions	D. Beaumel	8He	15.4AMeV	G3
18-sept	E430	48	Nuclear excitation of ^{57}Fe isomeric state by target electron capture in crystal channeling conditions	J.M. Daugas	56Fe	9.46AMeV	D4
21-sept	E430	104	Nuclear excitation of ^{57}Fe isomeric state by target electron capture in crystal channeling conditions	J.M. Daugas	57Fe	11.5AMeV	D4
26-sept	E404aS	20	Identification of gamma-rays in nuclei around the drip-line nucleus ^{130}Sm : probing the maximally deformed light rare-earth region	P. Nolan	83Kr	4.34AMeV	G1
27-sept	E404aS	24	Identification of gamma-rays in nuclei around the drip-line nucleus ^{130}Sm : probing the maximally deformed light rare-earth region	Nolan	83Kr	4.34AMeV	G1
29-sept	E404aS	168	Identification of gamma-rays in nuclei around the drip-line nucleus 130Sm : probing the maximally deformed light rare-earth region	Nolan	76Kr	4.34AMeV	G1
8-oct	E447S	24	Determination of ^{44}Ar(n,g)^{45}Ar and ^{46}Ar(n,g)^{47}Ar reaction rates by (d,p) transfer reaction	O. Sorlin	40Ar	10AMeV	G3
10-oct	E447S	80	Determination of ^{44}Ar(n,g)^{45}Ar and ^{46}Ar(n,g)^{47}Ar reaction rates by (d,p) transfer reaction	O. Sorlin	16Ar	10AMeV	G3
16-oct	P660	48	Interférence effects in electron emission from H_2 by fast ion impact	N. Stolterfoht	86Kr	60AMeV	D4 LISE
6-nov	Test	32	Test LISE2000	C. Stodel	18O	63AMeV	D4
8-nov	Test	24	Test RDT	H. Savajols	18O	5.3AMeV	G1 VAMOS

Date	exp #	Duration hours	Title	Spokes person	Beam	Energy	Cave
10-nov	E437a	96	From spherical ^{34}Si to deformed ^{32}Mg : ground state magnetic and quadrupole moments of Al-isotopes	P. Himpe	36S	77.5AMeV	D6
10-nov	E287c	96	Evolution of the N=28 shell gap in the Si isotopes	S. Grévy	36S	77.5AMeV	G3
16-nov	E287c	168	Evolution of the N=28 shell gap in the Si isotopes	S. Grévy	48Ca	60AMeV	G3
24-nov	E442S	15	Very high resolution spectroscopy of 19Ne for application to astrophysics	F. De Oliveira	12C1	1.2AMeV	G41
25-nov	E462	192	Very neutron rich calcium isotopes at N>=32 structure of nearly magic ^{54}Ca	M. Rejmund	48Ca	5,5AMeV	G1
7-déc	P675	12	Quid de la transition verre de Bose - liquide de vortex observée à haute température ?	A. Ruyter	208Pb	29AMeV	D1
9-déc	E287c	166	^{34,36}Ca : the reminiscence of the Z=20 "Mirror isle of inversion"	S. Grévy	48Ca	60AMeV	G3

EXPERIMENTS CONDUCTED IN SWIFT ION PHYSICS
YEAR 2003

Date	exp #	Duration hours	Title	Spokes person	Beam	Energy	Cave
27-mars	P609	128		Laurent	32S	95AMeV	D1
21-avr	P545	20	Effets du dépôt d'énergie électronique dans les dispositifs semi-conducteurs	A. Campbell	78Kr	73AMeV	D1
20-avr	Test	20		B. Lott	78Kr	73AMeV	G42
22-avr	Test	20		J. Lefrançois	78Kr	73AMeV	G41
1-mai	P645	32	Effets de l'irradiation sur les verres de Sialon dans le contexte de la transmutation des actinides	R. Dauce	86Kr	2,6AMeV	D1
3-mai	P634	10	Radiolyse des macromolécules biologiques par les ions lourds de TEL - 180 keVu/m. Modélisation des effets biologiques de la réaction 10B(n,a)7Li. 1 - Les protéines	M. Charlier	36Ar	95AMeV	D1
3-mai	P608	8	Irradiation de cellules humaines par les ions à TEL élevé : corrélation trace physique / trace biologique, implications de certaines lésions précoces dans l'instabilité chromosomique retardée.	I. Testard	36Ar	95AMeV	D1
3-mai	P647	12	Study of heavy ion-induced gene expression in recombinant human embryonic kidney cells	C. Baumstark	36Ar	95AMeV	D1
4-mai	P642	11	Detection of DNA double strand breaks, locally multiply damaged sites and chromosomal damage in human cells after exposure to heavy ions	D. Averbeck	36Ar	95AMeV	D1
4-mai	P608	12	Irradiation de cellules humaines par les ions à TEL élevé : corrélation trace physique / trace biologique, implications de certaines lésions précoces dans l'instabilité chromosomique retardée.	I. Testard	36Ar	95AMeV	D1
5-mai	P647	12	Study of heavy ion-induced gene expression in recombinant human embryonic kidney cells	C. Baumstark	36Ar	95AMeV	D1
30-mai	Test	28		M. Bajard	13C	75AMeV	G41
2-juin	P643	40	Simulation de la radiolyse alpha des déchets polymères dans des colis de déchets : émission de gaz	Y. N'Gono Ravache	13C	75AMeV	D1
3-juin	P612	24	Effet du TEL sur la morphologie et la structure des agrégats métalliques générés par rayonnement	H. Remita	13C	75AMeV	D1

Date	exp #	Duration hours	Title	Spokes person	Beam	Energy	Cave
15-juin	P626	24	Effets de la désorientation et l'enchevêtrement des défauts sur la dynamique des vortex en phase solide et liquide dans des monocristaux de Bi-2212. Mouvement des parois de domaines ferroélectriques dans des couches épitaxiales irradiées de Pb(Zr, Ti)O_3	A. Ruyter	208Pb	29AMeV	D1
17-juin	P616	8	Damage tracks in novel superconductors	C. Van der Beek	208Pb	29AMeV	D1
17-juin	P648	32	Irradiation d'alliages d'aluminium dans des phases quasicristallines et rhomboédriques	G. Coddens	208Pb	29AMeV	D1
30-juin	Test	4	Test J. Lefrançois		86Kr	43,1AMeV	G4
19-juil	P606	24	Effet du dépôt d'énergie par des ions lourds dans des dispositifs semiconducteurs	C. D'Hose	129Xe	50AMeV	D1/G4
20-juil	P545	16	Effets du dépôt d'énergie électronique dans les dispositifs semi-conducteurs	A. Campbell	129Xe	50AMeV	D1/G4
28-août	SME	32			129Xe	50AMeV	
31-août	SME	52			208Pb	4,5AMeV	
2-sept	SME	13			208Pb	4,5AMeV	
21-nov	P641	24	Radiolyse pulsée de l'eau à TEL élevé. 3 - Les radicaux libre OH	G. Baldacchino	13C	75AMeV	D1
22-nov	P656	32	Development of an optical delta-dose dosimeter	D. Broggio	13C	75AMeV	D1

EXPERIMENTS CONDUCTED IN SWIFT ION PHYSICS

YEAR 2004

Date	exp #	Duration hours	Title	Spokes person	Beam	Energy	Cave
3-mars	P662	8	Radiolyse des complexes acides nucléiques - protéines par les ions lourds de TEL > 180 keV/um.	M. Charlier	36Ar	95AMeV	D1
3-mars	P603	12	High LET particle-induced degradation of DNA bases	J.L. Ravanat	36Ar	95AMeV	D1
4-mars	P658	20	Etude de la réparation des cassures de l'ADN induites dans des cellules humaines irradiées par des ions lourds à TEL élevé. Implication de la réparation par jonction non homologue (NHEJ).	I. Testard	36Ar	95AMeV	D1
11-mars	test	40	Test EADS		129Xe	35AMeV	G41
23-juin	P633	4	Structure and reactivity of latent heavy-ion tracks	Y. Eyal	208Pb	29AMeV	D1
23-juin	P654	8	Pour une meilleure compréhension des processus de cristallisation des alliages amorphes à base de fer soumis à des fortes excitations électroniques	G. Rizza	208Pb	29AMeV	D1
23-juin	P680	8	Pour une meilleure compréhension des processus de cristallisation des alliages amorphes à base de fer soumis à des fortes excitations électroniques	G. Rizza	208Pb	29AMeV	D1
24-juin	P675	12	Quid de la transition verre de Bose - liquide de vortex observée à haute température ?	A. Ruyter	208Pb	29AMeV	D1
24-juin	SME	56			208Pb	29AMeV	
28-juin	P632	24	Apoptose induite par les ions carbone dans des cellules normales et tumorales : étude des mécanismes concernés et modulation phamacologique	J. Gueulette	13C	75AMeV	G41
29-juin	P661	24	Apoptose induite par les ions carbone dans des cellules normales et tumorales : étude des mécanismes concernés et modulation phamacologique	J. Gueulette	13C	75AMeV	G41
30-juin	P667	24	Mort cellulaire induite par des ions de hauts LET dans deux lignées tumorales humaines résistantes aux photons	Rodriguez Lafrasse	13C	75AMeV	G41
1-juil	P666	16	Mort cellulaire induite par des ions de hauts LET dans deux lignées tumorales humaines résistantes aux photons	M. Beuve	13C	75AMeV	G41
1-juil	P674	8	Etudes de systèmes dosimétriques en salle D1	A. Demeyer	13C	75AMeV	D1
1-sept	Test	40	Test ASCLEPIOS	Colin	13C	75AMeV	G4

Date	exp #	Duration hours	Title	Spokes person	Beam	Energy	Cave
16-oct	P679	24	Mesures et séparation des charges induites par ions lourds dans les composants microélectroniques.	J.E. Sauvestre	86Kr	60AMeV	D1
19-oct	P669	56	Measurement of correlated electron emission with the multidetector ARGOS	G. Lanzano	78Kr	64AMeV	G42
21-oct	P679	24	Mesures et séparation des charges induites par ions lourds dans les composants microélectroniques.	J.E. Sauvestre	78Kr	64AMeV	D1/G41
4-nov	Valorisation	16	ASTRIUM		129Xe	35AMeV	G41
5-déc	P654	8	Pour une meilleure compréhension des processus de cristallisation des alliages amorphes à base de fer soumis à des fortes excitations électroniques	G. Rizza	208Pb	29AMeV	D1
5-déc	P680	8	Pour une meilleure compréhension des processus de cristallisation des alliages amorphes à base de fer soumis à des fortes excitations électroniques	Rizza	208Pb	29AMeV	D1
6-déc	Valorisation	16	CNES		208Pb	29AMeV	G41

AVAILABLE IONS at GANIL

ION		PRODUCTION METHOD	COMPOUND	SAMPLE AVAILABLE AT GANIL
type	masse			
C	12	GAS	CO_2 - CH_3	YES
C	13	GAS	CO_2 - CH_3	YES
N	14	GAS	N_2	YES
N	15	GAS	N_2	YES
O	16	GAS	O_2	YES
O	17	GAS	O_2	YES
O	18	GAS	O_2 - CO_2	YES
F	19	GAS	SF_6	YES
Ne	20	GAS	Ne	YES
Ne	22	GAS	Ne	YES
Mg	24	MIVOC/OVEN	Mg / $MgC_{10}H_{10}$	YES
Si	28	GAS	SiH_4	YES
S	32	GAS	SF_6	YES
S	36	GAS	SF_6	YES
Ar	36	GAS	Ar	YES
Ar	40	GAS	Ar	YES
Ca	40	OVEN	Ca	YES
Ca	48	OVEN	Ca - CaO	NO
Cr	50	OVEN	Cr	NO
Cr	52	OVEN	Cr	YES
Cr	54	OVEN	Cr	YES
Fe	56	MIVOC	$FeC_{10}H_{10}$	YES
Ni	58	MIVOC/OVEN	$NiC_{10}H_{10}$/NiO/Ni	YES
Ni	64	MIVOC/OVEN	$NiC_{10}H_{10}$/NiO/Ni	NO
Cu	65	OVEN	Cu	NO
Zn	64	OVEN	Zn	YES
Zn	70	OVEN	Zn	NO
Ge	74	OVEN	GeO_2	NO
Ge	76	OVEN	GeO_2	NO
Se	80	OVEN	Se	YES
Kr	78	GAS	Kr	YES
Kr	84	GAS	Kr	YES
Kr	86	GAS	Kr	YES
Nb	93	ROD/SPUTTERING	Nb	YES

ION		PRODUCTION METHOD	COMPOUND	SAMPLE AVAILABLE AT GANIL
type	masse			
Mo	92	OVEN	MoO_3	YES
Mo	96	OVEN	MoO_3	YES
Ag	107	OVEN	Ag	YES
Ag	109	OVEN	Ag	YES
Cd	106	OVEN	CdO	NO
Sn	112	OVEN	Sn/SnO	NO
Sn	116	OVEN	Sn/SnO	NO
Xe	124	GAS	Xe	NO
Te	125	OVEN	Te	NO
Xe	129	GAS	Xe	YES
Xe	132	GAS	Xe	YES
Xe	136	GAS	Xe	NO
Sm	154	ROD	Sm_2O3	NO
Gd	155	ROD	Gd_2O3	NO
Gd	157	ROD	Gd_2O3	NO
Gd	158	ROD	Gd_2O3	NO
Ta	181	ROD/SPUTTERING	Ta	YES
Pb	208	OVEN	Pb	YES
U	238	SPUTTERING	U	YES

ACCELERATED BEAMS
WITH THEIR CHARACTERISTICS

* : The intensity with the following format " > xx " corresponds to a 400 W accelerated beam with the possibility to get higher power.
- The intensities correspond to a given energy. For a new energy a study must be done.
- The beams coming from CSS1 are available for the SME (Medium Energy Exit), with energies between 4 and 13 MeV/A. They can also be sent directly to all the experimental areas.

ION		CHARGE STATE	Isotopic enrichment	Max Source intensity	RF FREQUENCY	FINAL ENERGY	INTENSITY ON TARGET *
type	mass	source / final	%	µA	MHz	MeV/u	µAe
C	12	4/5/6			12.13	75	>2.7
C	12	4/6	99 %	100	13.45	95	>2.1
C	13	2/6	99 %	100	8.54	35	>5.2
C	13	3/6		100	10.97	60	>3
C	13	3/6		200	12.13	75	18.5
N	14	2/7	99 %	200	7.938	30	>6.6
N	14	3/7		200	13.45	95	>2.1
N	15	3/7	99 %	200	11.35	65	>2.9
N	15	4	100 %	100	13.45	1 (C0)	10
O	16	4/7/8			9.1	40	>5
O	16	3/8	99 %	200	9.52	44	>4.5
O	16	3/8		200	11.76	70	>2.8
O	16	4/8		200	13.45	95	>2.1
O	17	3/8	50 %	100	10.1	50	>3.8
O	17	4/8		100	12.75	84	>2.2
O	18	2/8	99 %	200	7.95	30	>5.9
O	18	3/8		200	10.1	50	>3.5
O	18	4/8	100 %	100	10.55	55	3
O	18	4/8		200	11.225	63	>2.8
O	18	4/8		200	12.2	76	>2.3
Ne	20	3/10	99 %	200	9.893	48	>4.1
Ne	20	5/10		200	13.45	95	>2.1
Ne	20	6/10		150	13.45	95	15.7
Ne	22	5/10	99 %	200	11	60	>3
Mg	24	5/12	79 %	6	11.77	70	1
Mg	24	7/12		10	13.45	95	1.5
S	32	9/16	95 %	26	13.45	95	4.1
S	36	(8)10/16	65 %	(40)/27	12.31	77.5	5.7
Ar	36	4/16	99 %	40	7.55	27.1	>5
Ar	36	6	99.5 %	100	8.07	4.9 (CSS1)	2.5
Ar	36	5/16		60	8.19	32	>5
Ar	36	5/17		60	8.77	37	>5

ION		CHARGE STATE	Isotopic enrichment	Max Source intensity	RF FREQUENCY	FINAL ENERGY	INTENSITY ON TARGET *
type	mass	source / final	%	µA	MHz	MeV/u	µAe
Ar	36	5/17		60	9.31	42	>4
Ar	36	5/17		60	9.478	44	>4
Ar	36	10/18		160	13.45	95	15.8
Ar	40	7/18	99 %	100	7.94	30	>5
Ar	40	6/15		100	8.66	36	>4
Ar	40	7/17		100	9.52	43.8	>3.8
Ar	40	7/17		100	9.6	45	>3.7
Ar	40	9/17		150	11.053	60.9	>2.7
Ar	40	7/17		100	11.77	70	>2.4
Ar	40	9/18		150	12.27	76.9	>2.3
Ca	40	7/18	97 %	5	7.94	30	0.5
Ca	40	9/18/19			10.1	50	0.8
Ca	40	6/19		5	10.1347	50.4	0.5
Ca	40	9/20		10	13.455	95	1.3
Ca	48	8	50 %	5	7.822	4.5 (CSS1)	4
Ca	48	8/18	65 %	10	9.397	6.56 (CSS1)	1
Ca	48	8(10)/19	56 %	40	11	60.3	4
Cr	50	11/22	93 %	4	10.81	58	0.45
Cr	50	13/23		4	12.62	82	0.6
Cr	52	10/23	84 %	5	12.15	75	0.8
Cr	54	8			7.974	4.75 (CSS1)	0.4
Fe	56	10	100 %	30	11.41	9.7 (CSS1)	2
Fe	57	10	100 %	30	11.41	9.7 (CSS1)	2
Fe	58	8	93 %	35	8.073	4.9 (CSS1)	5.2
Ni	58	9	100 %	10	7.6	4.3 (CSS1)	2
Ni	58	10/26		35	10.28	52	>3.4
Ni	58	12/26		15	11.38	65	>2.7
Ni	58	10/26		35	11.651	68.5	>2.6
Ni	58	10/26	68 %	35	11.95	72.5	>2.4
Ni	58	11/26		50	12.06	75	4.8
Ni	58	14/27		3	12.49	80	0.15
Ni	58	15/28	68 %	1	13.145	89.97	0.1
Ni	64	10/26	90 %	1à3	11.061	61	0.5
Ni	64	11/26		20	10.55	55	3.5
Cu	65	13/27	99 %	3	11.33	64.4	0.5
Zn	64	13/29	50 %	5	12.42	79	0.5
Zn	70	15/29	34 %	3	11.48	66	0.3 (enr:45%)
Ge	76	10	99 %	35	8.185	5 (CSS1)	8.5
Ge	76	13/30	75 %	2	11,1	61	0.2
Ge	76	14/30		3.5	10.9	59.1	0.7
Kr	78	15/32	100 %	30	11.31	64	1.7

ION		CHARGE STATE	Isotopic enrichment	Max Source intensity	RF FREQUENCY	FINAL ENERGY	INTENSITY ON TARGET *
type	mass	source / final	%	µA	MHz	MeV/u	µAe
Kr	78	15/33			11.8	70.4	7
Kr	78	16/33	100 %	40	11.65	68.5	4
Kr	78	16/34	99 %	25	11.99	73	2
Kr	84	14/33	90 %	50	11	60	>2.6
Kr	84	11/31		90	9.055	39.5	>3.7
Kr	84	12/31		50	9.41	42.9	>3.4
Kr	86	12			7.765	4.5 (CSS1)	10
Kr	86	10/30	99 %	100	8.55	35	>3.9
Kr	86	15/34		40	11	60	2
Kr	86	16/33		45	11	58	4.4
Kr	86	12/31		55	9.43	43.1	>3.3
Mo	92	16(17)/37	98 %	3	10.975	60	0.2
Nb	93	13/31	100 %	1.3	7.28	25	0.2
Nb	93	14/33		1.3	8.075	31	0.2
Nb	93	16/36		1	10.64	56	0.2
Cd	106	21/44	80 %	5	11.5	66.5	0.15
Ag	107	19/40	99 %	4	10.28	52	0.3
Ag	107	18/38		3	8.71	36.4	0.3
Ag	109	18/38		3	8.55	35	0.1
Sn	112	22/46	99 %	3	11.222	63	0.2
Sn	112	17/43		3	10.8	57.9	0.2
Sn	116	16/37	96 %	4	7.28	25	0.2
Sn	116	16/38		4	7.95	30	0.2
Te	125	17/38	95 %	1	7.28	25	0.05
Te	125	17/38		1	7.55	27	0.05
Xe	124	18/44		15	9.62	45	0.27
Xe	129	15			7.1	0.273 (C0)	6
Xe	129	14/37	78 %	30	7.55	27	0.5
Xe	129	15/38		30	7.935	30	0.5
Xe	129	15/41		30	8.012	30.65	1.8
Xe	129	17/42	100 %	20	8.55	35	0.3
Xe	129	18/44		35	9.52	44	2
Xe	129	20/44		25	9.4	42.8	1.3
Xe	129	19/46		35	10.09	50	2
Xe	132	18/42	65 %	30	8.48	34.44	1.5
Xe	132	18/45		30	9.649	45.4	1.8
Xe	136	19/46		13	9.649	45.4	1.8
Sm	154	20/46	98 %	3	8.207	32	0.1
Gd	155	19/47	95 %	3.5	8.672	36.1	0.1
Gd	157	19/47		3.5	8.562	35.1	0.1
Gd	158	19/47		3.5	8.5073	34.7	0.1

ION		CHARGE STATE	Isotopic enrichment	Max Source intensity	RF FREQUENCY	FINAL ENERGY	INTENSITY ON TARGET *
type	mass	source / final	%	µA	MHz	MeV/u	µAe
Ta	181	24/55	100 %	8	8.66	36	0.08
Ta	181	24/57		8	9.055	40	0.08
Pb	208	25	99 %	5	8.2	5 (CSS1)	0.4
Pb	208	23/56	99 %	5	7.82	29	0.1
U	238	31	99.3 %	0.25	9.38	6.6 (CSS1)	0.03
U	238	24/58	99 %	2	7.13	24	0.05

SPIRAL BEAMS
RADIOACTIVE ION BEAM INTENSITIES

The available SPIRAL radioactive beams are listed below as well as the primary beam characteristics on the ion source target (ECS) needed for the production.
The colored figures are the experimental results. The radioactive beam intensity expected is given in the Low Energy Beamline (LEB) before acceleration in the cyclotron CIME and on the experimental target at high energy after the acceleration.

Radioactive Beam (halflife)	Charge State	Intensity measured or expected (pps)		Energy Experimental or Min (MeV/nucleon)	Energy Experimental or Max (MeV/nucleon)	Primary Beam	Primary Beam Power on ECS Target (kW)	Primary Beam Energy (MeV/nucleon)
		LEB	Target*					
^{6}He (0.8s)	+1		$1.7\ 10^{7}$	3.2	7.3	C	1.2	75
	+1		$3.2\ 10^{7}$	5	7.3		1.2	
	+2	$2.8\ 10^{7}$	$5.6\ 10^{6}$	6.8	22.8		1.4	
^{8}He (0.12s)	+1	$2.6\ 10^{5}$	$5.2\ 10^{4}$	3.5	4.1	^{13}C	0.9	75
	+1	$3\ 10^{6}$	$6\ 10^{5}$	3.5	4.1		2.5	
	+2	1.3 to 1.5 10^{5}	2 to 3 10^{4}		15.4		1.4	
^{13}N (9.9min)	+1	$4.7\ 10^{7}$	N.F	N.F	N.F	$^{14}N^{7+}$	1.4	95
	+2	$8.4\ 10^{6}$	$1.7\ 10^{6}$	1.7	6.5			
	+3	$1.4\ 10^{6}$	$2.8\ 10^{5}$	3.7	14.5			
	+4	$1.9\ 10^{5}$	$3.7\ 10^{4}$	6.5	21			
^{14}O (70s)	+1	$1.3\ 10^{7}$	N.F	N.F	N.F	$^{16}O^{8+}$	1.4	95
	+2	$4\ 10^{6}$	$8\ 10^{5}$	1.7	5.6			
	+3	$1.6\ 10^{6}$	$3\ 10^{5}$	3.2	12.5			
	+4	$1.6\ 10^{6}$	$3\ 10^{5}$	5.6	19.3			
	+5	$4.1\ 10^{5}$	$8.2\ 10^{4}$	8.8	24.3			
	+6	$4.1\ 10^{5}$	$8.2\ 10^{4}$	12.6	25.4			
^{15}O (122s)	+1	$4.3\ 10^{8}$	N.F	N.F	N.F	$^{16}O^{8+}$	1.4	95
	+2	$1.3\ 10^{8}$	$2.6\ 10^{7}$	1.7	4.86			
	+3	$5\ 10^{7}$	$1\ 10^{7}$	2.8	10.9			
	+4	$5\ 10^{7}$	$1\ 10^{7}$	4.9	17.8			
	+5	$1.3\ 10^{7}$	$2.6\ 10^{6}$	7.7	22.9			
	+6	$1.3\ 10^{7}$	$2.6\ 10^{6}$	11	25.4			
^{17}Ne (0.11s)	+5			6	19.5	^{20}Ne	1.4	95
^{18}F (109min)	+4		$2\ 10^{5}$	7.0	7.0	^{20}Ne	0.3	95
^{18}Ne (1.7s)	+2	$5.7\ 10^{7}$	$1.1\ 10^{7}$	1.7	3.25	^{20}Ne	1.4	95
	+4	$3\ 10^{6}$	$1\ 10^{6}$	7.0	12.95		0.3	
	+5	$3.2\ 10^{6}$	$6.5\ 10^{5}$	5.34	18		1.4	
	+7	$5.2\ 10^{6}$	$1.1\ 10^{6}$	10.4	24		1.4	
	+8	$1.2\ 10^{6}$	$2.4\ 10^{5}$	13.6	24.8		1.4	
	+10	$6.6\ 10^{3}$	$1.3\ 10^{3}$	21.2	24.8		1.4	

Radioactive Beam (halflife)	Charge State	Intensity measured or expected (pps)		Energy Experimental or Min (MeV/nucleon)	Energy Experimental or Max (MeV/nucleon)	Primary Beam	Primary Beam Power on ECS Target (kW)	Primary Beam Energy (MeV/nucleon)
		LEB	Target*					
^{19}Ne (17s)	+5	1.8 10^{8}	3.7 10^{7}	4.8	17	^{20}Ne	1.4	95
^{19}O (26.9s)	+3	3.8 10^{5}	7.2 10^{4}	2.8	10.9	^{36}S	0.9	77.5
^{20}O (13.5s)	+1	2.4 10^{5}	4.8 10^{4}	2.8	10.9	^{36}S	0.9	77.5
^{21}O (3.4s)	+1	1.2 10^{4}	2.4 10^{3}	2.8	10.9	^{36}S	0.9	77.5
^{22}O (2.25s)	+4	1 10^{3}	2 10^{2}	2.8	10.9	^{36}S	0.9	77.5
^{23}Ne (37s)	+5	5 10^{6}	1 10^{6}	3	11.4	^{36}S	1.4	77.5
^{24}Ne (3.4min)	+5	10^{6}	2 10^{5}	10	10	^{36}S	1.4	77.5
^{25}Ne (0.6s)	+4	1.7 10^{5}	3.4 10^{4}	1.9	6.9	^{36}S	0.8	77.5
^{26}Ne (0.23s)	+5	1.1 10^{4}	3 10^{3}	10	10	^{36}S	0.8	77.5
^{27}Ne (32ms)	+5	5 10^{2}	1 10^{2}	2.6	9.3	^{36}S	0.8	77.5
^{31}Ar (15ms)	+3	2.1 10^{1}	4 10^{0}	1.8	2.4	^{36}Ar	1.1	95
	+6	4.4 10^{0}	1 10^{0}	2.6	10.2		1.1	
^{32}Ar (98ms)	+9	10^{3}	2 10^{2}	5.5	18.5	^{36}Ar	1.1	95
^{33}Ar (173ms)	+8	9.1 10^{4}	1.8 10^{4}	4.1	15	^{36}Ar	1.1	95
^{34}Ar** (844ms)	+7	3.8 10^{6}	7.7 10^{5}	2.9	11.0	^{36}Ar	1.4	95
	+8	6.4 10^{6}	1.3 10^{6}	3.9	14.8		1.4	
^{35}Ar (1.78s)	+8	1.6 10^{8}	3 10^{7}	3.6	13.7	^{36}Ar	1.1	95
^{42}Ar** (33yr)	+8	5.2 10^{7}	10^{7}	2.5	9.54	^{48}Ca$	0.6	60
^{43}Ar** (5.4min)	+8	3 10^{7}	6 10^{6}	2.4	9.1	^{48}Ca$	0.6	60
^{44}Ar (11.8min)	+9	10^{6}	2 10^{5}	10.8	10.8	^{48}Ca$	0.6	60
^{45}Ar** (21.5s)	+8	7.5 10^{5}	1.5 10^{5}	2.2	8.3	^{48}Ca$	0.6	60
^{46}Ar (8.4s)	+9	10^{5}	2 10^{4}	10.3	10.3	^{48}Ca$	0.6	60
^{72}Kr (17s)	+11	2 10^{2}	4 10^{1}	1.8	6.3	^{78}Kr	0.4	68.5
^{73}Kr (27s)	+11	3 to 6 10^{3}	6 10^{4}	1.8	6.2	^{78}Kr	0.4	68.5
^{74}Kr (11.5min)	+11	6 10^{4}	1.5 10^{4}	2.6	2.6	^{78}Kr	0.4	68.5
^{75}Kr (4.3min)	+11	5 10^{5}	1 10^{5}	1.8	5.8	^{78}Kr	0.4	68.5
^{76}Kr (14.8h)	+11	3 10^{6}	6 10^{5}	2.6	2.6	^{78}Kr	0.4	68.5
	+11	3 10^{6}	10^{6}	4.4	4.4		0.4	
^{77}Kr (74.4min)	+11	3 10^{6}	6 10^{5}	1.8	5.5	^{78}Kr	0.4	68.5
^{79}Kr (35h)	+15	5.9 10^{6}	1.2 10^{6}	2.5	9.5	^{78}Kr	0.8	68.5
^{81}Kr (2.3 10^{5}yr)	+15	2.5 10^{6}	5 10^{5}	2.4	9	^{78}Kr	0.8	68.5

* Available intensity for the experiment.
** Computed figures
N.F = not feasible
^{48}Ca$ = ^{48}Ca is dependent on physicists.

6

APPENDIX #2 : LIST OF PUBLICATIONS

ARTICLES :

Recycling effect of germanium on ECR ion source
Lehérissier P., Barué C., Canet C., Dubois M., Dupuis M., Flambard J.L., Gaubert G., Jardin P., Lecesne N., Lemagnen F., Leroy R., Pacquet J.Y.
GANIL – Caen

NIM B211 (2003) 53

Le système de mesure 3D portable à bras six axes dans la métrologie des accélérateurs de particules
Beunard R.
GANIL – Caen

Revue XYZ 95 (2003) 43

Minimono: an ultracompact permanent magnet ions source for singly charged ions
Gaubert G., Barué C., Canet C., Cornell J., Dupuis M., Farabolini W., Flambard J.L., Gorel P., Jardin P., Lecesne N., Lehérissier P., Lemagnen F., Leroy R., Pacquet J.Y., Saint-Laurent M.G., Villari A.C.C.
GANIL - Caen

Review of Scientific Instruments, Volume 74 , Fascicule 2. (2003) 956-960

Transport and cooling of singly charged noble gas ion beams
Ban G., Darius G., Durand D., Flechard X., Herbane M., Labalme M., Lienard E., Mauger F., Naviliat-Cuncic O., Guenaut C., Bachelet C., Delahaye P., Kellerbauer A., Maunoury L., Pacquet J.Y.
LPC Caen, CSNSM – Orsay, CERN – Genève, CIRIL – Caen, GANIL – Caen,

NIM A 518 (2004) 712-720

Atom-to-ion transformation time in singly charged ECRISs
Jardin P., Farabolini W., Gaubert G., Pacquet J.Y., Cornell J., Durantel F., Huet-Equilbec C., Lecesne N., Leroy R., Saint-Laurent M.G., Barué C., Canet C., Dubois M., Dupuis M., Flambard J.-L., Leherissier P., Lemagnen F., Tuske O., Villari A.C.C.
GANIL – Caen
NIM B 225 (2004) 374-382

Status of the light ion source developments at CEA/Saclay
Gobin R., Beauvais P.Y, Bogard D., Charruau G., Delferriere O., De Menezes D., France A., Ferdinand R., Gauthier Y, Harrault F., Mattei P., Benmeziane K., Leherissier P., Paquet J.Y., Ausset P., Bousson S., gardes D., Olivier A., Celona L., Sherman J.
CEA Saclay – Gif-sur-Yvette, LPGP and Univ. Paris-Sud – Orsay, GANIL – Caen, CNRS – Orsay, INFN LNS – Catania, LANL – Los Alamos
Review of Scientific Instruments 75, 5 (2004) 1414

CONFERENCES :

World trends in cyclotron developments for nucler physics and applications

Baron E.
GANIL – Caen
Nukleonika 48, suppl. 2 (2003) S3.
XXXIII European Cyclotron Progress Meeting
Warsaw (POLAND)
17 septembre 2002

SPIRAL – A new radioactive beam facility

Lieuvin M.
GANIL – Caen
Nukleonika 48, suppl. 2 (2003) S149.
XXXIII European Cyclotron Progress Meeting
Warsaw (POLAND)
17 septembre 2002

Recent development for high intensity beams at GANIL

Moscatello M.H., Anger P., Berthe C., Bertrand P., Bru B., David L., Di Giacomo M., Jamet Ch., Ozille M., Pellemoine F., Petit E., Savalle A., Vignet J.L.
GANIL – Caen
Nukleonika 48, suppl. 2 (2003) S155.
XXXIII European Cyclotron Progress Meeting
Warsaw (POLAND)
17 septembre 2002

Beam dynamics studies in SPIRAL2 Linac

Duperrier R., Uriot D., Pichoff N., Bertrand P., Bru B., Savalle A., Varenne F., De Conto J.M., Froidefond E., Biarotte J.L.
CEA Saclay – Gif-sur-Yvette, Cea – Bruyères-le-Châtel, GANIL – Caen, LPSC – Grenoble, IPN – Orsay
2003 Particle Accelerator Conference

Proceedings of the 2003 Particle Accelerator Conference
Portland (USA)
12 mai 2003

LIONS LINAC : a new particle in cell code for LINACS

Bertrand P.
GANIL – Caen
2003 Particle Accelerator Conference

Proceedings of the 2003 Particle Accelrator Conference

Portland (USA)
12 mai 2003

Status report on ECR ion source operation at GANIL
Leherissier P., Barue C., Canet C., Dubois M., Dupuis M., Flambard J.L., Gaubert G., Jardin P., Lecesne N., Lemagnen F., Leroy R., Pacquet J.Y., Pellemoine-Landre F.
GANIL - Caen

Review of Scientific Instruments, Volume 75 , Fascicule 5. (2004)1488-1491

International Conference on Ions Sources 10
ICIS 2003
Dubna (RU)
08 septembre 2003

Visible light spectrometry measurements for studying an ECRIS plasma and especially applied to the MONO1001 ion source
Tuske O., Maunoury L., Pacquet J.-Y., Barue C., Dubois M., Gaubert G., Jardin P., Lecesne N., Leherissier P., Lemagnen F., Leroy R., Saint-Laurent M.G., Villari A.C.C.
GANIL - Caen

Review of Scientific Instruments, Volume 75 , Fascicule 5. (2004) 1529-1531

International Conference on Ions Sources 10
ICIS 2003
Dubna (RU)
08 septembre 2003

Radioactive ion beam production at GANIL: status and prospectives

Leroy R.
GANIL - Caen

Review of Scientific Instruments, Volume 75 , Fascicule 5. (2004) 1601-

International Conference on Ions Sources 10
ICIS 2003
Dubna (RU)
08 septembre 2003

Latest results obtained at GANIL with new target-source systems dedicated to radioactive ion production
Jardin P., Saint-Laurent M.G., Farabolini W., Gaubert G., Angelique J.C., Cornell J.C., Dubois M., Gibouin S., Lecesne N., Leroy R., Maunoury L., Pacquet J.Y., Pellemoine F., Stodel F., Tuske O., Verney D., Villari A.C.C., Barue C., Canet C., Dupuis M., Durantel F., Flambard J.-L., Huet-Equilbec C., Leherissier P.,
Lemagnen F.
GANIL - Caen

Review of Scientific Instruments, Volume 75 , Fascicule 5. (2004) 1617-1620

International Conference on Ions Sources 10
ICIS 2003
Dubna (RU)
08 septembre 2003

MONO1001 : a source for singly charged ions applied to the production of multicharged fullerene beams

Maunoury L., Andersen J.U., Cederquist H., Huber B.A., Hvelplund P., Leroy R., Manil B., Pacquet J.Y., Pedersen U.V., Rangamma J., Tomita S.

CIRIL – Caen, DPA Univ. of Arhus – Arhus, Univ. of Stockholm – Stockholm, GANIL – Caen,

Review of Scientific Instruments, Volume 75 , Fascicule 5. (2004) 1884-1887

International Conference on Ions Sources 10
ICIS 2003
Dubna (RU)
08 septembre 2003

Beam optical design of a multi charge ion recirculator for charge breeders

Cee R., Mittig W., Villari A.C.C.

GANIL – Caen

Proceedings of EPAC 2004 (2004) 1267-1270

EPAC 2004, 9th European Particle Accelerator Conference
Lucerne (SUI)
5-9 juillet 2004

GANIL status report

Chautard F., Jacquot B., Savalle A., Baelde J.L., Braue C., Berthe C., Colombe A., David L., Dolegieviez P., Jamet C., lecahrtier M., Leherissier M., leroy R., Moscatelo M.H., Petit E., Sénécal G., Varenne F.

GANIL – Caen

Proceedings of EPAC 2004 (2004) 1270

EPAC 2004, 9th European Particle Accelerator Conference
Lucerne (SUI)
5-9 juillet 2004

Possibilities for experiments with rare radioactive ions in a storage ring using individual injection

Meshkov I., Sidorin A., Smirnov A., Syresin E., Trubnikov G., mittig W., Roussel-Chomaz P., Katayama T.

JINR – Dubna, GANIL – Caen, CNS – Saitama

Proceedings of EPAC 2004 (2004) 1393

EPAC 2004, 9th European Particle Accelerator Conference
Lucerne (SUI)
5-9 juillet 2004

Longitudinal resonances and emittance growth using QWR/HWR in a LINAC

Bertrand P.

GANIL – Caen

Proceedings of EPAC 2004 (2004) 2011

EPAC 2004, 9th European Particle Accelerator Conference
Lucerne (SUI)
5-9 juillet 2004

Preliminary design of the RF system for the SPIRAL2 LINAC
Di Giacomo M., Ducoudret B., Leyge J.F., Denis J.-F., Desmons M., luong M., Mosnier A.
GANIL – Caen, SACM – CEA – Saclay

Proceedings of EPAC 2004 (2004) 2014

EPAC 2004, 9th European Particle Accelerator Conference
Lucerne (SUI)
5-9 juillet 2004

Status report on the beam dynamics developments for the SPIRAL2 project
Duperrier R., Uriot D., Pichoff N., Bertrand P., Varenne F., De Conto J.-M. Froidefond E., Biarotte J.L.
CEA Saclay – Gif-sur-Yvette, CEA – Bruyères-le Châtel, GANIL – Caen, LPSC – Grenoble, IPN – Orsay

Proceedings of EPAC 2004 (2004) 2020

EPAC 2004, 9th European Particle Accelerator Conference
Lucerne (SUI)
5-9 juillet 2004

SPIRAL2 RFQ design
Ferdinand R., Congretel G., Curtoni A., Delferriere O., France A., Leboeuf D., Thinel J., Toussaint J.C., Di Giacomo M.
DSM DAPNIA/SACM CEA Saclay – Gif-sur-Yvette, GANIL – Caen

Proceedings of EPAC 2004 (2004) 2023

EPAC 2004, 9th European Particle Accelerator Conference
Lucerne (SUI)
5-9 juillet 2004

PREPRINTS :

GANIL A 03 01
Recycling effect of germanium on ECR ion source

Leherissier P., Barué C., Canet C., Dubois M., Flambard J.L., Gaubert G., Jardin P., Lecesne N., Lemagnen F., Leroy R., Pacquet J.Y.
GANIL – Caen

GANIL A 03 02
Mono 1001 : source for singly charged ions applied to the production of multicharged fullerene beams

Maunoury L., Andersen J.U., Cederquist H., Huber B.A., Hvelplund P., Leroy R., Manil B., Pacquet J.Y., Pedersen U.V., Rangamma J., Tomita S.
CIRIL – Caen, Univ. of Arhus – Arhus, Stockholm Univ. – Stockholm, GANIL – Caen

GANIL A 03 03
World trend in cyclotron developments for nuclear physics ans applications

Baron E.
GANIL – Caen

GANIL A 03 04
Status report on ECR ion source operations at GANIL

Lehérissier P., Barué C., Canet C., Dubois M., Dupuis M., Flambard J.L., Gaubert G., Jardin P., Lecesne N., Lemagnen F., Leroy R., Pacquet J.Y., Pellemoine-Landré F.,
GANIL – Caen

GANIL A 04 01

Visible light spectrometry measurements for studying an ECRIS plasma and especially appied to the MONO1001 ion source

Tuske O., Maunoury L., Pacquet J.Y., Barué C., Dubois M., Gaubert G., Jardin P., Lecesne N., Leherissier P., Lemagnen F., Leroy R., Saint-Laurent M.G., Villari A.C.C.
GANIL – Caen, CIRIL - Caen

GANIL A 04 02

The portable six-axis-arm 3D measuring system : precise metrology applications for experimental equipment at GANIL

Beunard R.
GANIL – Caen

GANIL A 04 03
Atom-to-ion transformation time in singly-charged ECRISs

Jardin P., Farabolini W., Gaubert G., Pacquet J.Y., Cornell J., Durantel F., Huet-Equilbec C., Lecesne N., Leroy R., Saint-Laurent M.G., Barué C., Canet C., Dubois M., Dupuis M., Flambard J.L., Leherissier P., Lemagnen F., Tuske O., Villari A.C.C.
GANIL – Caen

GANIL A 04 04
Radioactive ion beam facilities in Europe. Current status and future development

Cornell J.
GANIL – Caen

GANIL A 04 05
SPIRAL2 at GANIL

Mosctello M.H.
GANIL – Caen

GANIL A 04 06
GANIL Status Report

Jacquot B., Chautard F., Savalle A.
GANIL – Caen

PREPRINTS ABOUT GANIL :

CERN LHC-Project-Report-799
Characterization and performance of the CERN ECR4 ion source

Andresen C., Chamings J., Coco V., Hill C.E., Kuchler D., lombardi A., Sargsyan E., Scrivens R.
CERN – Genève

CERN LHC-Project-Report-800
GTS-LHC : a new source for the LHC ion injector chain

Hill C.E., Küchler D., Scrivens R., Hitz D., Guillemet L., leroy R., Pacquet J.Y.
CERN – Genève, CEA – Grenoble, GANIL – Caen

REPORTS :

GANIL R 03 03
Fringe field minimisation of solenoids

Bertrand P.
GANIL - Caen

GANIL R 03 04
Proposition d'amélioration du tri en masse dans le cyclotron CIME
Bertrand P.
GANIL - Caen

GANIL R 03 07
Production of phosphorous and carbon ions with MONO 1001
Pacquet J.Y., Leroy R., Barué C., Canet C., Dubois M., Dupuis M., Durantel F., Flambard J.L., Gaubert G., Jardin P., Kantas S., Lecesne N., Lehérissier P., Lemagnen F., Maunoury L., Saint-Laurent M.G., Tuske O., Villari A.C.C.
GANIL – Caen, Pantechnik – Caen, CIRIL - Caen

GANIL R 03 08
Production of multi-charged phosphorus ions with ecris« SUPERSHyPIE » at GANIL
Pacquet J.Y, Leroy R., Maunoury L., Barué C., Canet C., Dubois M., Dupuis M., Durantel F., Flambard J.-L., Gaubert G., Huet-Equilbec C., Jardin P., Kantas S., Lecesne N., Lehérissier P., Lemagnen F., Saint-Laurent M.G., Tuske O., Villari A.C.C.
GANIL – Caen, PANTECHNIK - Caen, CIRIL – Caen

GANIL R 04 01
Beam optical calculations for SPIRAL2

Cee R.
GANIL - Caen